University of Kerbala

College of Science

Department of Chemistry

A Convenient Green Method to Synthesize Luminescent Carbon Dots from Edible Carrot and Its Applications

A thesis

Submitted to the Council of the College of Science, University of Kerbala, in Partial Fulfillment of the Requirements for the Degree of Master in Chemistry

By

Huda Radhi Mohaisen

Supervised by

Prof. Dr. Baker A. Joda **Prof. Dr. Adnan I. Mohammed**

2023 A.D. **1444 A.H.**

بِسْمِ اللَّهِ الرَّحْمَٰنِ الرَّحِيمِ

يَرْفَعِ اللَّهُ الَّذِينَ آمَنُوا مِنكُمْ وَالَّذِينَ أُوتُوا الْعِلْمَ دَرَجَاتٍ وَاللَّهُ بِمَا تَعْمَلُونَ خَبِيرٌ ﴿١١﴾

صَدَقَ اللهُ العَلِيُّ العَظيم

سورة المجادلة

الآية (11)

Dedication

Praise be to Allah, the maximum amount of praise, and thanks be to Allah before and after.

To the Prophet Muhammad (may God bless him and his family and grant them peace) and his honorable family (peace be upon them).

To the one who paved the way to walk through, and strived and sacrificed to reach where I am now

My dear father (may God have mercy on him)

To whom gave all the giving and was with me and supported and encouraged me at all times

My dear mother

To whom gave an advice and support

My dear sister

To whom supported me and drew my strength from them

My Dear brothers

To whom shared this journey and took the road with me

My dear friend

I present to you the fruit of my scientific effort

((Acknowledgement))

First of all, I would like to say a great thank you to my God who granted me this opportunity…….

I would also like to thank my supervisors, Dr. Baker A. Joda and Dr. Adnan Ibrahim Mohammed for their guidance, directions and scientific advice, which were very helpful…….

I would like to thank Department of Chemistry - College of Science - University of Kerbala…….

I would like to thank a number of people for their assistance and support, namely Dr. Luma M. Ahmed, Dr. Thaer M. Madlool, Dr. Ayad and Dr. Ali Atia…….

I would like to express a special thanks to my mother, brothers, sisters and daughter for their prayers and support…

THANK YOU ALL!

((Supervisor Certification))

We certify that this thesis, entitled (**A Convenient Green Method to Synthesize Luminescent Carbon Dots from Edible Carrot and Its Applications**) has been prepared under our supervision at the Department of Chemistry, College of Science, University of Kerbala in partial fulfillment of the requirements of the degree of Master of Science in Chemistry.

Signature:

Name: Dr. Baker. A. Joda
Title: Professor
Address: University of Kerbala, College of Science, Department of Chemistry
Date: / /2023

Signature:

Name: Dr. Adnan I. Mohammed
Title: Professor
Address: University of Kerbala, College of Science, Department of Chemistry
Date: / /2023

In view of the available recommendations, I forward this thesis for debate by the examining committee.

Signature:

Name: Dr. Luma Majeed Ahmed
Title: Professor
Head of Department of Chemistry, College of Science/ University of Kerbala
Date: / /2023

((Examination Committee Certification))

We are the examining committee, certify that we have read the thesis titled (**A convenient green method to synthesize luminescent carbon dots from edible carrot and its applications**) and examined the student (Huda Radhi Mohaisen) in its contents and in our opinion, it is adequate as a thesis for the Degree of Master of Science in Chemistry.

Signature:

Name: Dr. Bushra Basheer Qassim
Title: Professor
Address: University of Baghdad, College of Science, Department of Chemistry.
Date: / /2023

(Chairman)

Signature:

Name: Dr. Ahmed Fadhil Khudhair
Title: Professor
Address: University of Baghdad, College of Science, Department of Chemistry.
Date: / /2023

(Member)

Signature:

Name: Dr. Rahman Tama Haiwal
Title: Professor
Address: University of Kerbala, College of Science, Department of Chemistry.
Date: / /2023

(Member)

Signature:

Name: Dr. Baker. A. Joda
Title: Professor
Address: University of Kerbala, College of Science, Department of Chemistry.
Date: / /2023

(Member & Supervisor)

Signature:

Name: Dr. Adnan. I. Mohammed
Title: Professor
Address: University of Kerbala, College of Science, Department of Chemistry.
Date: / /2023

(Member & Supervisor)

Approved by the council of the science

Signature:

Name: Dr. Jasem Hanoon Hashim Al-Awadi
Title: Professor
Address: Dean of College of Science, University of Kerbala

Date: 6 / 7 /2023

Abstract.

In this study, a simple single-stage procedure depending upon refluxing Iraqi edible carrot with aqueous trisodium phosphate (TSP) has been used to synthesize blue color luminescent carbon dots (CDs). Optimization study indicate that refluxing 5 g of carrot in 100 mM TSP aqueous solution for 120 min is adequate to produce highly luminescent blue CDs. The Fourier-transform infrared (FTIR) spectrum of carrot extract (CE) and carbon dots (CDs) is explained that the -C=O peak observed in 1740 and 1650 cm−1 in the CE was completely lost in CDs, indicate that the carbonyl group was undertook carbonization and form more sp2 hybridized carbon. Furthermore, the 1H NMR spectra of CE and CDs showed that the number of signals observed between 3 and 4 ppm in the CE was reduced considerably in CDs, indicating that some sugar residues undergone carbonization. These results confirmed that the carbohydrates present in the carrot undergone carbonization to produce luminescent CDs. Scanning Electron Microscopy (SEM) images showed that CDs are almost spherical in shape and the size is around 6.40 – 25.76 nm. Energy dispersive X-ray (EDX) spectrum confirmed the presence of carbon in the samples. The CDs produced are used as luminophore to image bacteria through fluorescence microscopy. CDs have membrane good permeability and minimum toxicity against Gram-negative and Gram-positive bacteria. The CDs capability for direct reduction of silver ions to elemental silver (Ag^0) and gold ions to elemental gold (Au^0) without additional reducing and stabilizing agent was demonstrated. The resulting Ag and Au nanoparticles have a size of (20.40 – 59.44 nm) and (14.57 – 38.33 nm), respectively. Significantly higher values of Prothrombin Time (PT) and Activated partial Thromboplastin time (APTT) are found with AgNPs when compared with those without AgNPs, at the probability value of $P = 0.05$. On the other hands, there is no any significant effect of health status, gender, and smoking activity on the values of PT and APTT.

Table of Contents

List of Tables

List of Figures

Abbreviation

AgNPs	Sliver Nano Particles
AOR	Alcohol Oxidation Reaction
APTT	Activated Partial Thromboplastin Time
AuNPs	Gold Nano Particles
CDs	Carbon Dots
CE	Carrot Extract
CNDs	Carbon Nano Dots
CPDs	Carbonized Polymer Dots
CQDs	Carbon Quantum Dots
DDW	Distilled Deionized Water
EDX	Energy Dispersive X- ray Spectroscopy
EM	Electromagnetic
GQDs	Graphene Quantum Dots
KE	kinetic Energy
MWA	Microwave Ablation
OER	Oxygen Evolution Reaction
PBS	Phosphate Buffer Solution
PET	Polyethylene Terephthalate
ORR	Oxygen Reduction Reaction
PT	Prothrombin Time
PL	Photoluminescent
SEM	Scanning Electron Microscope
SWCNTs	Single -Wall Carbon Nanotubes
TSP	Tri Sodium Phosphate
XPS	X- ray Photoelectron Spectroscopy
1HNMR	Proton Nuclear magnetic resonance spectroscopy

Chapter One
General Introduction

Chapter One

General Introduction

1.1 Carbon Dots (CDs)

Carbon dots (CDs) were recognized since 2004 through the cleansing of Single-Walled Carbon Nanotubes (SWCNTs) through preparative electrophoresis. They can define as fluorescent small carbon nanoparticles and their sizes are less than 10 nm. The CDs have several applications such as bioimaging, biosensing, drug delivery, disease detection, materials science, and synthetic chemistry. These materials are low production costs, water-soluble, photo-chemically, and physio-chemically stable. Recently, the applications, production, and of CDs have maintained the attention of many scientists because of it is essential to develop different morphologies, sizes, and specific CDs for future research[1].

Generally, the modifications of surface for carbon nanoparticles with other molecules such as organic materials or polymeric are used to create the CDs. There are several methods were developed to prepare the CDs, for example, electrochemical oxidation, laser ablation, supported synthesis, and combustion/thermal MWA heating. Furthermore, solvothermal, hydrothermal, and microwave-assisted methods are useful because of their low-cost and simple operation [1].

The use of natural samples to produce CDs has several advantages such as being cost-effective, appropriate, and easily available in natural environments. For instance, in the preparation of CDs from banana juice using slow heating, and without the oxidizing agent, organic salt was used to synthesize green luminescent oxygenous CDs (~ 3 nm) [2]. The results show that the CDs are centration, excitation wavelength, and pH-dependent luminescent behavior in the visible scale. Furthermore, a suitable approach was utilized to supply fluorescent and water-

soluble carbon nanoparticles through a hydrothermal process by using the pomelo peels to use as a source for carbon [1]. A previous study has developed a new method to synthesize water-soluble fluorescent CDs by using watermelon peel as a reproducible and raw carbon resource via low-temperature carbonization and simple filtration, as shown in Figure 1.1 [2]. The resulting CDs had small particle sizes (approximately 2 nm) and were more stable in a wide range of pH values (2–11), acceptable fluorescence lifetimes, high blue luminescence, and at high salt concentrations. Interestingly, this method is able for the wide range production of water-soluble CDs. In addition, the CDs particles can use to provide live cell imaging. Therefore, these carbon NPs can consider high-performance optical imaging probes.

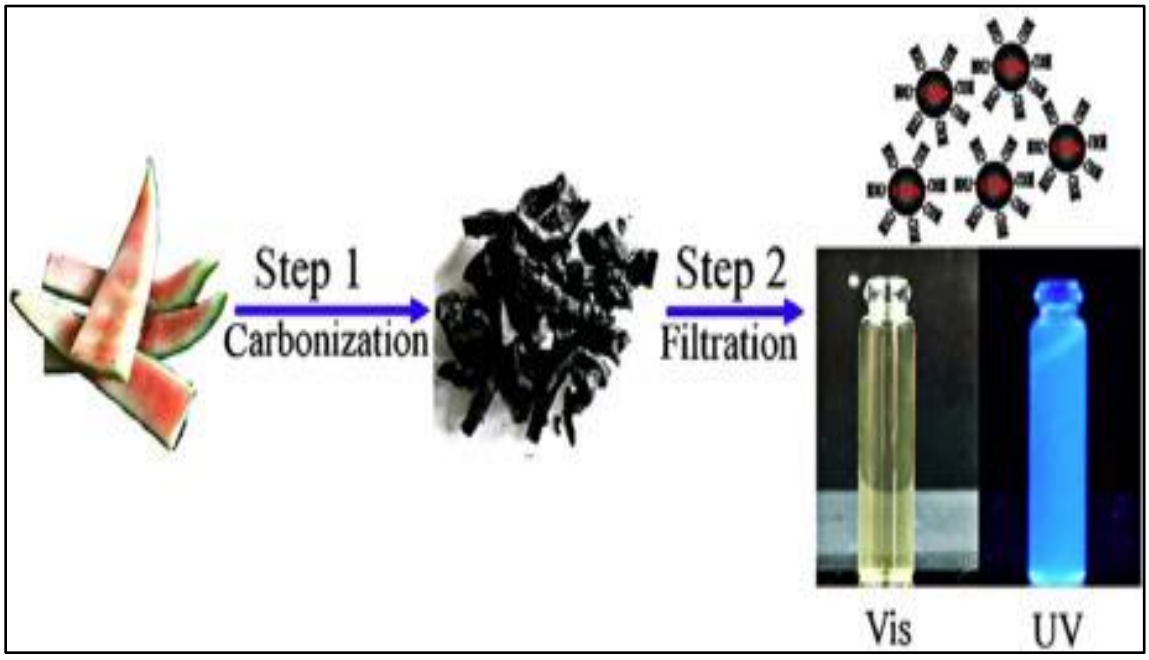

Figure 1.1: A schematic diagram of the preparation method for CDs from watermelon peel [2].

Carbon dots, a young member of the carbon nanomaterial family, are quasi-spherical nanoparticles, which have fluorescent properties as their key characteristic Carbon dots (C-dots) are quasi-spherical particles with a diameter of less than 10 nm

that were discovered while purifying single-walled carbon nanotubes, as shown in Figure 1.2. a series of different parameters that affect the properties of carbon dots have been investigated, including temperature, starting pH, as well as precursor concentration. Carbon atoms with sp^2/sp^3 hybridization make up C-dots chemically. C-dots have unique photophysical and chemical features when compared to other carbon allotropes [3, 4].

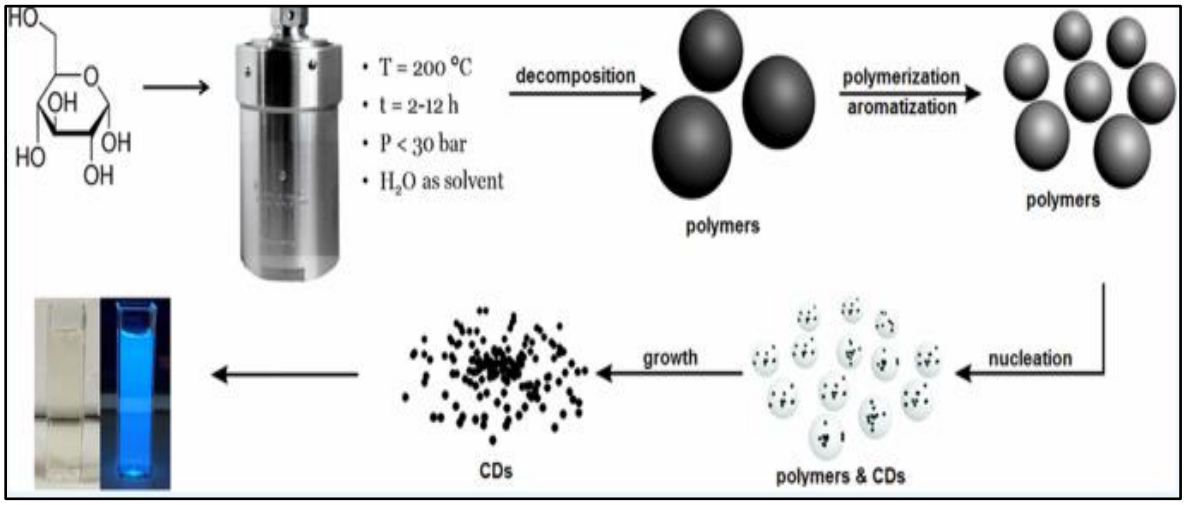

Figure.1.2. Stages of synthesis carbons dots.

C-dots have attracted a great deal of interest and have considerable potential in biological applications. Also, biocompatibility has been touted as C-dots' primary advantage in the field of NPs applications. C-dots are mostly made of carbon, which is a common and safe element. Their structure and electronic properties are different from those of other NP families [5, 6].

1.2 Chemical and Physical Properties of Carbon Dots

Carbon dots (CDs) have unique physical and chemical properties as well as optical properties, for examples fluorescence [7], luminescence [8], and photoluminescence [9]. Moreover, they exhibit biocompatibility [10], hydrophilicity [11], chemical stability [12], electroconductivity [13], high reactivity, surface functionality, and low toxicity [14]. The existence of numerous functionalities and various sizes are

accountable for their wide-ranging physical and chemical properties. These properties can be enhanced using different procedures to adjust their size, surface functionality, and chemical structure [15-17].

1.2.1 Electrochemical Properties of Carbon Dots

Carbon dots have currently related in the area of electrochemistry and electrocatalysis depending on of the following advantages:

- CDs exhibit exceptional charge transferability, enhanced electroconductivity, larger effective surface area, and lesser toxicity, as well as being comparatively cost-effective [18-20].
- the functional groups presenting on the surface of carbon dots such as hydroxy, carboxy and amine can transfer a large number of sites for the surface modification and also use to improve the activity of electrocatalytic by accelerating the intermolecular electroconductivity [21, 22].
- when carbon dots use heteroatom such nitrogen, phosphorous, sulfur and boron, they become anesthetic. the intramolecular charge transferability can be clearly enhanced by using of the electronic contribution of carbon dots [23, 24].
- through the electrochemical reactions such as oxygen evolution reaction (OER), hydrogen evolution reaction (HER), oxygen reduction reaction (ORR), and alcohol oxidation reaction (AOR), electrocatalysis process remarkably improve by carbon dots [25].

1.2.2 Visual Properties of CDs

These Properties can be classified into:

1.2.2.1 Ultraviolet-Visible Absorption

Usually, the UV-vis analysis is used to clarify the basic chemical structure of CDs. It was found that the kind of functional groups in the surface, methods of CDs synthesis, and chemical nature can be indicated by transition of the CDs skeleton such as n- π* (C=O, C-N, C-S, and π-π* (C=C), etc.). This means that sp2 hybridization of the π electrons and n-π* transition for the absorption bands of CDs can be exhibited at the region of 273 nm and 342 nm respectively [26]. The absorption of bands position can be affected by the mixture of the same C atom but various N sources [27]. The UV-vis peaks of the CD's molecular structure may fluctuate due to the attendance of hetero atoms, for examples Se, S, B, P, O, and N [28, 29].

1.2.2.2 Photoluminescence

The photoluminescent (PL) of the CDs is the considered the most fantastic characteristic feature. This characteristic gives a wide range of field applications. The transition of a thermally activated electron from the ground state to the excited state leads to transformation photoluminescence in the near-infrared area CDs [30]. The formation of CDs with specific shapes and various luminescent behaviors, namely deep ultraviolet emission, green, blue, red, yellow, and white have been resulted by the various synthetic approaches along with different starting materials. Since variable carbon sources can lead to the fabrication of CDs by various ways, the PL behavior also depends upon several factors such as size, pH, and solvent. Usually, the CDs display symmetrical and broad spectra across the range of wavelengths as a result of the diverse electronic transition pathways, [31-33].

1.2.2.3 Electron Transfer of CDs

Another characterized property of carbon dot is acting as an electron acceptor and donor. The CDs can use along with ionic liquids for energy uses as nanofluids which contain a mixture of organic and inorganic hybrid systems. This mixture can use as separators and electrolytes in the field of energy storage [34]. Photocatalysis is most important application of CDs. The previous studies indicated that the photocatalytic performance of the amorphous CDs and graphitic was produced saccharides such as fructose and glucose, and citric acid [35].

1.2.2.4 Cytotoxicity and Photostability of CDs

CDs are required for diverse applications because fascinating biocompatibility and relatively less toxicity. Both in vitro and in vivo conditions, the cytotoxicity of CDs are studied. The photostability of CDs is a key feature to discover their utilizing as fluorescent probes [36, 37].

1.2.2.5 Emerging property: chirality of CDs

In recent years, researchers have made more efforts to improve chiral CDs for their application in different fields such as bioimaging, chiral catalysis, sensing of chirality, biomedicine, chiral catalysis, and separation of chiral molecules. Usually, the “bottom-up” method produces good chiral CDs due to the precursor molecules themselves being chiral and therefore do not require the introduction of chiral ligands during the synthesis method [38, 39].

1.3 Classification of carbon dots.

CDs can be classified into several types, as shown in Figure1.3.

Figure1.3: The classification of CDs, their properties, synthesis approaches, characterization techniques, and applications in health care [40]

1.3.1 Graphene quantum dots (GQDs)

GQDs are nanoparticles with only two dimensions. They are made up of one or more layers of graphene sheets and form when graphitic material is peeled off. CQDs are quasi spherical nanoparticles with a crystalline graphitic core that are produced by thermally treating suitable precursors at elevated temperatures (T > 300 °C) [41, 42]. GQDs are pieces of graphene that are made up of one or more sheets of graphene with visible graphene lattices and chemical groups on or within interlayer defects. These features are what make GQDs stand out, as shown in Figure1.4 The lateral dimensions of a typical anisotropic graphene sheet are less than 20 nm, while its height is less than 2.5 nm [43]. In addition, it should be emphasized that both the quantum confinement effect of GQD sizes and the quantum confinement effect of the conjugated domains that are isolated by defects on the graphene plane can be referred to as the quantum confinement effect. When the oxygen element concentration is raised, more conjugated-domains function as the fluorescence centers. It is known that the natural luminescence of CQDs and the quantum confinement effect caused by their small size are caused by the crystal lattices and chemical groups on their surfaces. Controlling the photoluminescence wavelength by adjusting the size of CQDs is a big advancement [44, 45].

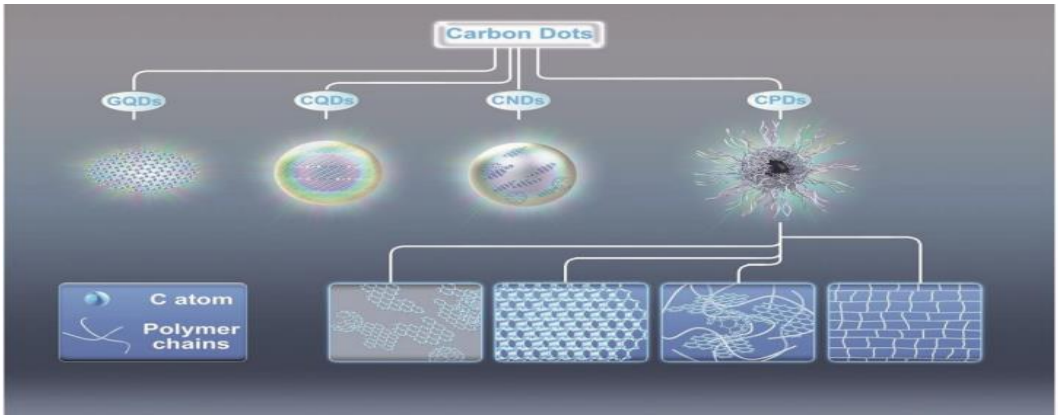

Figure.1.4: Classification of CDs: including (GQDs), (CQDs), (CNDs), and (CPDs), the possible structures of carbon core of CPDs [45].

Graphene-based composites may be utilized in sensors, depending on the need. Various graphene-based composites (metal nanoparticles, metal oxides, carbon hybrids) are currently being used to develop a variety of electrochemical and biosensors [46]. The enormous potential of graphene–metal chalcogenide composites for the detection of chemicals, biomolecules, and bio macromolecules is the focus of our research. Graphene–metal chalcogenide compounds have several benefits compared to other composite materials that use as an electrochemical sensor. The advantages increase from the hybridization of graphene and metal chalcogenides, namely polonies, selenides, sulfides, and tellurides but not oxides. The surface area and high electrical conductivity of the graphene can contribute to redox centers imparted by the metal: high current; and chalcogenide sites are highly advantageous for electro catalytic sensing of a broad range of molecules [47-49].

1.3.2 Carbon Quantum Dots.

In 2004 the first discovery of carbon quantum dots (CQDs) occurred during the purification of single-walled carbon nanotubes [48]. CQDs have a multilayer crystalline graphitic core with a crystalline lattice [49]. A Nano carbon material in the carbon family, zero-dimensional (0D) carbon quantum dots (CQDs) have gained increasing attention in recent years due to their remarkable characteristics of low cost, nontoxicity, large surface area, high electrical conductivity, and abundant surface functional groups.

CQDs emerge as promising functional materials for applications in energy-conversion sectors involving electro catalysis due to their rapid electron transfer and large surface area. In addition, the abundant functional groups on the surface of CQDs provide an abundance of anchoring sites and active sites for the design of multicomponent and high-performance composite materials [50].

Importantly, the heteroatoms in the CQDs can change the charge distribution in a way that encourages electron transfer through internal interactions. This is important for improving the performance of electro 6 catalytic reactions [51-54]. CQDs are created by functionalizing the surfaces of nanoparticles of carbon and polymeric and organic material.

The majority of preparation techniques involve the carbonization of carbon-containing precursors. This method yields CQD with highly variable optical properties but less controllability [55, 56].CQDs that are passivated have strong fluorescence and weak selector chemiluminescence. CQDs have been evaluated successfully in surface passivation as they have the ability to improve brightness because of long wavelengths and decreasing quantum yield. This is because their structures appear as layers and crystalline phases. CQDs that are passivated have strong fluorescence and weak electrochemiluminescence [57].

Numerous methods for the synthesis of CQDs have been developed, including electrochemistry [58], electrochemical oxidation treatments [59], carbonization methods [60], microwave synthesis routes [61], combustion, ultrasonic-assisted routes [62], hydrothermal/solvent heat treatments [63], and acidic oxidation, green synthesis, among others [64]. While numerous of these production methods need toxic or costly precursors, it is difficult to modify the complex reaction conditions. Therefore, research into new approaches and environmentally friendly precursors for synthesizing CQDs is still required. In the last century, many precursors for the synthesis of CQDs, for example, citric acid, phenyl-indamine, and ethylenediamine, have been identified. In recent years, several researchers have investigated the synthesis of CQDs utilizing natural products as starting materials. Examples include gelatin, human hair, honey, rose-heart radish, silk, and apple juice. To be both ecofriendly and easy to get, it is essential to find starting materials that are compatible with living things and break down naturally [65].

1.3.3 Carbon Nano Dots (CNDs)

Rapid development of carbon nanodots (CNDs) as phosphorescence candidates was studied due to their comparatively simple preparation procedure, high biocompatibility, and unique optical properties make them particularly intriguing in the area of biotechnology [66]. Due to the efforts of scientists, phosphorescent CNDs have a significant role in the development of optoelectronic apparatuses at room temperature. [67]. Ultraviolet (UV) phosphorescent CNDs that emit high-energy photons for an extended period of time 7 have not yet been realized. The development of UV phosphorescent CNDs become important in terms of their application in UV light-emitting devices [68].

1.3.4 Carbonized Polymer Dots (CPDs)

Carbonized polymer dot (CPD) is a revised term for the subclass of CDs consisting of a carbonized core and a polymer shell. The majority of CDs synthesized "bottom-up" from molecules or polymers should be CPDs. CPDs are subjected to dehydration and crosslinking [69]. CPD performance is primarily determined by the equilibrium between polymerization and carbonization [70]. The CPDs are used as excellent materials for catalysis, optoelectronic device construction, and ion detection due to they are green environment-protecting materials, have carbon content and special structures, high photo-stability, low toxicity, and tunable photoelectric properties [71].

1.4 Applications of Carbon Dots (CDs)

CDs can use in several biomedical applications such as medication transfer, biosensors, and bioimaging. CQDs play important role in optronics, sensors, and catalysis based on their electronic properties and good optical [57], as illustrated in Figure1.5.

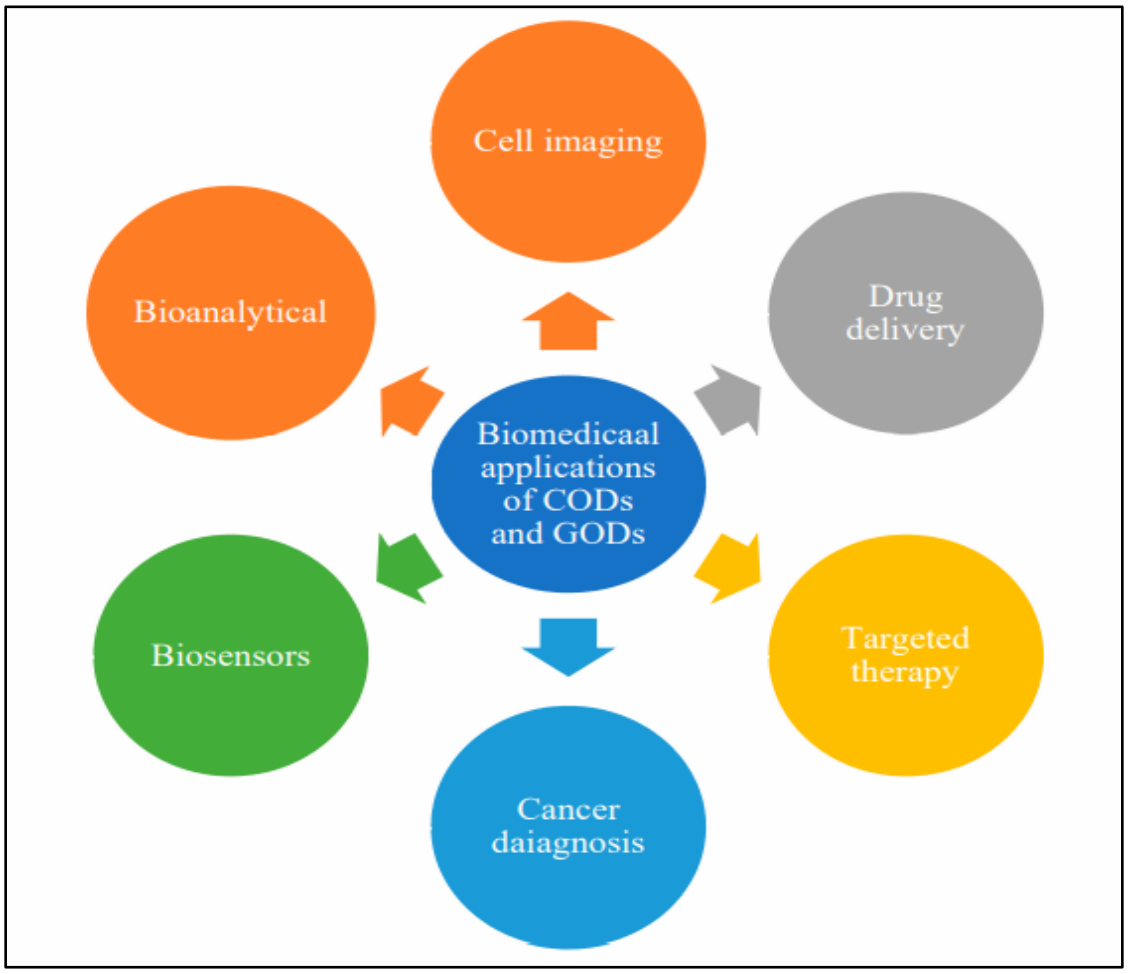

Figure 1.5: Biomedical applications of CODs [57].

1.4.1 Bioimaging

Bioimaging is a technique for imaging and direct observation of biological methods in real time which is often used to obtain information from the 3D morphology of the noted sample from the outside [72]. A previous study has reported several applications of C-dots in the biological field such as bioimaging [73].

1.4.2. Biosensors

The CQDs were utilized as biosensors because they have excellent biocompatibility, excellent photostability, nontoxicity, and high-water solubility. In addition, can be used for tracking pH, glucose, cellular copper, etc [74-76]. as shown in Figure 1.6.

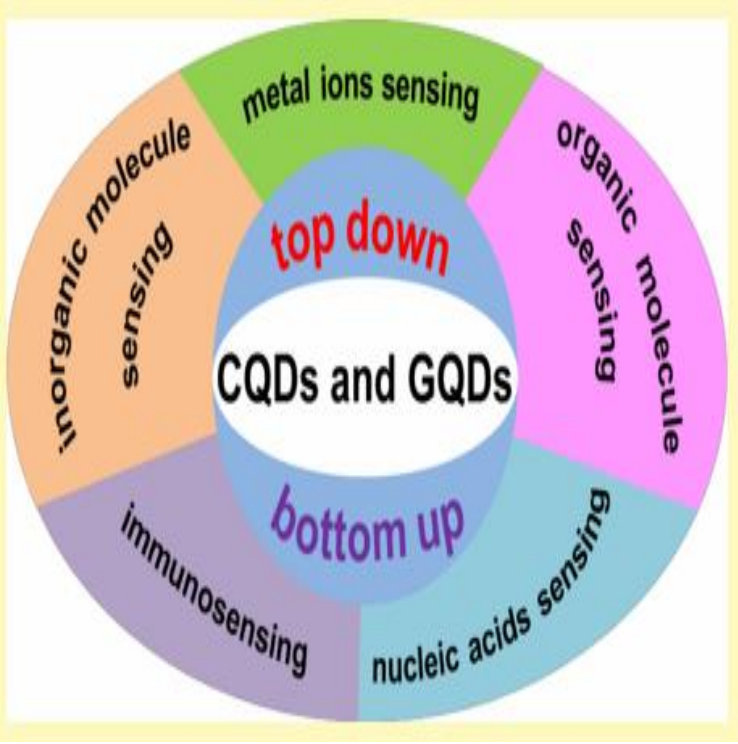

Figure 1.6: Molecules and metals sensing for CQDs and GQDs [59].

1.4.3 Drug Delivery

The important applications of CQDs' are included drug carriers, monitoring drug release, and fluorescent tracers because it is nontoxicity and biocompatibility. The non-toxicity and biocompatibility of CQDs' give evidence for using CQDs as photosensitizers in the treatment of cancer cell damage [77]. Several studies explained that CDs have been utilized for the delivery of numerous drugs in humans and animals. As previous mention, the main advantage of CDs is a carrier drug for damaged tissues due to their important properties [78]. The absorption of CDs as a carrier by cells is faster because CDs have small size and good surface area [79-81].

1.4.4 Catalysis

Carbon dots become efficient catalysts or photocatalysts when there sizes less than 10 nm. Various CQD forms have ability to absorb lights of different wavelengths due to the versatility of surface modification so that they are considered good prospects for photocatalytic applications. Photocatalytic H_2 development in UV-Vis light demonstrated enhancing by the composites of P_{25} TiO_2 modified by CDs. The separation competence of the P_{25} electron-hole pairs increase by the electron's repository in CDs. [81, 82]. [90]

1.5 Green Chemistry

It is an environmentally friendly method that can be used for various applications in chemistry [83]. The important fields that are improved by green chemistry are sustainability for living practices, economics, and development [84, 85] .

1.5.1 Principle of green chemistry

In 1998, Paul Anastas and John Warner introduced the Twelve Principles of Green Chemistry, as shown in Figure1.7. They are a guiding framework for the design of new chemical products and processes. The guiding framework of the design of new chemical products and processes can occur by principle of green chemistry [86, 87].

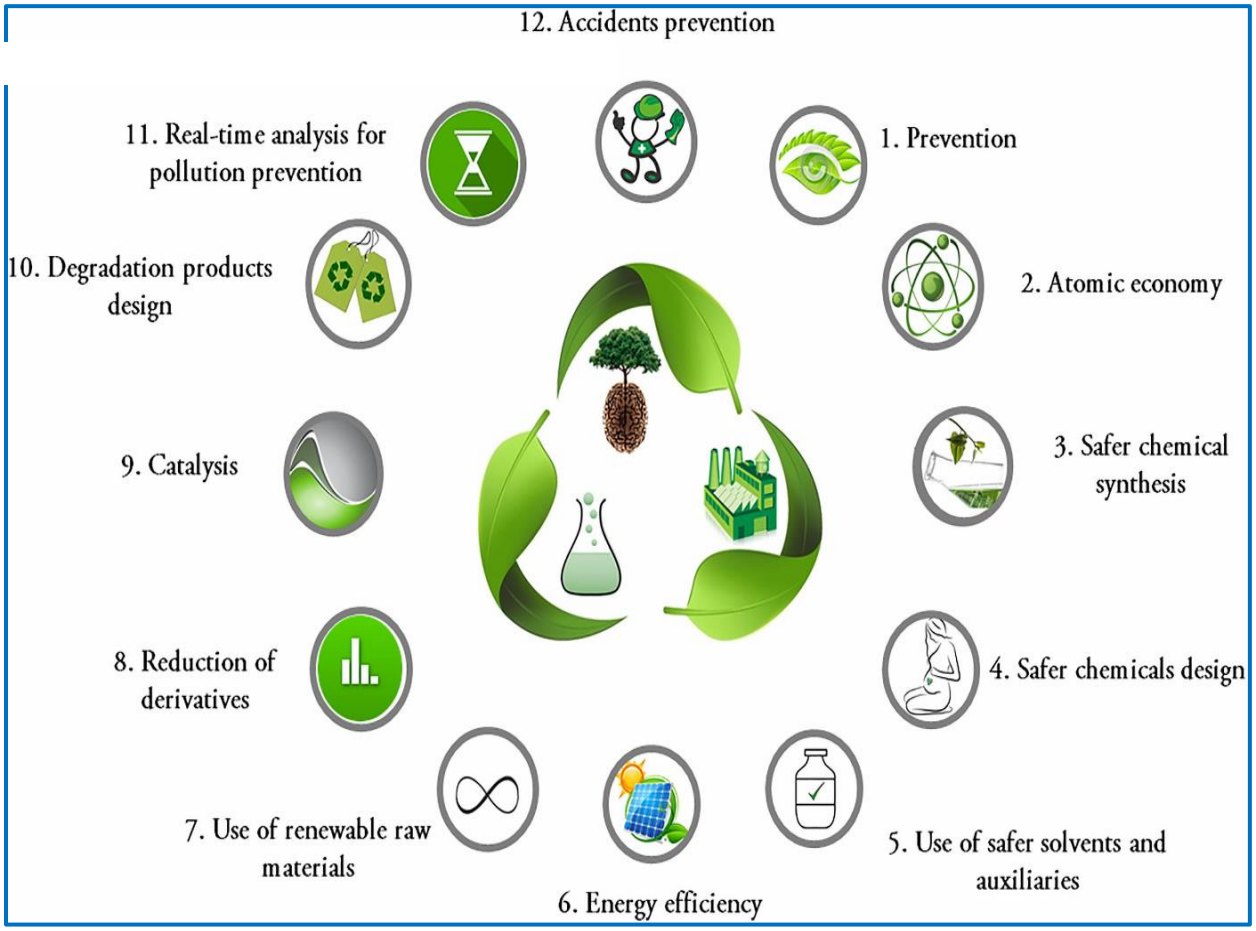

Figure 1.7: Principles of Green Chemistry proposed by Anastas and Warner [88]

1.6 Literature Review

Recently, human carbon dots (CDs) have been recognized as an invaluable materials and good area for research.

Bui Thi Hoan and et al. were synthesized highly luminescent carbon dots (C-dots) by the one-pot simple hydrothermal method directly from lemon juice using different temperatures, time, aging of precursors, and diluted solvents to control the luminescence of C-dots. They found that C-dots had strong green light emission with quantum yield in the range of 14.86 to 24.89% as a function of hydrothermal temperatures [89].

Another study is conducting for the synthesis of CDs form banana peel waste by a simple hydrothermal method. The resulting CQDs have a narrow size distribution, and the average particle size was measured as 5 nm. The nitrogen-containing and oxygen-containing functionalities on/in the surface of carbon structure were observed in the resulting CQDs. CQDs emit intense blue fluorescence under the excitation of UV-light (365 nm) with a good quantum yield of 20% without any surface passivation chemicals. Besides, CQDs exhibit excellent water solubility and excitation-dependent emission performance. Furthermore, the banana peel waste-derived CQDs had almost no photobleaching under UV-light irradiation for a long-time, suggesting that they have high photostability. Since no chemical reagent was involved in the synthesis of CQDs, the synthesized CQDs were confirmed to have lower toxicity for nematodes even at a high concentration of 200 $\mu g\ mL^{-1}$. Because of the intense fluorescence with excellent fluorescence stability and biocompatibility, CQDs can be used for bioimaging in nematodes [90].

The most interesting and appealing characteristic of CDs is the great intensity of their fluorescence emission that originates from quantum confinement (QC) occurring when the exciton's Bohr radius is bigger than the average size of CDs [91].

Clinical decision support (CDS) provides clinicians, staff, patients or other individuals with knowledge and person-specific information, intelligently filtered or presented at appropriate times, to enhance health and health care. CDS encompasses a variety of tools to enhance decision-making in the clinical workflow. These tools include computerized alerts and reminders to care providers and patients; clinical guidelines; condition-specific order sets; focused patient data reports and summaries; documentation templates; diagnostic support, and contextually relevant reference information, among other tools [92].

CDs are considered very important for many fields. Strong fluorescence quenching effect of Fe (III) on SiCQDs can be used for its selective detection among general metal ions. Specific electron transfer between SiCQDs and hydrogen peroxide enables SiCQDs as a sensitive fluorescence sensing platform for hydrogen peroxide. The subsequent fluorescence recovery induced by removal of hydrogen peroxide from SiCQDs due to formation of the stable adducts between hydrogen peroxide and melamine was taken advantage of to construct effective sensor for melamine [93]. These highly biocompatible DNA–CDs can serve as a new type of fluorescent vehicle for cell imaging and drug delivery studies. Our research may hasten the development of CDs for prominent future biomedical applications [94]. As prepared AgNPs appears yellow in color and showed the characteristic surface plasmon resonance [95].

CDs can be applied in many fields as Photocatalysis [96], luminescent device [97], chemical sensing [98] and biosensor [99]. A large variety of techniques have been developed to fabricate CQDs since their discovery. Generally, synthetic methods taken for CQD preparation are divided into two routes: top-down and bottom-up methods. The top-down approach mainly refers to the destruction or dispersion of carbonaceous macromolecules such as graphite, nano-diamonds, carbon nanotubes, and activated carbon into nano-sized CQDs by physical, chemical, or electrochemical methods, whereas in the bottom-up process, small carbonaceous molecules such as citric acid, glucose, and sucrose go through a series of polymerization and carbonization reactions by chemical reactions to produce CQDs [100-104]. There are four green method s for producing of carbon dots. These methods include hydrothermal, solvothermal, dry heating and microwave [105-111].

1.7 Aim of Study

The aims of this study are to:

- Use a green procedure to produce the CDs from Iraqi edible carrots by using available laboratory glassware and chemicals.
- Utilize the CDs to prepare the metal nanoparticles (Ag & Au).
- apply the use of CDs for bioimaging of positive and negative bacteria models.
- Use the nanoparticles to determine the values of PT and APTT.

Chapter Two
Experimental Part

2.0 Experimental

The sample collection and preparation procedures that were implemented for carrot and blood matrices have been illustrated in this Chapter, as shown in Section 2.3. The fundamental methods utilized for the synthesized of carbon dots (CDs) are described in Section 2.4. Several techniques were used to clarify the preparation and applications of CDs such as Fourier Transform Infrared FTIR Spectroscopy, Fluorescence Microscope, Proton Nuclear Magnetic Resonance (HNMR), Scanning Electron Microscope (SEM), and X-ray Photoelectron Spectroscopy (XPS).

2.1 Instrumentation

There are several types of techniques were used in this study, as shown in **Table 2.1**.

Table 2.1: Analytical techniques and tools are used in this study.

No.	Instrument	Source & Model	Places
1	UV-vis double beam spectrophotometer with a quartz cell of 1ml	UV. spectrophotometer 1800 pc (Japan) (Shimadzu)	University of Karbala, Science college
2	Scanning Electron Microscopy (SEM)	Fisher Scientific, USA	Al- Khora office in Baghdad
3	Hotplate with a magnetic stirrer	Electrothermal, England	University of Karbala, Science college
4	Centrifuge	(Germany)	University of Karbala, Science college
5	Fourier-Transform infrared Spectroscopy (FT-IR)	Shimadzu, 8400S, Japan	Iran University of Science and Technology
6	Nuclear Magnetic Resonance Spectroscopy (HNMR)	A Bruker 300 MHz, Varian, America	Iran University of Science and Technology
7	Energy dispersive X-ray Spectroscopy (EDX)	Fisher Scientific, USA	Al- Khora office in Baghdad
8	X-Ray Photoelectron spectroscopy (XPS)	Japan, Shimadzu	Iran University of Science and Technology

9	Fluorescence Microscopy	Zeiss, Germany	University of Babylon, College of Science
10	UV lamp	Japan, Shimadzu	University of Karbala, Science college
11	Thrombotimer (4-channel)	Germany	Teaching Al-Handia Hospital

2.2 Reagents and Chemicals

There are several chemicals have been used in this study to prepare the sample and drugs, as described in **Table 2.2**.

Table 2.2: Chemicals used in this study along with their manufacturers.

No.	Material	purity	Company
1	Tri- sodium phosphate $Na_3 PO_4$ (TSP)	99.99	Central Drug House (CDH) India
2	Silver nitrate $AgNO_3$	99.99	Thomas baker India
3	Gold chloride $AuCl_4.3H_2O$	99.99	Central Drug House (CDH) India
4	Potassium dihydrogen phosphate KH_2PO_4	99.99	Central Drug House (CDH) India
5	Di sodium hydrogen phosphate Na_2HPO_4	99.99	Central Drug House (CDH) India
6	Prothrombin time (PT)	99.00	Les Hautes Rives 02160, France
7	Activated partial Thromboplastin time (APTT)	99.00	Les Hautes Rives 02160, France
8	Calcium chloride KIT $CaCl_2$	99.99	Canada
9	Potassium Citrate $K_3C_6H_5O_7$	99.99	Nipigon Health Corp, Canada

2.3 Sample Collection and Preparation

2.3.1 Materials

The edible carrots were obtained from a supermarket in Karbala. Chemical materials such as Na_3PO_4 (TSP) and $NaBH_4$ were obtained from Central Drug House (P) Ltd - CDH. $AgNO_3$ was obtained from Thomas baker. $AuCl_3$ was purchased from the Central Drug House (CDH) in India, as shown in **Table 2.2**. Distilled Deionized Water (DDW) was utilized throughout this study.

2.3.2 Preparation of Samples

In general, the material samples were either solid or liquid, therefore, various procedure were used to make them ready for analysis.

2.3.2.1 Preparation of CDs

Approximately five grams of Iraqi carrot (black or orange) were cut and placed in a flask, then 25 mL of 100 mM Na_3PO_4 (TSP) solution was added to this flask. The solution was refluxed by fitting a condenser on a round bottom flask, then placed on a magnetic stirrer hot plate. After two hours of heating at 60 ± 5 °C, the solution color was changed from colorless into brown at the end. This result indicates that carbonization yields CDs. Solutions were filtered by using a filter with a size of 0.45 µm. Then, the solutions were put in a clean test tube. The obtained solutions were irradiated with an ultraviolet light at wavelength of 360 nm to confirm the synthesis of CDs [112].

2.3.2.2 Preparation of Metal Nanoparticles

In this procedure, 200, 400, and 600 µL of CDs were added to the solution of (9.8 ml) distilled deionized water including 1 mM of $AuCl_3$ or $AgNO_3$. Then, the

solutions were left unstirred for 10 or 12 hrs. The formation of NPs confirms when the color of the solution is changed by using 200 μL of CDs and 10 hrs [112].

2.3.2.3 Live Cell Imagining

Generally, the CDs were applied to make images of the live cells of Gram-negative and Gram-positive bacteria, such as E. coli and S. aureus, respectively [113]. Therefore, 1 mL of created CDs were incubated overnight along with cultured bacterial cells at condition of 0.5–0.6 optical density, wavelength at 660 nm, time of 2 hrs., temperature of 37°C in the dark. The cells were centrifuged (10 minutes at 1500 rpm), then washed three times with phosphate buffer solution (PBS). In the end, the particles were collected and suspended in a buffer solution. A blue-filtered Nikon Eclipse fluorescence microscope was used to observe the bacterial cell suspension by placing a drop of the cell on a cover slip of the microscope [112].

2.3.3 Clinical Study

2.3.3.1 Preparation of Blood Samples

In this study, blood samples were taken from ninety people (healthy and patients) (n=90) from Kerbala, and their ages ranged from 25 - 65 years, as shown in Table 2.3. All the samples were collected in the Teaching Al-Handia Hospital, laboratory of diagnosis. At least 2 mL of peripheral blood samples were collected using 3.2% sodium citrate tubes to prevent the clotting process from starting before the test [114]. Blood samples were centrifugated at 6000 rpm for 15 minutes in order to separate blood cells. Then, the mixture is left at 37°C of the period of 1-2 min. Excess quantities of ionized calcium were added to the mixtures to reduce the sodium citrate and allow clotting to start. Samples were analyzed using a Thrombotimer 4-channel instrument to determine the values of Prothrombin time (PT) and Activated Partial

Thromboplastin Time (aPTT). A plasma sample without NPs was used as a control. Neoplastin CI plus 5 kit was used to determine PT, while C.K. prest 2 reagent calcium (50 µL) was used to measure aPTT [115]. In this part, the coagulation factors have been determined, as shown in the following sections.

Table 2.3: Study populations for different blood samples collected from Karbala, Iraq.

Health Status	Gender	Smoking Activity	No. of Samples
Healthy	**Male**	**Smokers**	**15**
		Non-smoker	**7**
		Total	**22**
	Female	Smokers	**0**
		Non-smoker	**8**
		Total	**8**
	Total	Smokers	**15**
		Non-smoker	**15**
		Total	**30**
***Patient**	Male	Smokers	**21**
		Non-smoker	**15**
		Total	**36**
	Female	Smokers	**9**
		Non-smoker	**15**
		Total	**24**
	Total	Smokers	**30**
		Non-smoker	**30**
		Total	**60**
Total	**Male**	Smokers	**36**
		Non-smoker	**22**
		Total	**58**
	Female	Smokers	**9**
		Non-smoker	**23**
		Total	**32**
	Total	Smokers	**45**
		Non-smoker	**45**
		Total	**90**

***They have coagulation and take Aspirin.**

2.3.3.2 Prothrombin Time test (PT)

The PT test is utilized to monitor patients taking drug and to identify clotting problems. This test is timed from the addition of the $CaCl_2$ until the plasma clots within the 11 -15 second range [116].

2.3.3.3 Partial Thromboplastin Time test (PTT)

The activated PTT represents the required time for a clot. Generally, the time for clot is equal to 35 seconds [117].

2.4 Instrumentation

The following subsections show the analytical techniques used in this study.

2.4.1 Fourier-transform infrared spectroscopy (FTIR)

The IR range of the spectrum includes radiation with wavelengths ranging from 10^3 to 10^5 nm. This region is divided into three parts, namely near-, mid-, and far-IR, as shown in **Table 2.4** [118].

Table 2.4: IR spectral regions.

Region	Wavelength (λ), μm	Wavenumber (ν), cm^{-1}	Frequencies (ν), Hz
Near	0.78 to 2.5	12800 to 4000	$3.8x10^{14}$ to $1.2x10^{14}$
Middle	2.5 to 50	4000 to 200	$1.2x10^{14}$ to $6.0x10^{12}$
Far	50 to 1000	200 to 10	$6.0x10^{12}$ to $3.0x10^{11}$
Most used	2.5 to 15	4000 to 670	$1.2x10^{14}$ to $2.0x10^{13}$

In this region, absorption of radiation can occur by characteristic organic molecules resulting in vibrational, rotational, and blending modes, but the molecule will remain in its ground state.

The main use of FTIR with NMR and MS revolutionized organic chemistry due

to it decreased the time to confirm compound identification 10- 1000-fold. **Figures 2.1 and 2.2** show the general Scheme which examines the functional groups existing along with frequency region - 3600 cm^{-1} to 1200 cm^{-1}.

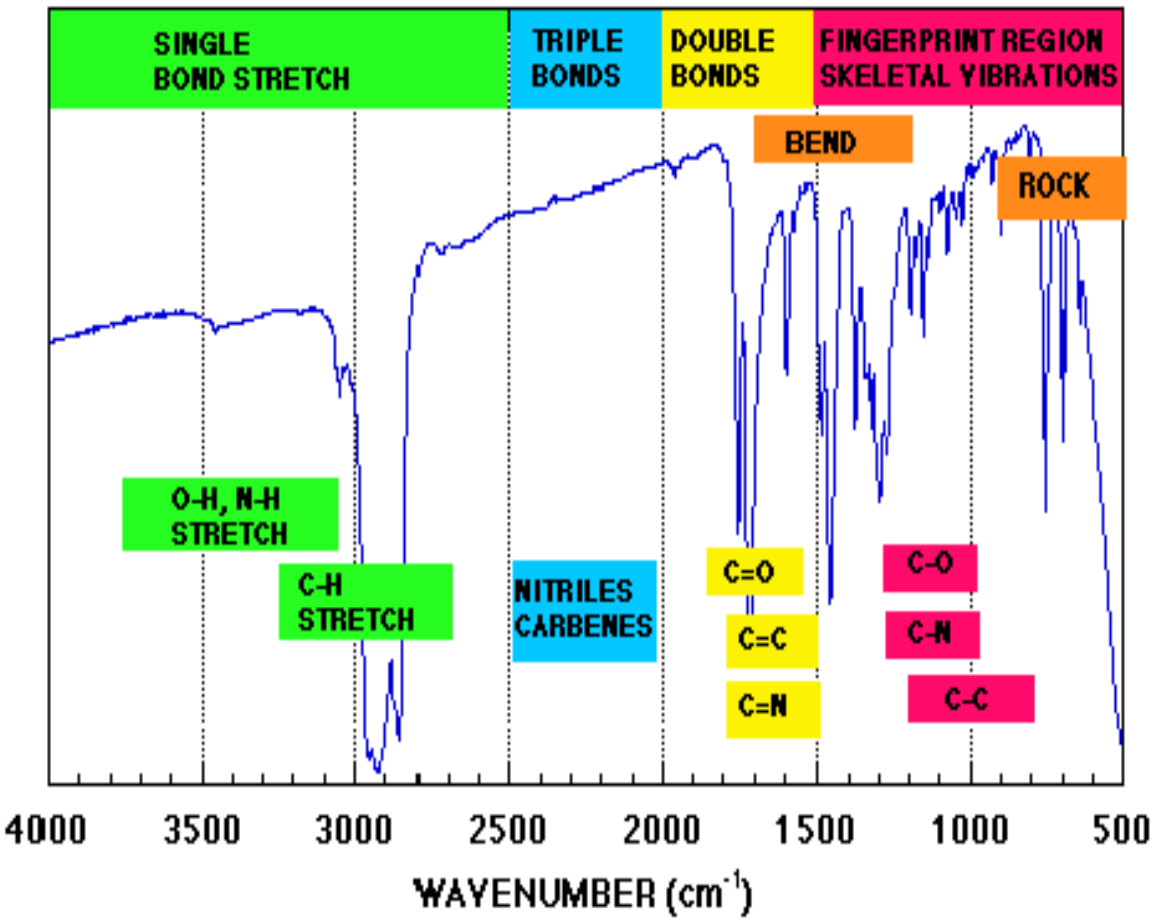

Figure 2.1: Functional groups are present at group frequency regions [119].

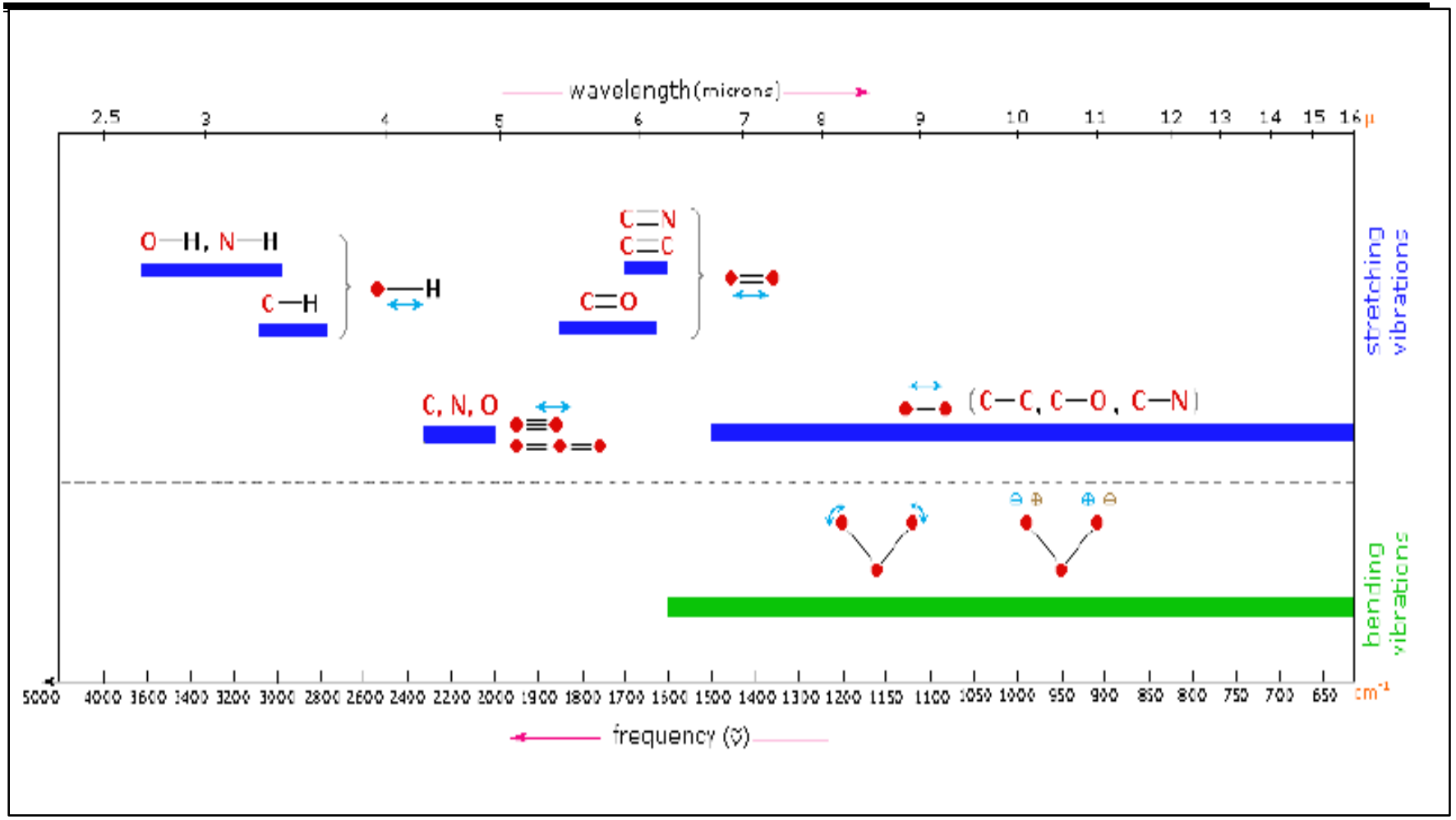

Figure 2.2: Group frequency regions at FT-IR chart [120].

2.4.2 X-ray Photoelectron Spectroscopy

X-ray photoelectron spectroscopy (XPS) is one of the most used surface analysis techniques. This technique is usually used to analyze the materials [121]. In XPS, the sample is irradiated with soft x-rays (energies lower than ~6 keV), and the kinetic energy of the emitted electrons is analyzed, as shown in **Figure 2.3**. The emitted photoelectron is the result of the complete transfer of the x-ray energy to a core-level electron [122].

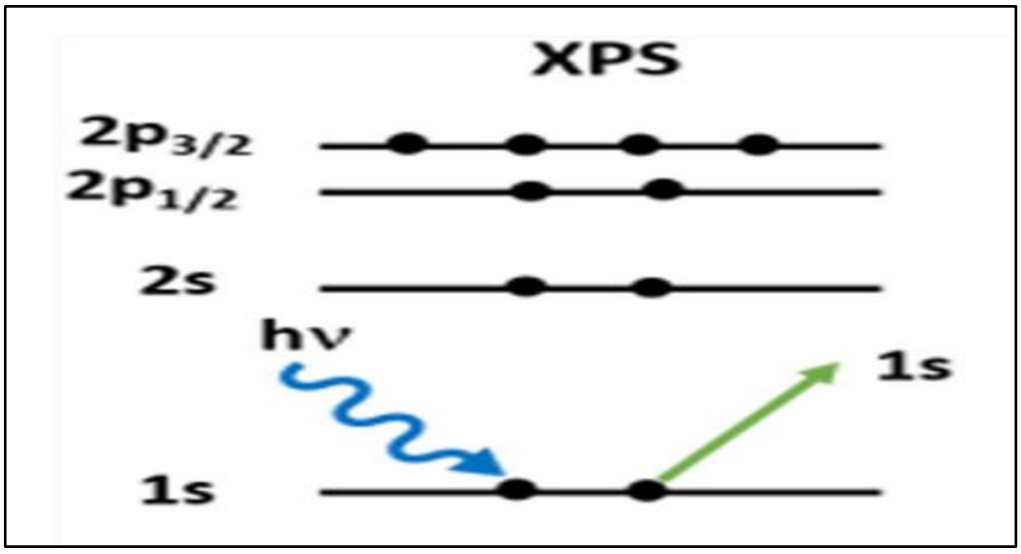

Figure 2.3: The emission of a photoelectron [120].

Figure 2.4 show the XPS survey spectra of polyethylene terephthalate (PET). This Survey can use to obtain basic elemental information and to look for the presence of unexpected elements in the sample [122].

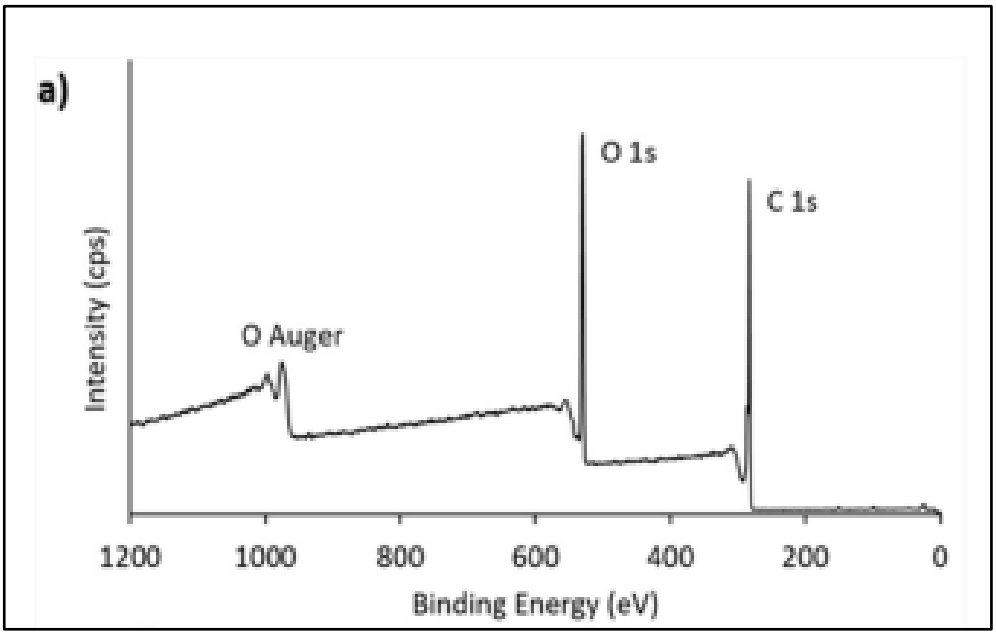

Figure 2.4: XPS survey spectrum for several elements [120].

2.4.3 Proton Nuclear magnetic resonance (H NMR) spectroscopy

This technique is used to determine the energy absorbed due to the changes in the nuclear spin state. The application of NMR spectroscopy to the study of proteins and nucleic acids has provided unique information on the dynamics and chemical kinetics of these systems. Furthermore, this technique can also provide structural information for the solutions of nucleic acids and proteins. Generally, 1H and 13C are the significant NMR functional nuclei in organic chemistry, but not all nuclei are suitable for NMR [123].

The location (chemical shift, δ) and shape (splitting or multiplicity) of the NMR signals provides valuable information about the chemical environment of the nuclei [124], as shown in Figure 2.9.

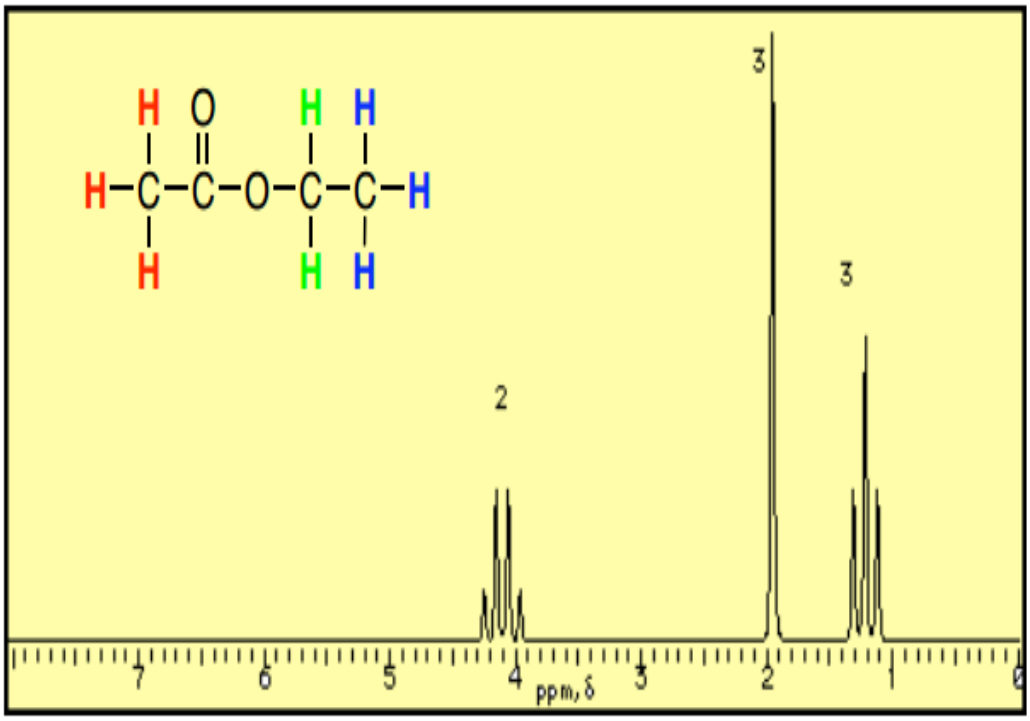

Figure 2.5: The location (chemical shift, δ) and shape (splitting or multiplicity) of the NMR signals.

2.4.4 Scanning Electron Microscopy (SEM)

Scanning Electron Microscopy (SEM) is a useful technique for the following purposes [125]:

The surface features of an object or how it looks, its texture (Topography);

The shape and size of the particles making up the object (Morphology);

- The elements and compounds that the object is composed of and the relative amount of them (Morphology); and
- How the atoms are arranged in the object (Crystallography).

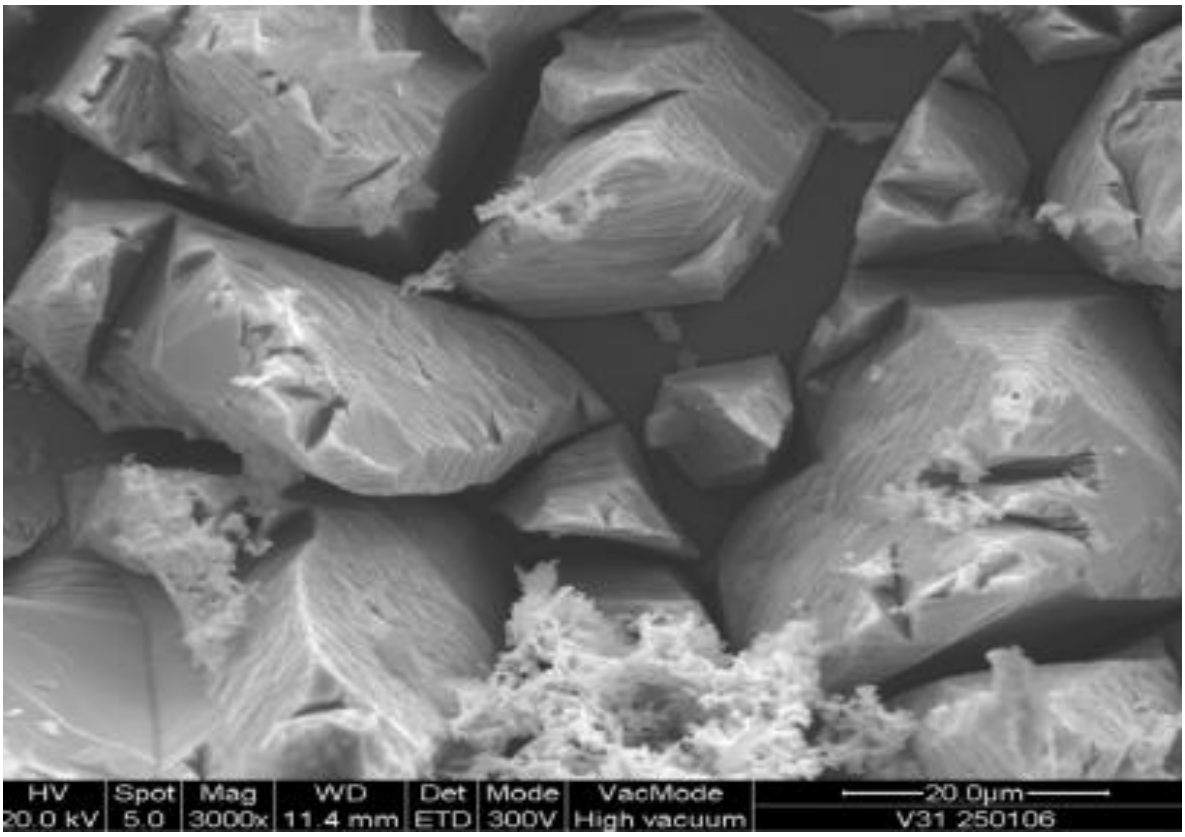

Figure 2.6: SEM image.

2.4.4.1 Effect of Accelerating Voltage

the resolution is improved with increased accelerating voltage.

2.4.4.2 Effect of Working Distance

The depth of field increases with working distance.

2.4.4.3 Effect of Spot Size

The depth of field is improved in the lower spot size image.

2.4.5 Energy dispersive X-ray spectroscopy (EDX)

It is one of the analytical techniques that allow the chemical characterization and elemental analysis of materials. In this technique, a sample will excite by energy and some of this energy will dissipate by ejecting a core-shell electron. Then, one of the outer-shell electrons has a higher energy to fill its place. This will lead to the release of the difference in energy as an X-ray that has a typical spectrum depending upon its atom of origin. The main advantage of this analysis is to use to carry out the compositional analysis for the volume of the sample that was excited by the energy source [126]. Therefore, qualitative analysis (position of the peaks in the spectrum) and quantitative analysis (intensity of the signal corresponds to the concentration) can apply to the elements in the samples.

Chapter Three
Results and Discussion

3.0 Introduction

In this chapter, the results of the synthesis of CDs and its applications in different fields have been described. The results of FT-IR, H NMR, EDX, SEM, and XPS were reported and discussed for prepared CDs, as shown in Sections 3.1.1.1-3.1.1.5. For application purposes EDX, and SEM have also been performed for silver and gold nanoparticles, as shown in Sections 3.1.2.1-3.1.2.2. In addition, Fluorescence Microscope was used to identify the ability to use CDs to image the live cells, namely Gram-positive bacteria S. aureus and Gram-negative bacteria, E. coli., as shown in Section 3.1.2.1. Furthermore, the CDs were also used to prepare the metal nanoparticles, namely for silver and gold, as described in Section.

3.1 Results and Discussion

The findings of CDs were divided into two parts, synthesis of CDs and its applications.

3.1.1 Synthesis of Carbon Dots (CDs)

In this synthesis, a simple procedure was used by mixing the edible carrot and aqueous trisodium phosphate (TSP), then the mixture was refluxed in order to prepare blue color luminescent carbon dots (CDs). Generally, heating carbohydrates by using a strong alkali such as NaOH is recognized for preparing CDs [127]. In this study, trisodium phosphate (TSP) was replaced instead of sodium hydroxide due to sodium hydroxide can make important damage when not managed safely. In addition, using a 1% solution of trisodium phosphate is adequately alkaline with pH 12 [128]. It was found that the carrot materials recognize a rich source for free sugars [129]. Therefore, it was used to synthesize CDs by heating it for 3 - 5 hours in water to generate a pale-yellow solution of carrot extract (CE). A previous study has shown

that the aqueous solution of carrot extract exposed the existence of amino acids and carbohydrates. The brown color of the solution is referred to the synthesize of CDs throughout the method of carbonization [130].

A 3-D fluorescence technique was used to determine the optimal peak and wavelength of excitation and emission for CDs, as shown in Figure 3.1. It was found that the emission spectrum of CDs at 450 nm is varying from the excitation spectrum wavelength, as presented in Figure 3.2. This represents the typical emission of the blue luminescent fluoroiphore, as reported in the literature [130]. Figure 3.2 explains that the 2-D excitation spectra showed a maximum wavelength of 365 nm by setting the emission maximum at 450 nm [131].

Several techniques were used to produce luminescent CDs such as Fourier-transform infrared (FTIR), Scanning Electron Microscopy (SEM),1H NMR spectroscopy, X-ray photoelectron spectroscopy (XPS).

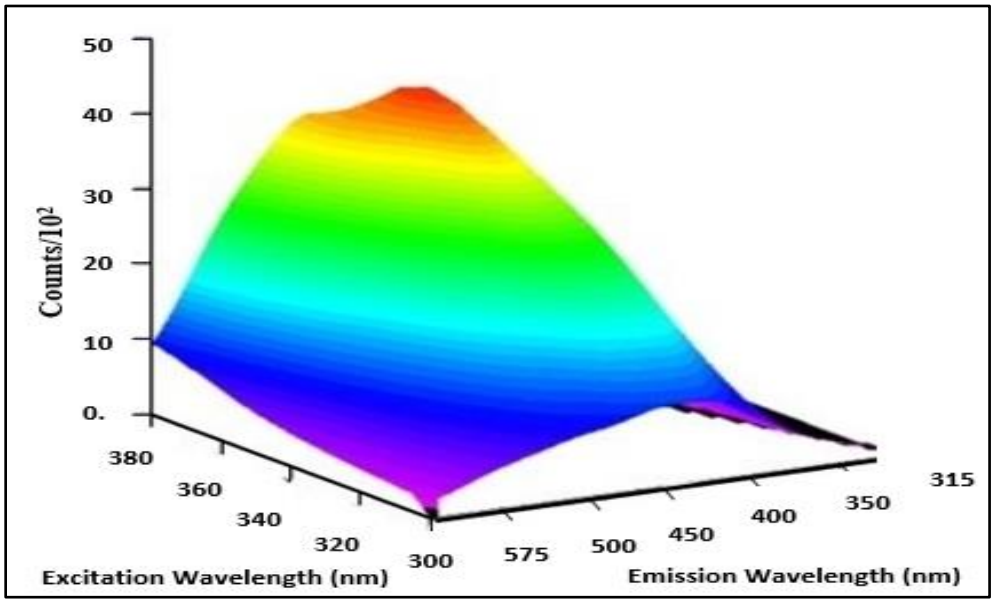

Figure 3.1: 3-D fluorescence spectra of CDs

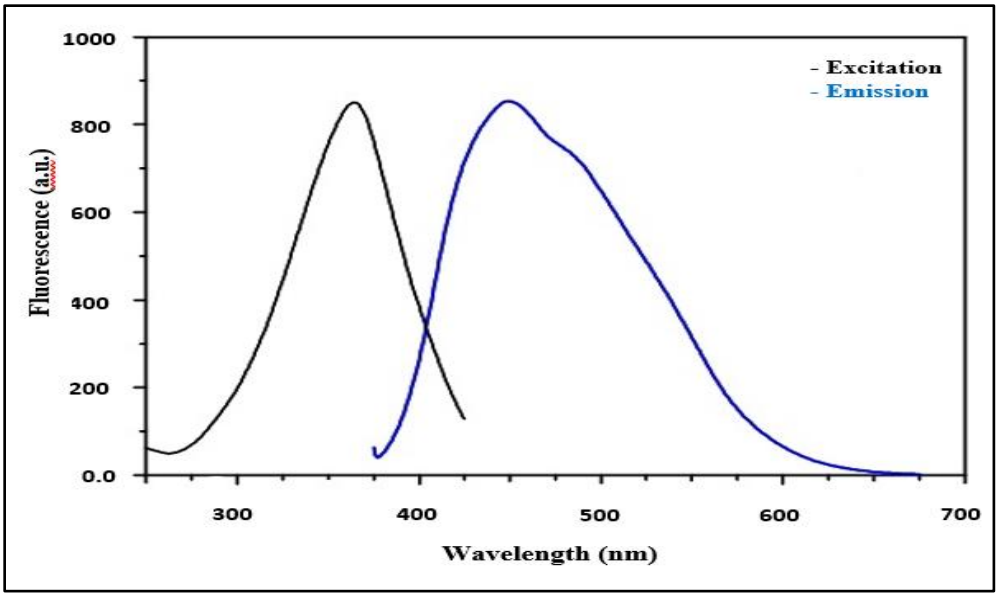

Figure 3.2: Excitation and emission spectra of CDs.

3.1.1.1 FT-IR analysis of Carbon Dots

The results show that the Carbon Dots (CDs) produced during the carbonization process. This result is suggested that there are numerous functional groups working to protect the CDs. These functional groups were studied using FTIR spectrum, and results of CDs and Carrot Extract (CE) obtained from orange carrots are shown in Figures 3-3 and 3-4. The peaks corresponding to -OH (broad) and -NH (stretching) were seen at 3236 and 3259 cm^{-1}, respectively. The peaks associated to -CH (stretching) were found at 2916, 2850 cm^{-1} and 2924 cm^{-1}. On the other hand, the peaks associated with bending vibrations of -CH were found at 1396 and 1400 cm^{-1}. The peaks corresponding to pyranose form of sugar were found at 1045 and 1072 cm^{-1}. The peaks at 1566 and 1585 cm^{-1} is associated with C=C (vibrations). The results indicate that CDs have a sharp peak at 1566 cm−1 in comparison to CE. On the other hand, there are two peaks, namely 1728 and 1647 cm^{-1} were found to corresponding to -C=O in the carrot extract, while these peaks were lost in CDs. This result indicates that the carbonyl group-including phytonutrients suffer

carbonization and produce more sp2 hybridized carbon. Figure 3.5 indicates that the peaks associated with the functional groups are approximately found in CE and C

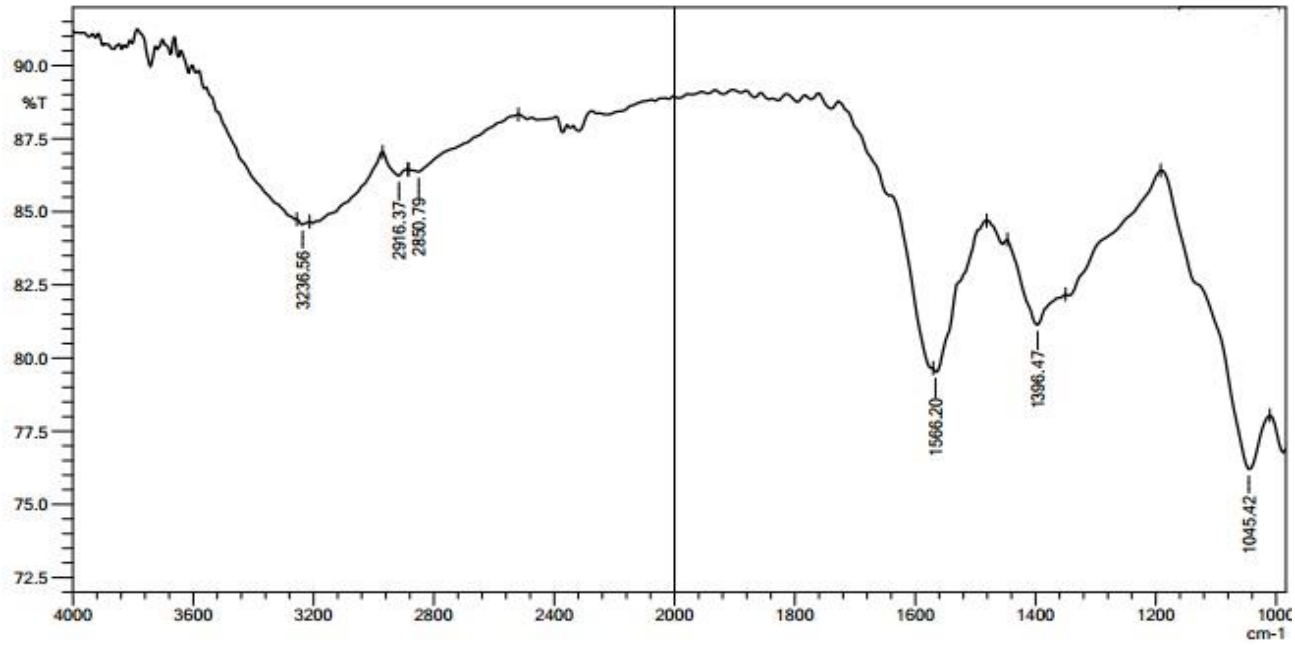

Figure 3.3: FTIR spectra of carbon dots (CDs) extracted from orange carrot.

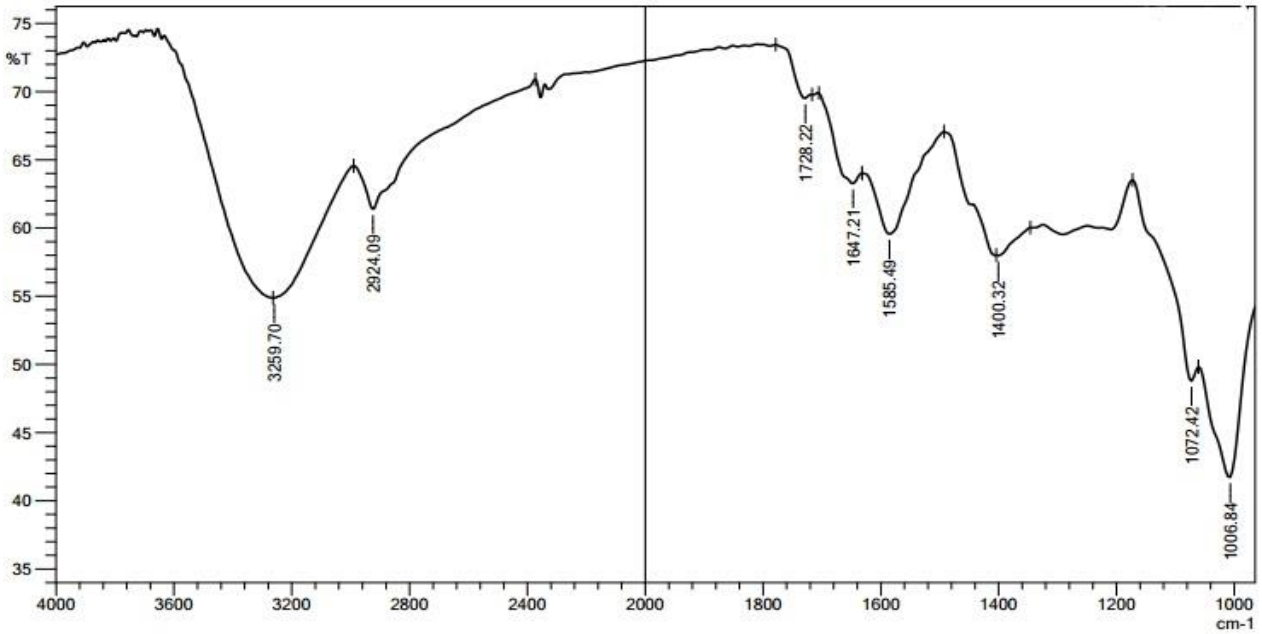

Figure 3.4: FTIR spectra of orange carrot extract (CE).

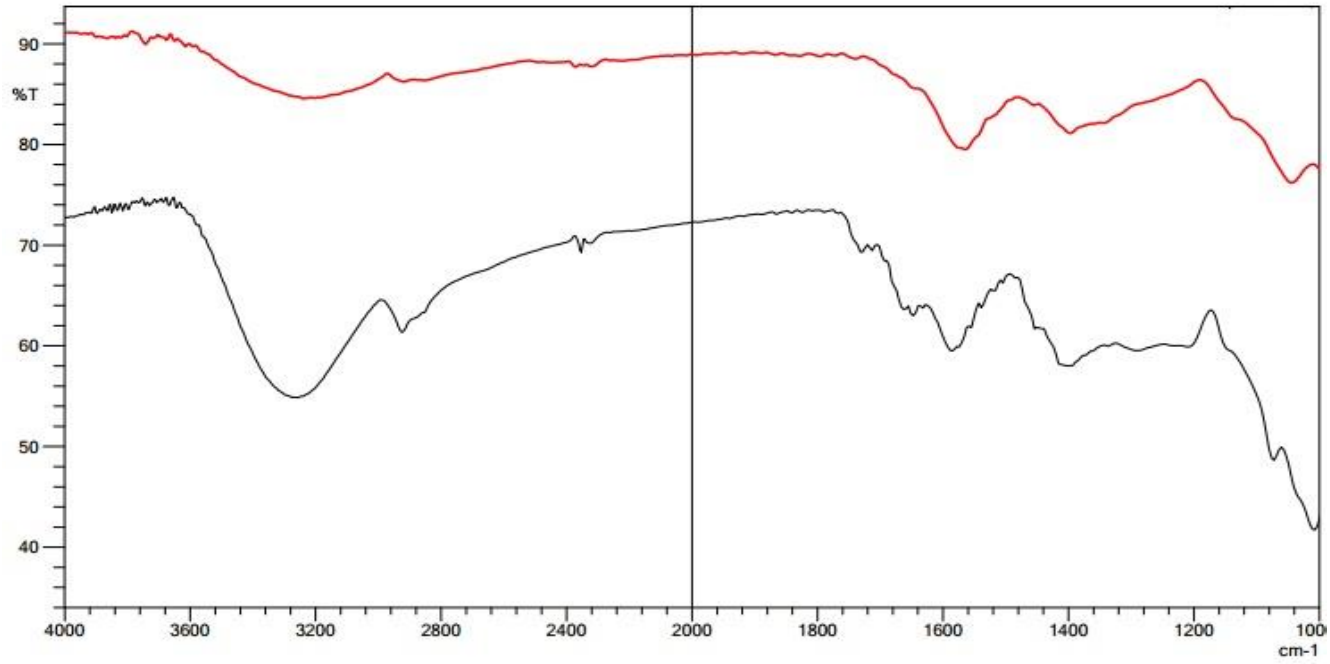

Figure 3.5: FTIR spectrum of orange CE (black color) and CDs (red color).

3.1.1.2 X-ray photoelectron spectroscopy (XPS)

The X-ray photoelectron spectroscopy (XPS) was used to analyze the functional group found on the CDs surface as shown in the XPS spectrum (Figures 3.6 and 3.10). The elemental information and unexpected elements in the sample have been determined by using the XPS spectrum. It was found that the CDs sample contains carbon and oxygen as expected [132]. Figure 3.6 shows the XPS survey spectrum of CDs which is including two peaks (binding at 285 and 535 eV) associated with C1s and O1s, respectively. The spectrum of C1s XPS is showed three carbon type at 284, and 286 eV, which can be associated with C-C/C=C, and C-O, respectively. The results are agreement with those reported by using FTIR study and indicate that C=C may be result in a series of emissive traps between π and π* to yield blue-emitting CDs [132].

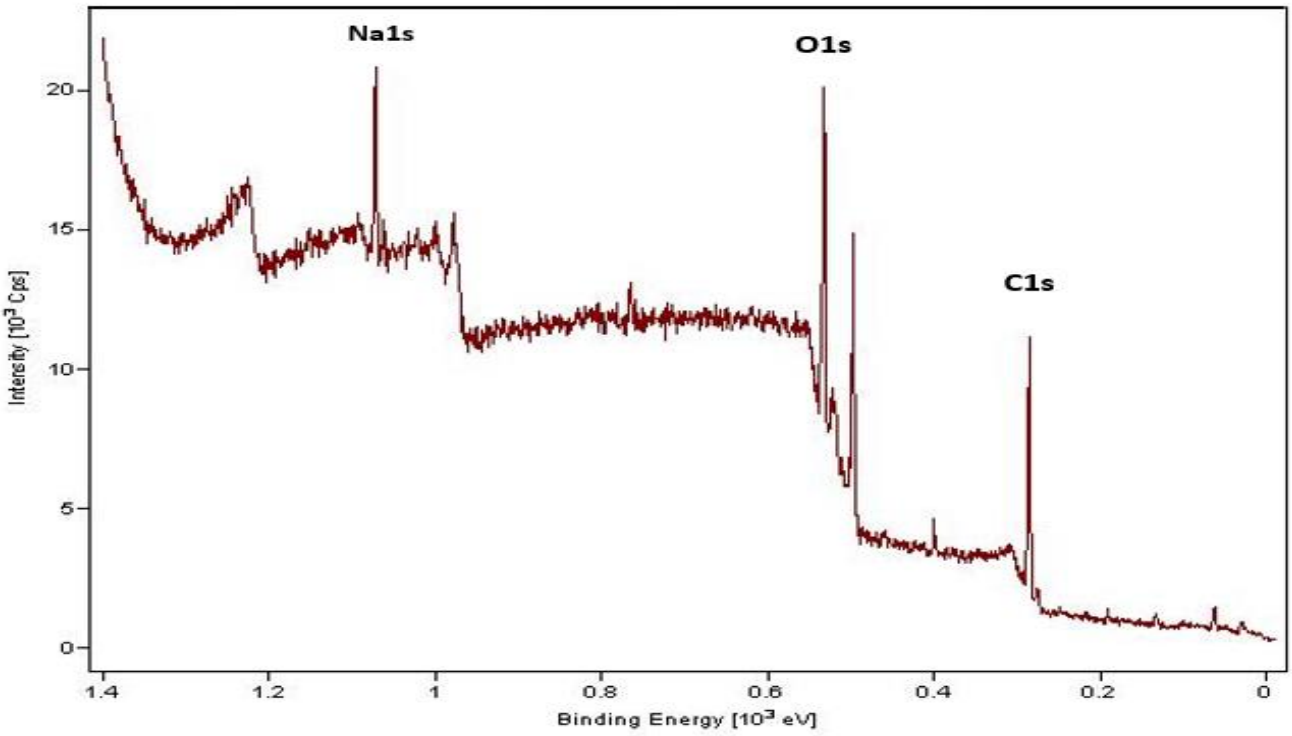

Figure 3.6: XPS spectrum of orange carrot CDs

3.1.1.3 Energy Dispersive X-Ray Spectroscopy (EDX)

Energy-dispersive X-ray analysis (EDX) is a method utilized for the determination of nanoparticles (NPs) by SEM. In this method, the NPs are measured by activation utilized an EDS X-ray spectrophotometer, which is presented in modern SEM [133]. The results confirmed that the carbon is found in the samples. Figure 3.7 (a) shows a peak around 0.25 keV is the binding energy of the carbon in CDs NPs. Therefore, an EDX spectrum was used to identify carbon inside the NPs. The spectrum of X-ray (EDX) confirms the presence of C (24.3 Wt%), N (3.1 Wt%), O (30.0 Wt%), Na (13.6 Wt%), Mg (0.5 Wt%), Al (0.2 Wt%), Si (19.9 Wt%), P (1.9 Wt%), Cl (0.5 Wt%), K (1.5 Wt%), Ca (4.1 Wt%), Fe (0.2 Wt%), and Ni (0.1 Wt%) in the carrot composite (Figures 3.7 (b) and 3.7 (c)**).**

(a)

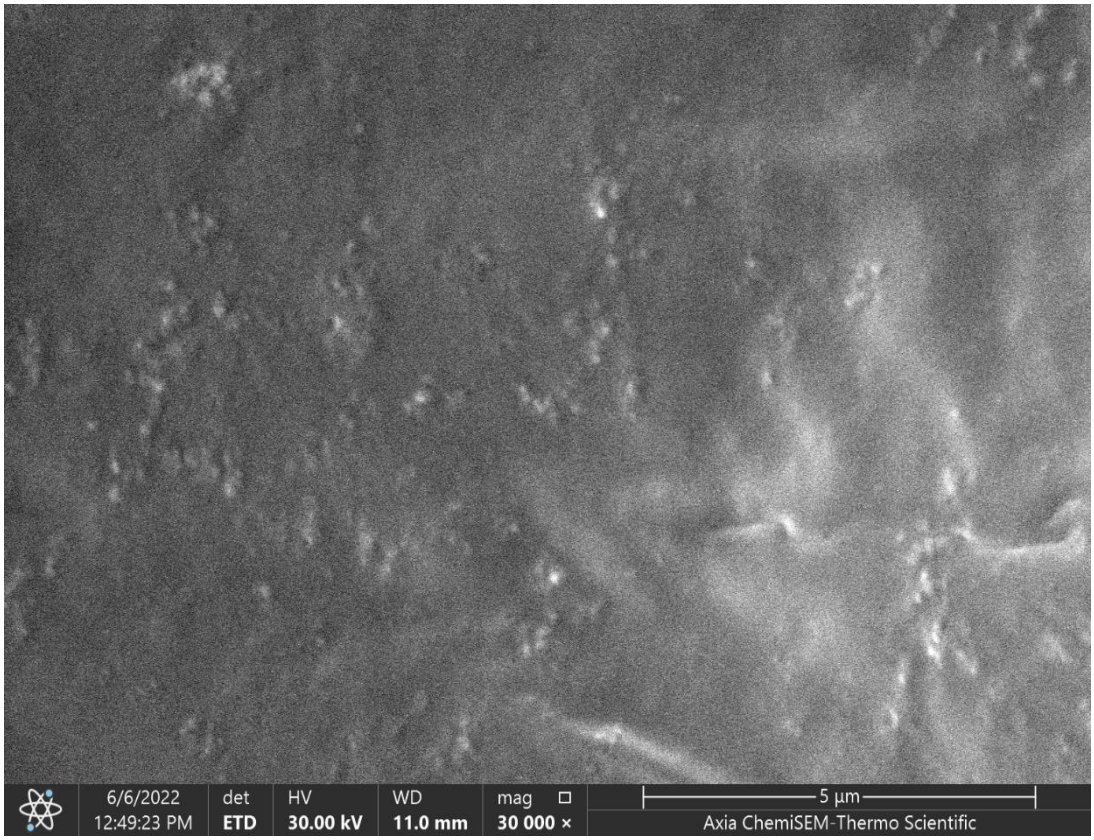
6/6/2022
12:49:23 PM
det
ETD
HV
30.00 kV
WD
11.0 mm
mag
30 000 ×
5 µm
Axia ChemiSEM-Thermo Scientific

(b)

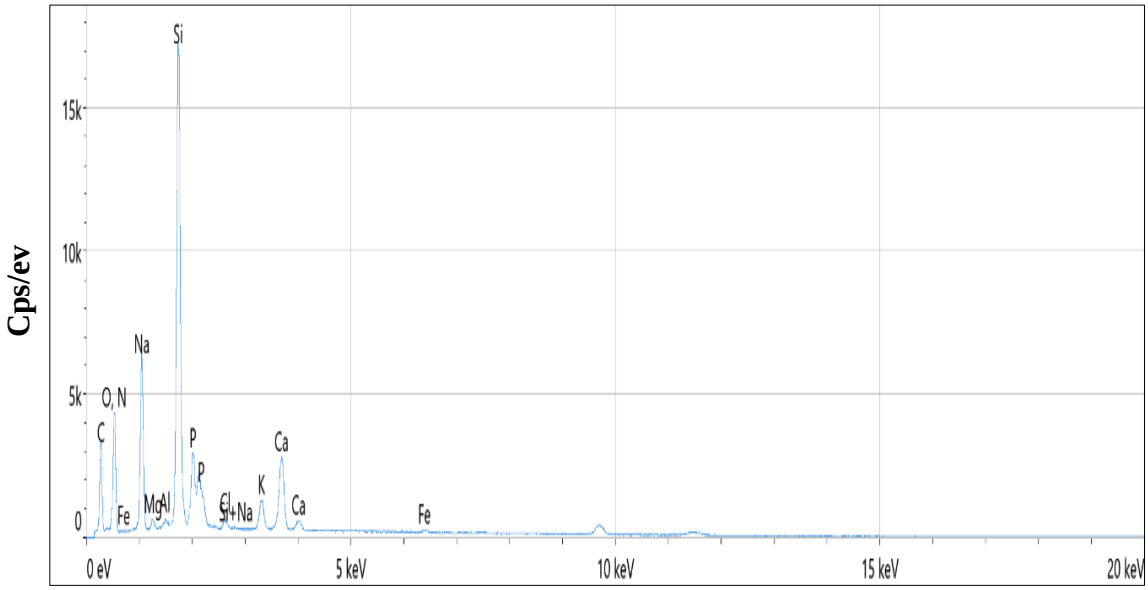
Cps/ev
15k
10k
5k
0
Si
Na
O, N
C
Fe
Mg
Al
P
P
Si+Na
K
Ca
Ca
Fe
0 eV
5 keV
10 keV
15 keV
20 keV

(c)

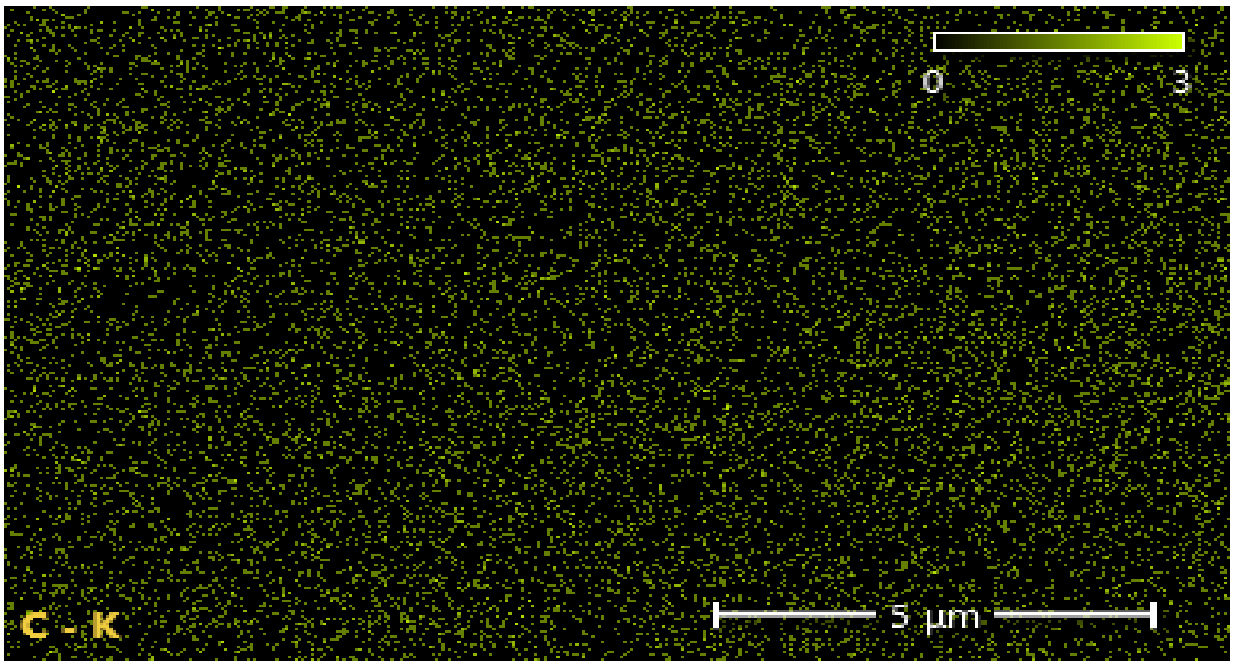

Figure 3.7: (a) SEM image, (b) EDX analysis, and (c) Elemental mapping analysis of CDs particles by using an orange carrot.

3.1.1.4 1HNMR spectra

In the last few decades, important efforts of research have been spent to understand the mechanism of the formation of CDs [131, 134, 135]. Generally, the suggested mechanisms of bottom-up synthesis depend on the following steps: (i) pyrolysis of carbon-rich precursors at elevated temperatures; which leads to (ii) carbonization and nucleation; followed or accompanied by (iii) surface passivation with stabilizing agents [136].This is suggested that any carbohydrate-containing C, H, and O in the ratio of 1:2:1, where H and O exist in a form that allows dehydration under hydrothermal conditions, can be used for the preparation of CDs, as shown in Figure 3.8.

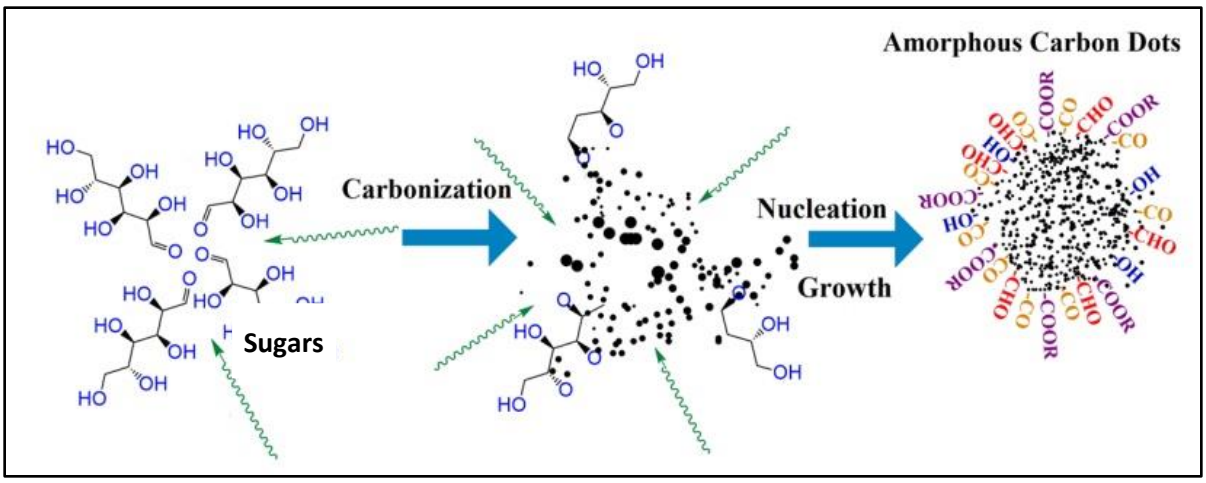

Figure 3.8: Schematic diagram of the mechanism of formation of self-passivated CDs from sugars [131].

A Bruker 300 MHz apparatus was used to measure the 1HNMR spectrum. The 1HNMR spectra of Carbone dots (CDs) and carrot extract (CE) are shown in Figure 3.9. It was found that signals found for 3 and 4 ppm in the CE disappeared completely in the case of carbon dots. This result confirms that sugars have suffered from the carbonization process. The resonance associated with the protons involved in methyl and methylene is found between 1 and 2 ppm. But the resonance of 2.5 ppm is corresponding to the protons connected to carbonyl groups. Comparison between CE and CDs showed the peak at 2.2 ppm disappears completely in CDs compared CE. The main reason is that the carbonyl residues disappeared, and the aromatic clusters are formed. Based on the above evidence and reports from others, the phytonutrients suffer from the two process such as dehydration and decomposition in the presence of sodium phosphate and the yields formed may suffer polymerization to form clusters[134, 135]. Once these clusters reach the critical supersaturating concentration, they will undergo carbonization and aromatization, resulting in a nuclear burst of aromatic clusters to produce blue color-emitting CDs.

(a)

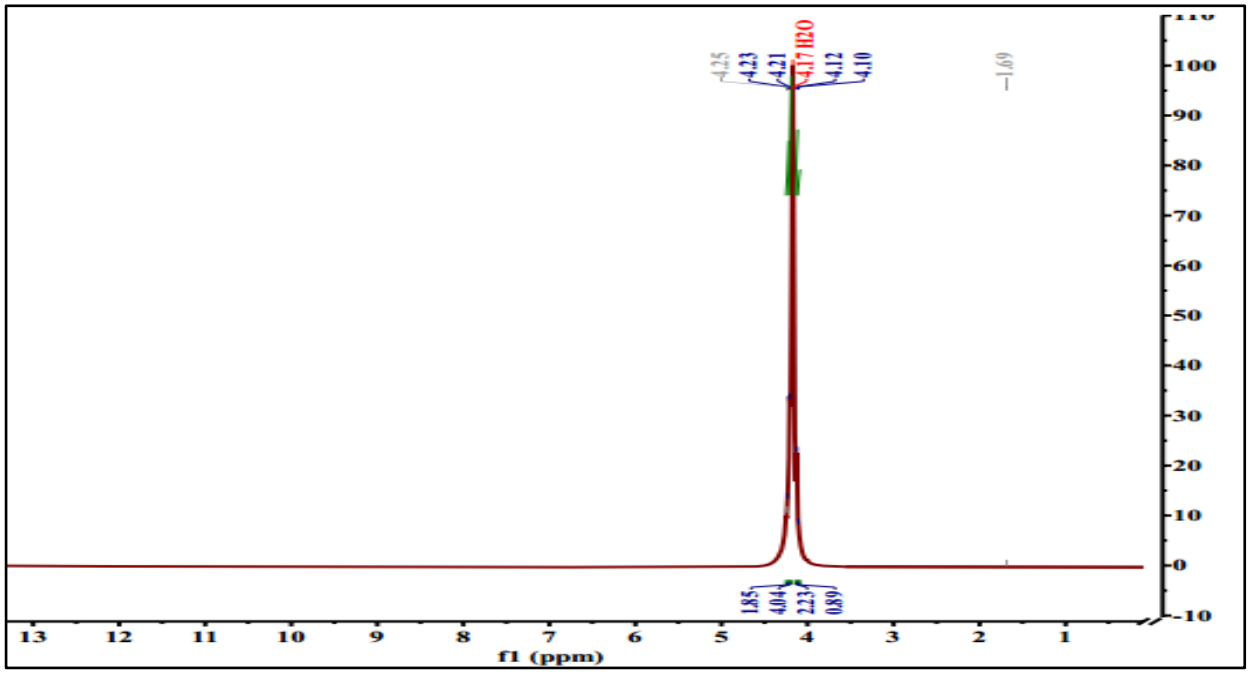

(b)

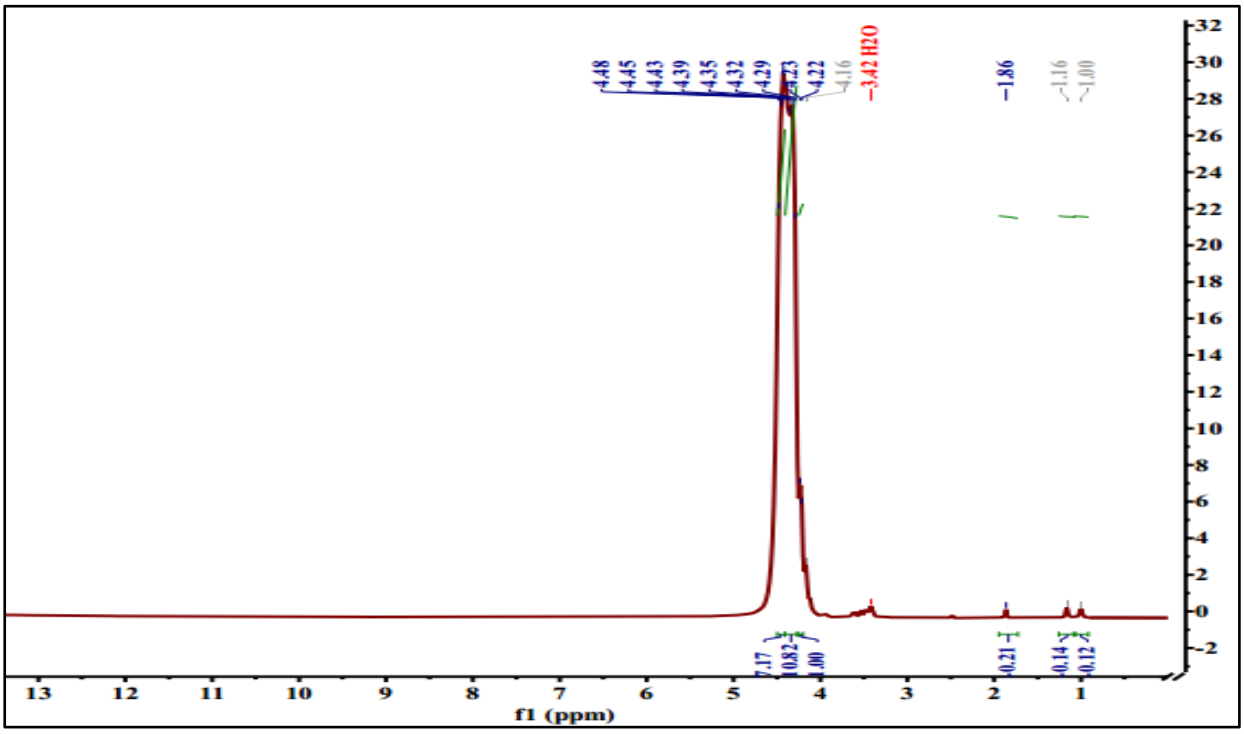

Figure 3.9: 1H NMR spectra of (a) carbon dots and (b) carrot extract

3.1.1.5 Scanning Electron Microscopy (SEM)

A scanning electron microscope (SEM) was used to produce images of CDs samples by scanning the surface with a focused beam of electrons. These electrons will interact with atoms in the CDs sample, producing various signals that contain information about the surface topography and composition of the sample. Figure 3.10 shows the Scanning electron microscope (SEM) and High-Resolution SEM images of pure carbon dots (CDs). The results show that the size of CDs obtained from carrot was found in the range of 6.40 – 25.76 nm, as shown in Figure 3.10 (a). The SEM morphology of the synthesized of CDs is shown that the carbon dots are approximately spherical, uniform in distribution and size, and it might have a strong agglomeration effect, as presented in Figure 3.10 (b).

(a)

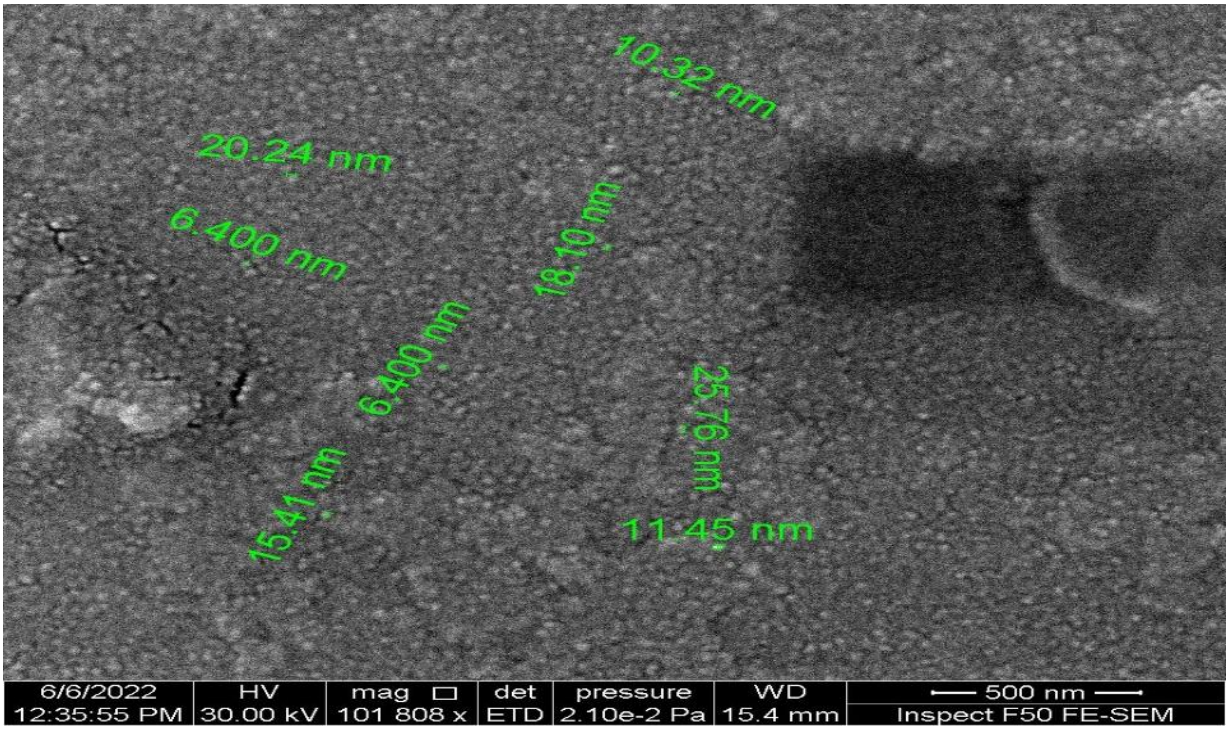

(b)

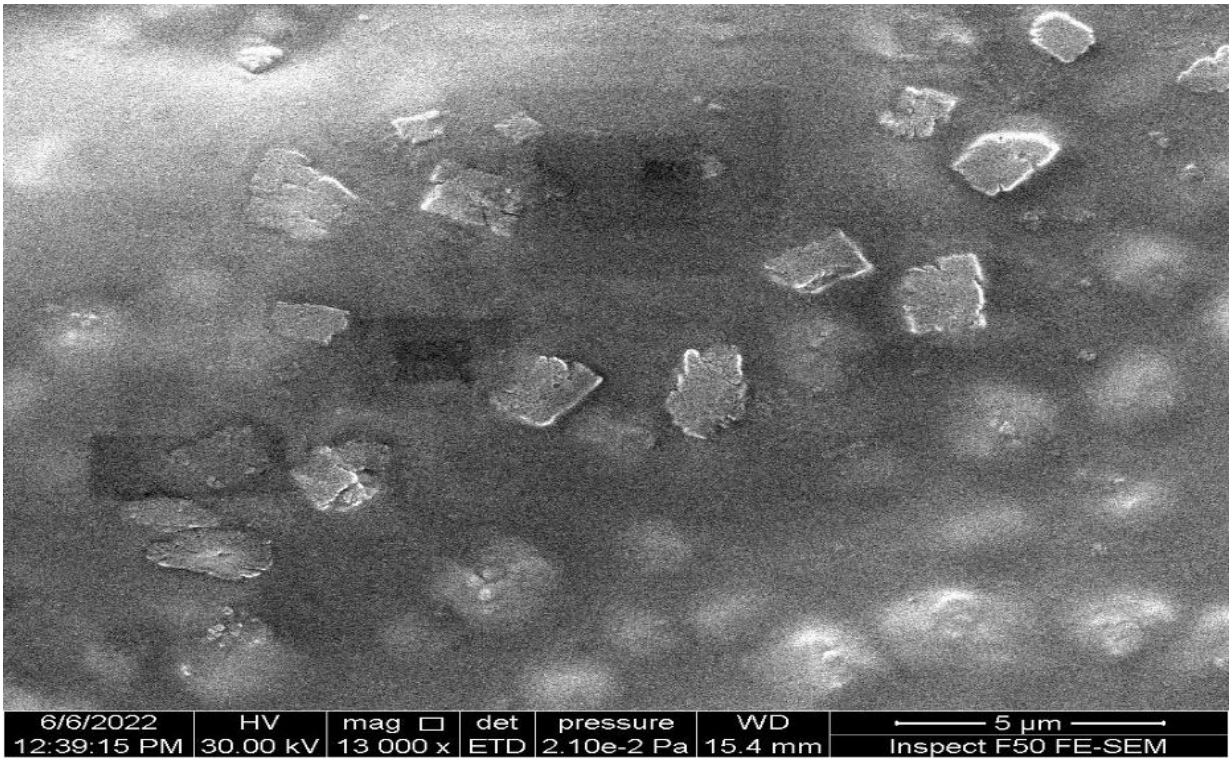

Figure 3.10: SEM images of CDs: (a) SEM image: and (b) High-resolution SEM image.

3.1.2 Applications

3.1.2.1 Live cell imagining

In this research, the probability of applying CDs to imaging live cells by fluorescence microscopy has been investigated. Therefore, two types of organisms were selected for this bioimaging study namely, E. coli and S. aureus. The bacteria cells were pre-exposed to CDs and washed by using PBS buffer and drop-cast onto a cover slip. As a result, in the viewing by using a blue filter through a fluorescence microscope, luminescent blue cells have been observed. It was found that E. coli and S. aureus were found to have clearly visible rod-shaped morphology and cocci-shaped morphology, respectively through labeling with blue fluorescence CDs, as shown in Figure 3.11. Significantly, CDs labels both E. coli and S. aureus

nevertheless of their variance in the outer membrane constituents. However, further research is needed to outline the mechanism of labeling.

(Bright field) **(Fluorescence)**

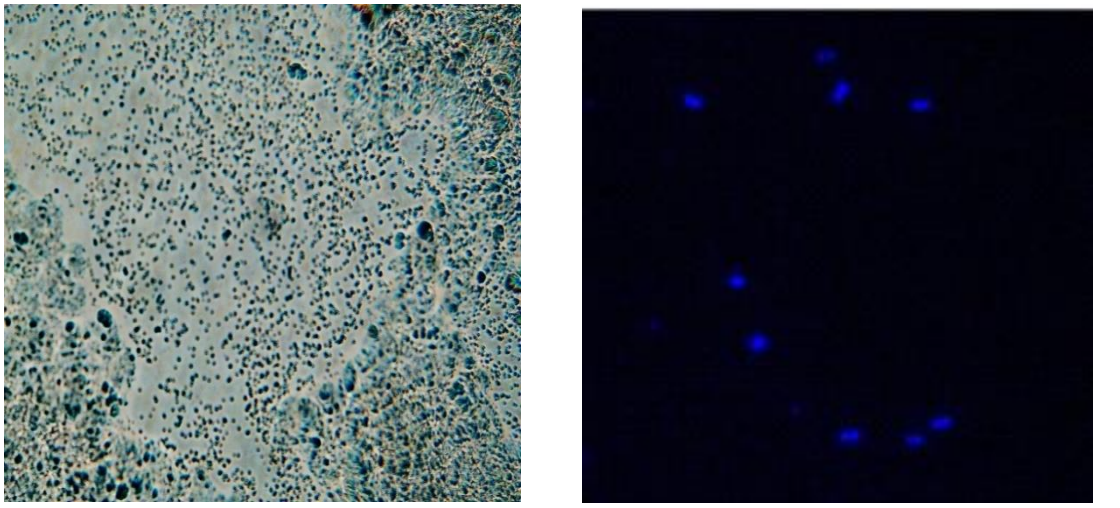

(a)

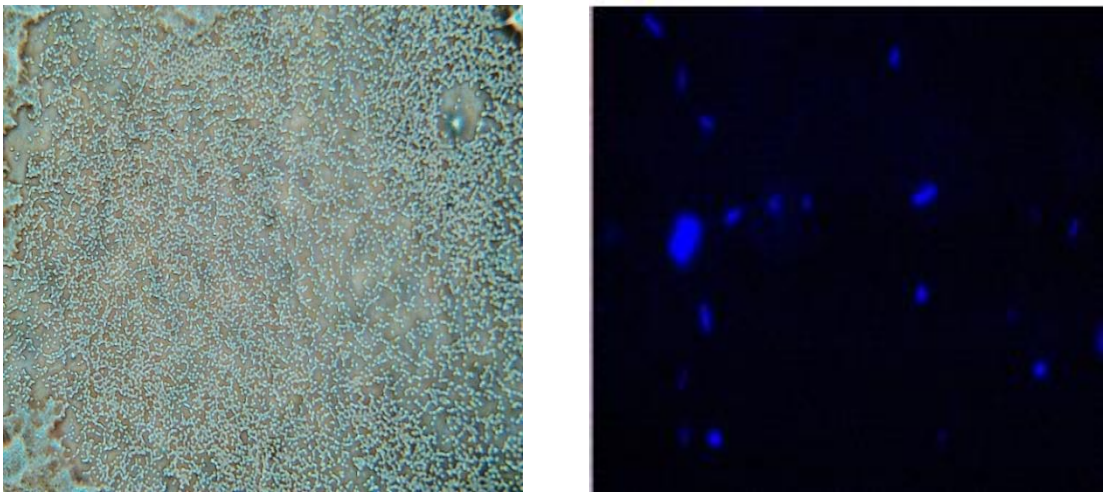

(b)

Figure 3.11: Fluorescence pictures of (a) E. coli and (b) S. aureus cells marked with carbon dots.

3.1.2.2 Metal Nanoparticles

The results from the X-ray (EDX) spectrum confirmed that Ag and Au are found in the solutions. The results show that the peaks around 2.1 and 3.6 Kev is the binding energy of gold and silver, respectively in the sample, as shown in Figure 3.12. In addition to Ag and Au, there are several metals have been found in the samples. As described in Section 3.1.13, the nanoparticles are analyzed by activation using an EDX-ray spectrophotometer, which is generally present in modern SEM, therefore, Figure 3.13 shows the SEM images for As and Au. Silver and gold mapping analysis are also shown in Figure 3.14.

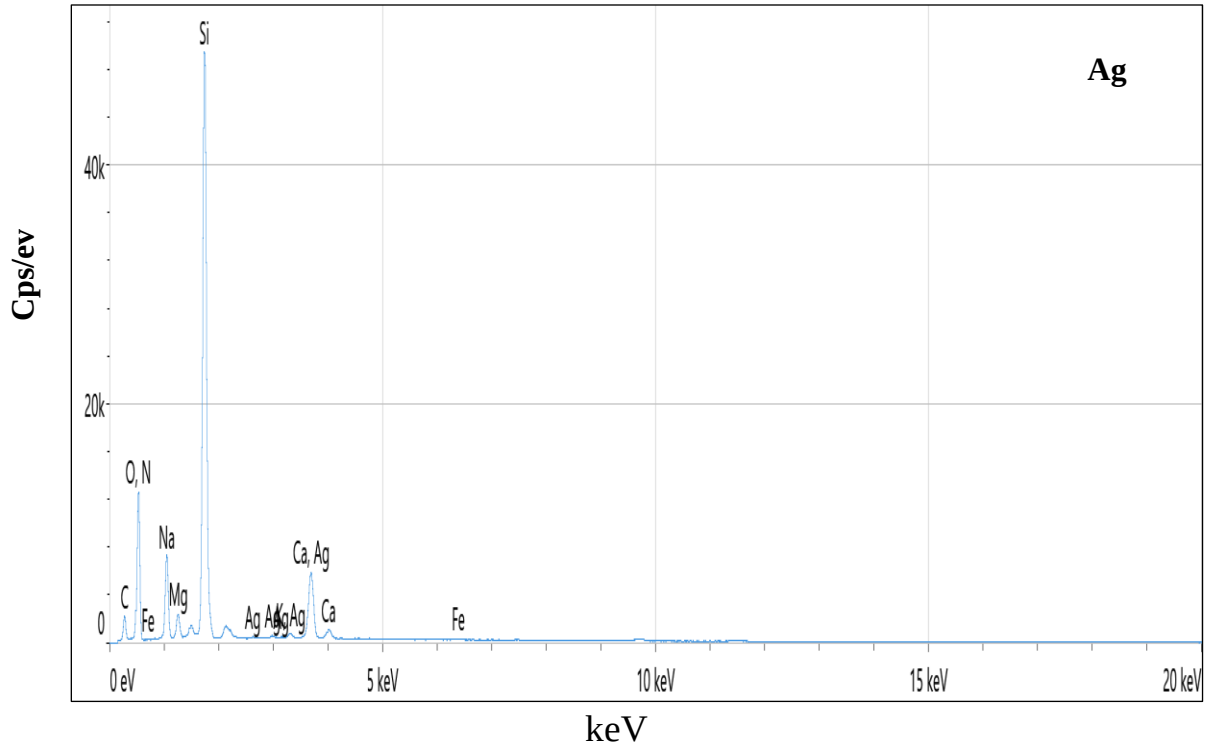

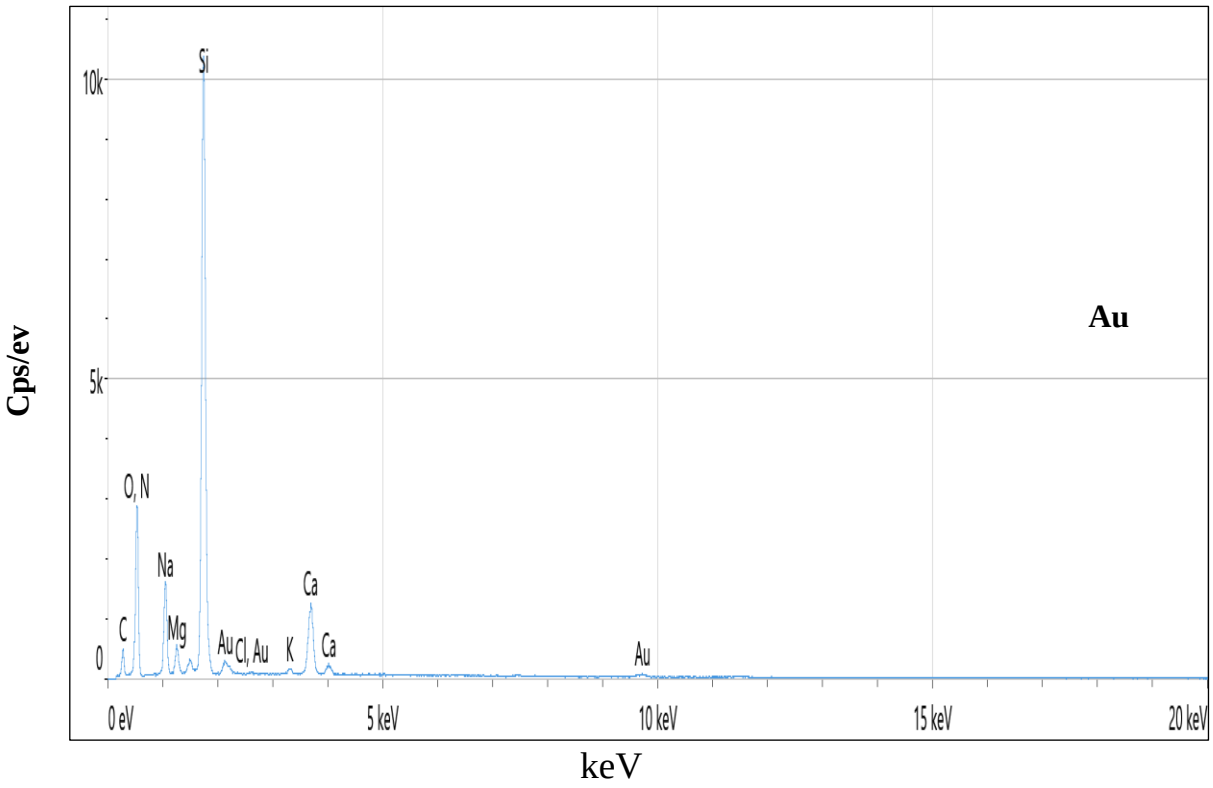

Figure 3.12: EDX analysis for Ag and Au.

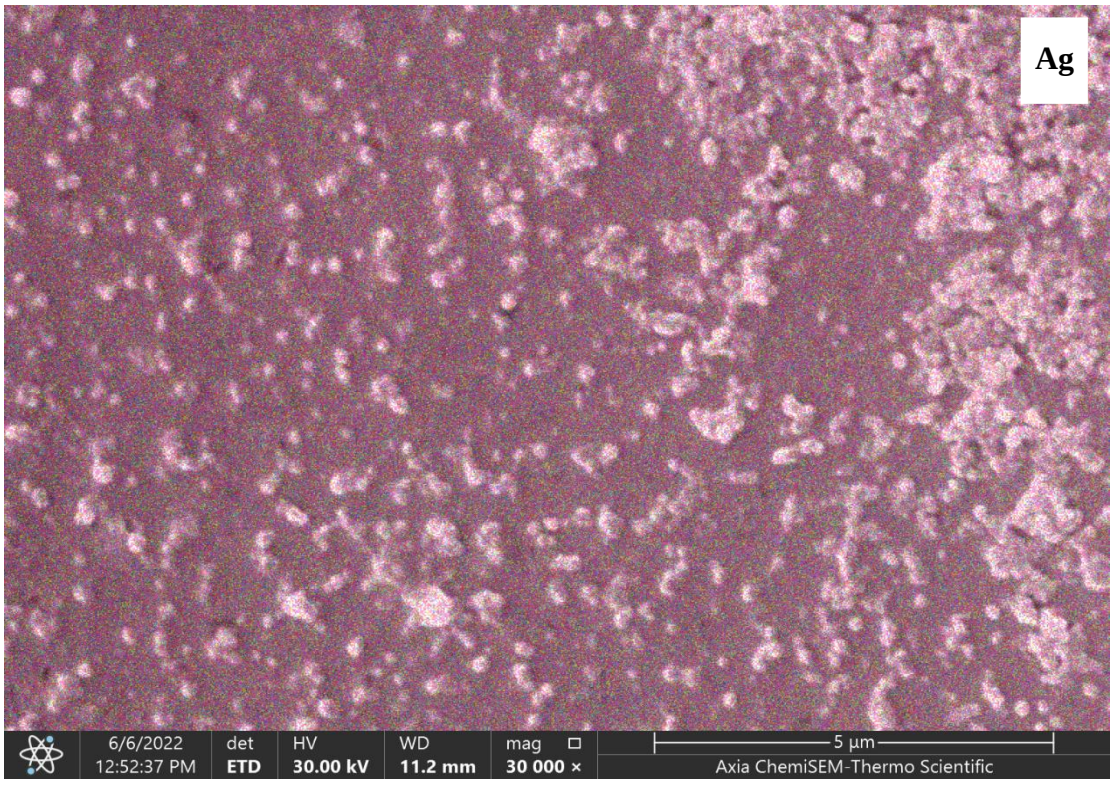

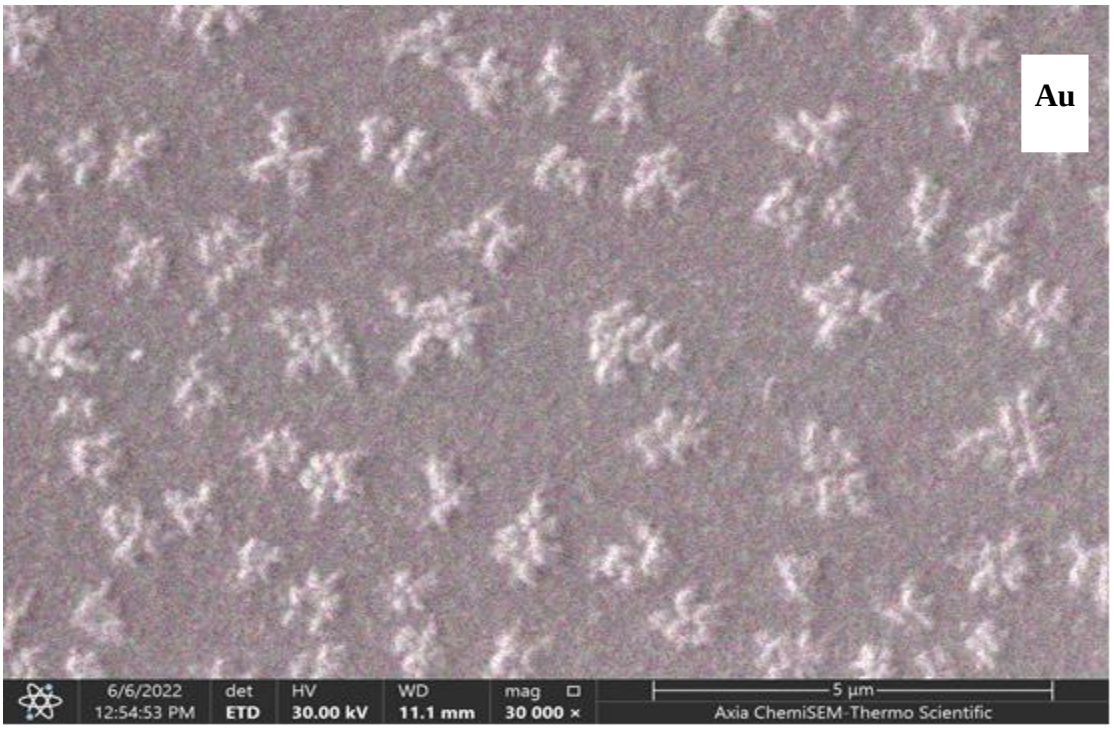

Figure 3.13: SEM images for Ag and Au

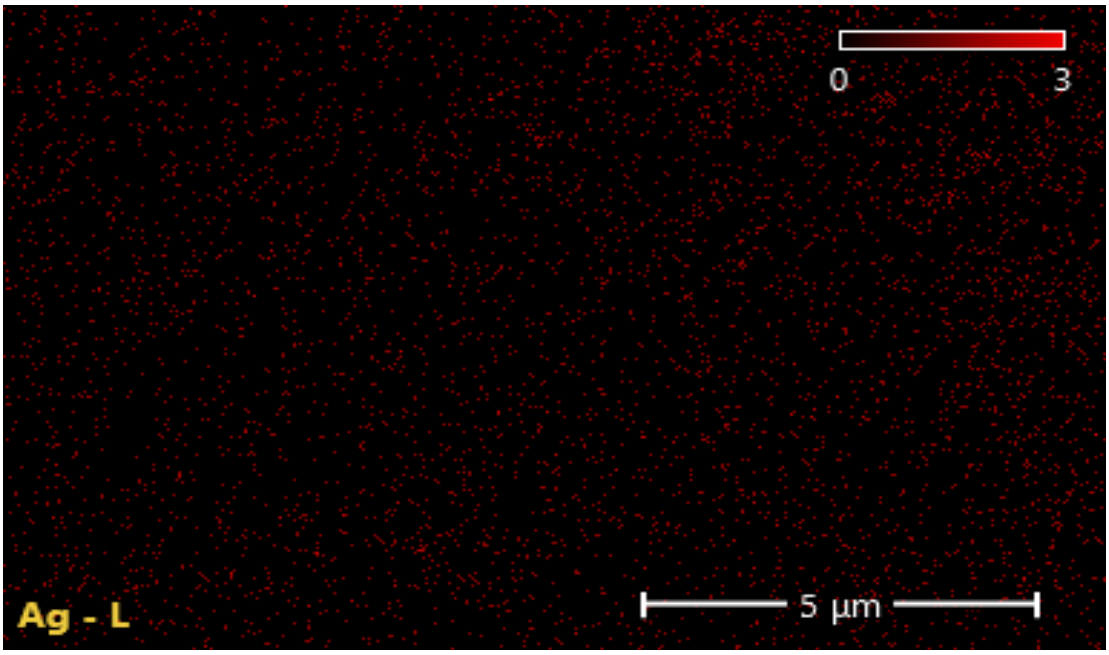

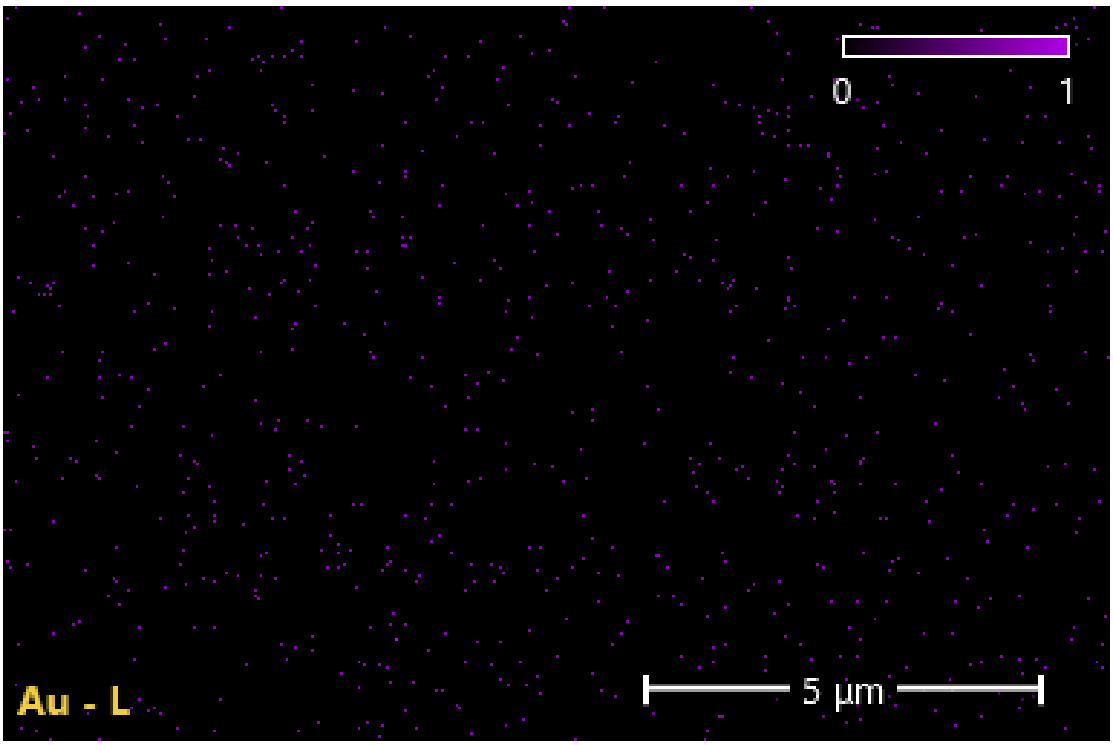

Figure 3.14: Elemental mapping analysis of Ag and Au

Figures 3.15 and 3.16 show the Scanning electron microscope (SEM) and High-Resolution SEM images of silver and gold. The results show that the size distributions of Ag and Au are narrow in the range of 20.40 – 59.44 and 14.57 – 38.33 nm, respectively. The high-resolution SEM images of Ag and Au are reported in Figure 3.15.

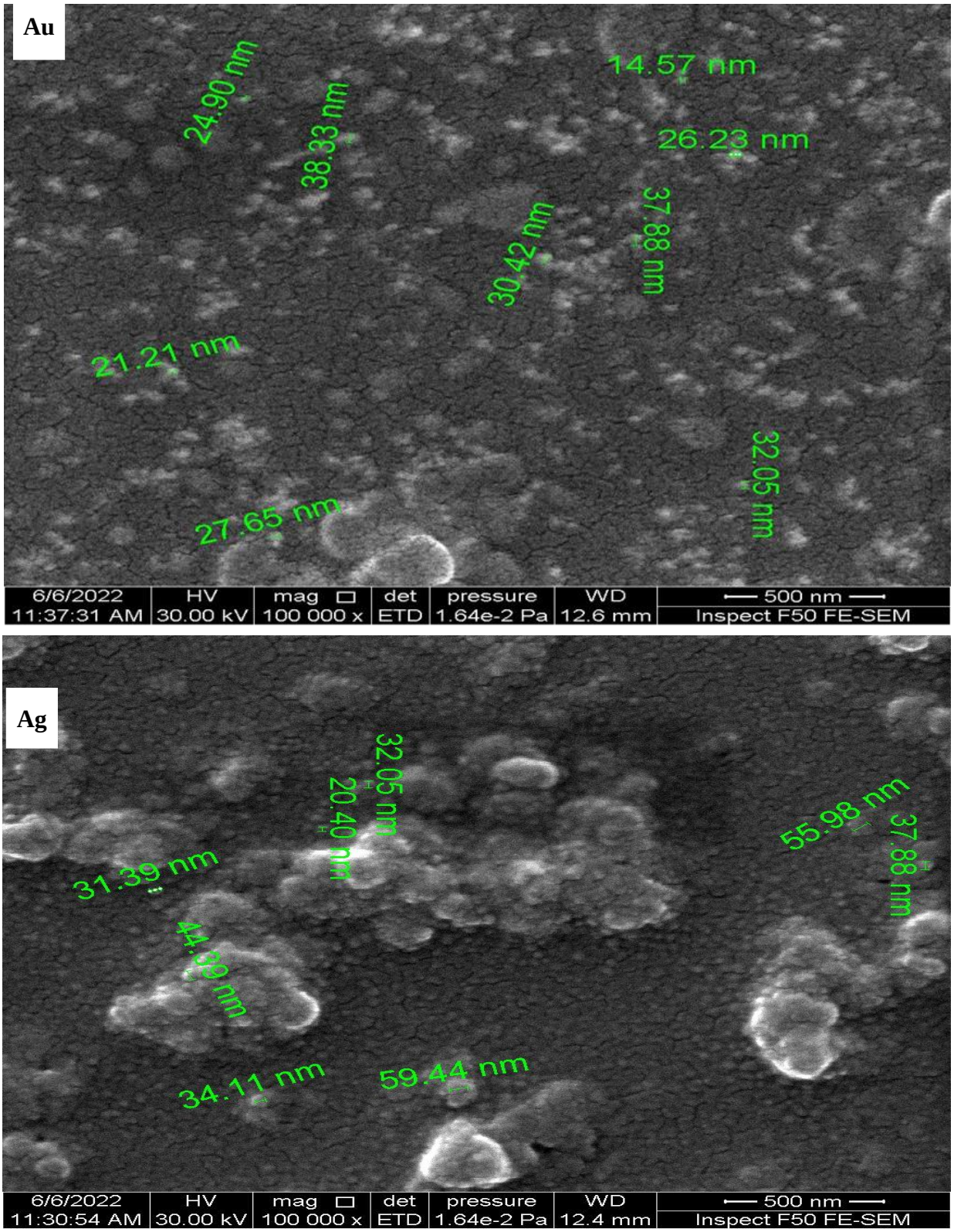

Figure 3.15: SEM images of Au and Ag.

Interestingly, the images obtained from SEM are like those reported by using EDS X-ray spectrophotometer present in modern SEM. The control procedures implemented by adding silver and gold to CE are shown no color change for more than 48 hrs. This result is indicating that the CE is not able to produce NPs. These results indicate that the CDs obtained from CE have the ability to reduce Ag^{+} and Au^{+3} to Ag and Au nanoparticles, respectively. Moreover, CDs can also stabilize these nanoparticles versus aggregation.

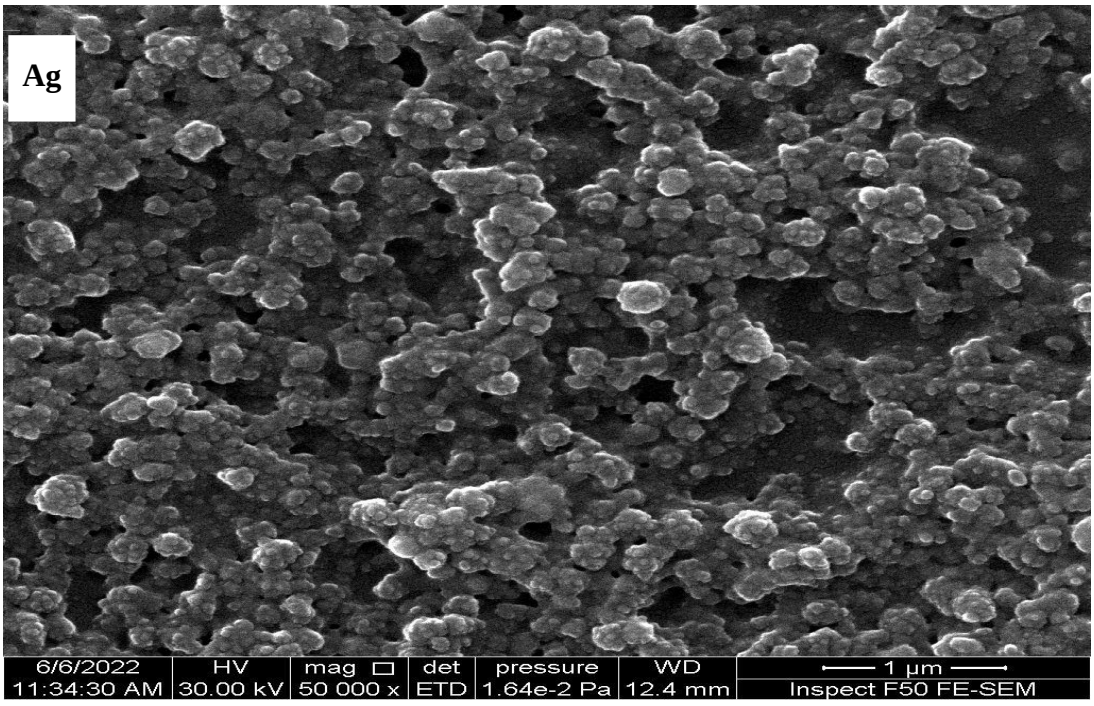

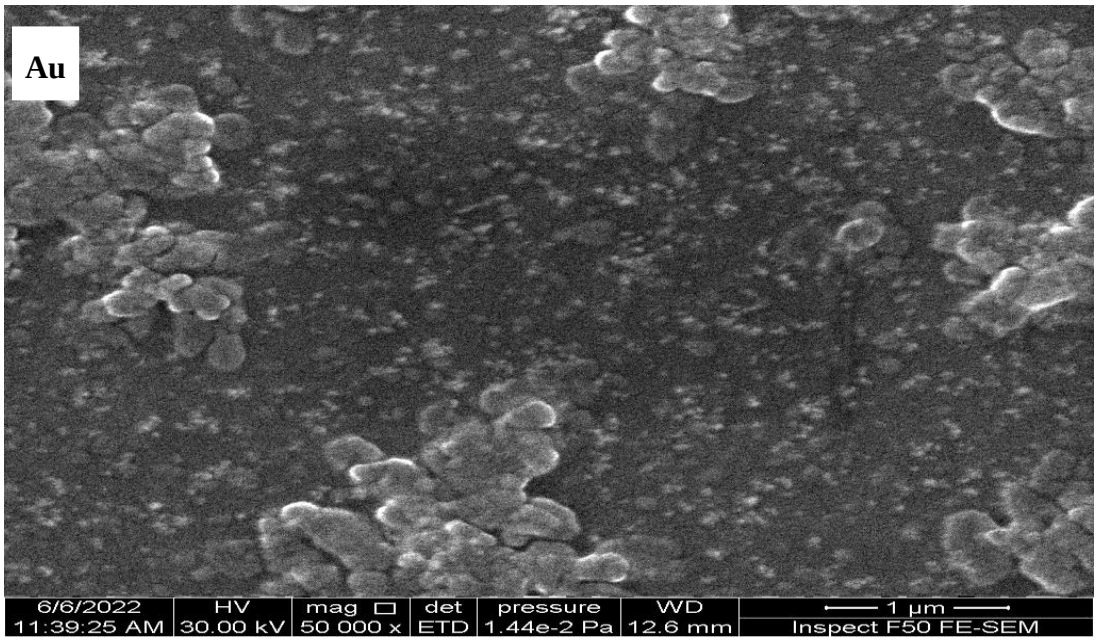

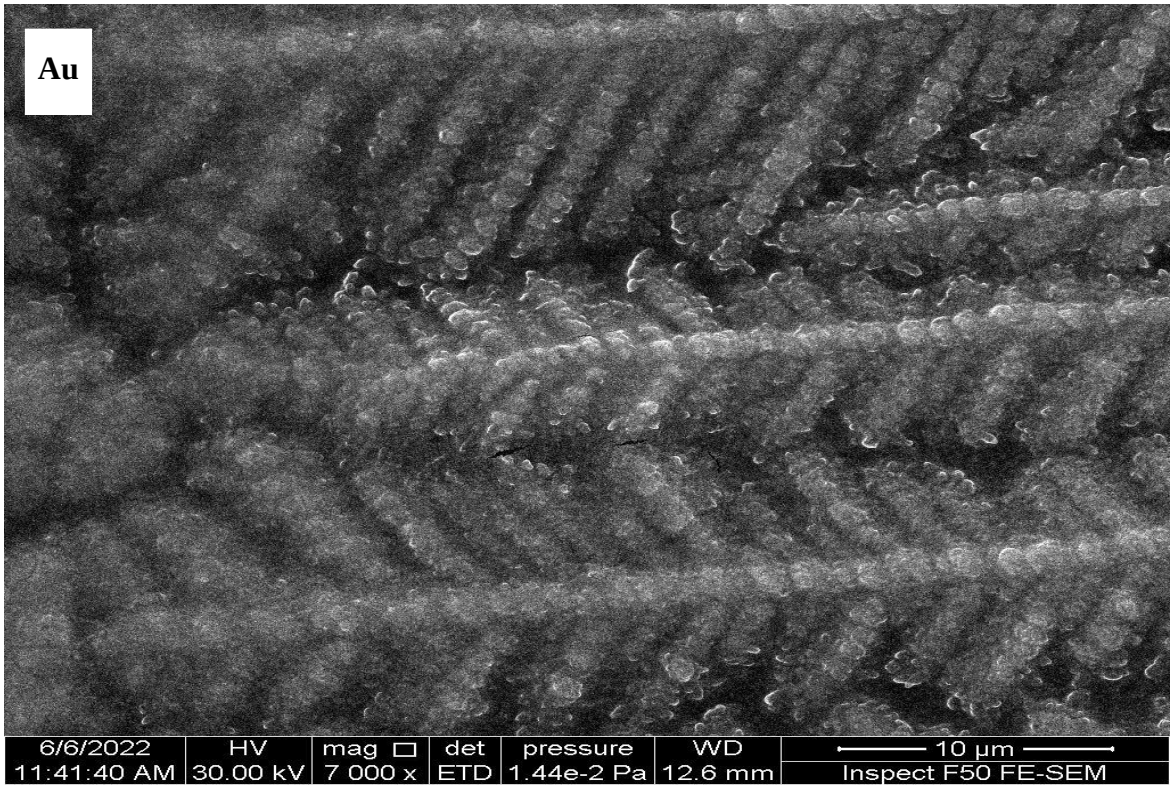

Figure 3.16: High-resolution SEM images for Ag and Au.

Chapter Four
Clinical Application

4.0 Introduction

This chapter has described the results of the clinical application by measuring the values of coagulation factors, namely Prothrombin Time (PT) and Activated Partial Thromboplastin Time (APTT) in the blood samples (healthy and those with high blood viscosity) (n=90), described in Section 2.3.3.1. The influence of AgNPs, health status, gender, and smoking activity on the es of PT and APTT were investigated. The aim of this chapter was to diagnose the levels of clotting disorders in patients who continue taking certain medications.

4.1 Statistical Study

A statistical study is used to assess the values of PT and APTT in the blood samples in order to investigate the relationships between AgNPs, PT, and APTT levels against several factors such as smoking activity, health status, and gender. The values of arithmetic mean, standard deviation, paired t-tests, and two-tailed t-tests have been determined in this study (refer to Appendix C).

4.2 Results and Discussion

4.2.1 Influence of AgNPs Concentration

The influence of AgNPs concentration on the values of PT and APTT was investigated. The results present that the higher effect of the concentration of AgNPs on the PT and APTT was 100 μg/ml, as shown in Figures 4.1 and 4.2. However, the higher values of PT (13.40) and APTT (42.28) are found by using 100 μg/ml of AgNPs compared with other concentrations. Therefore, this concentration was used for future studies [137].

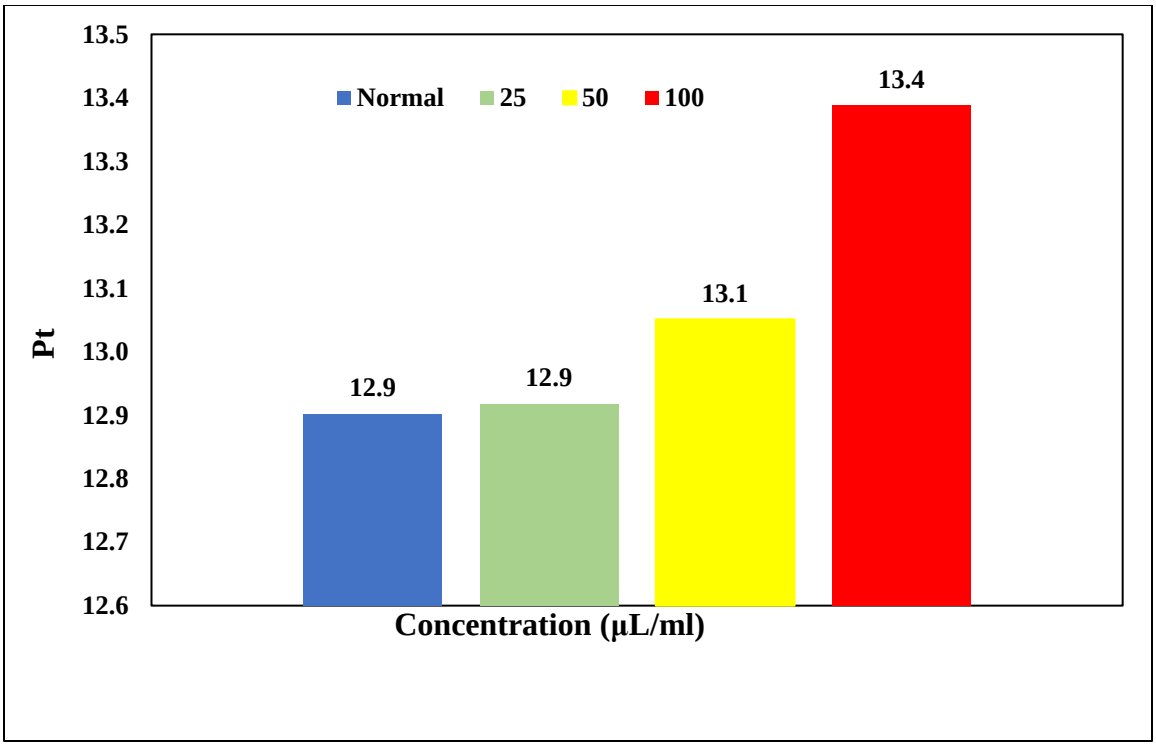

Figure 4.1: The effect of AgNPs concentration on the PTs (n=90).

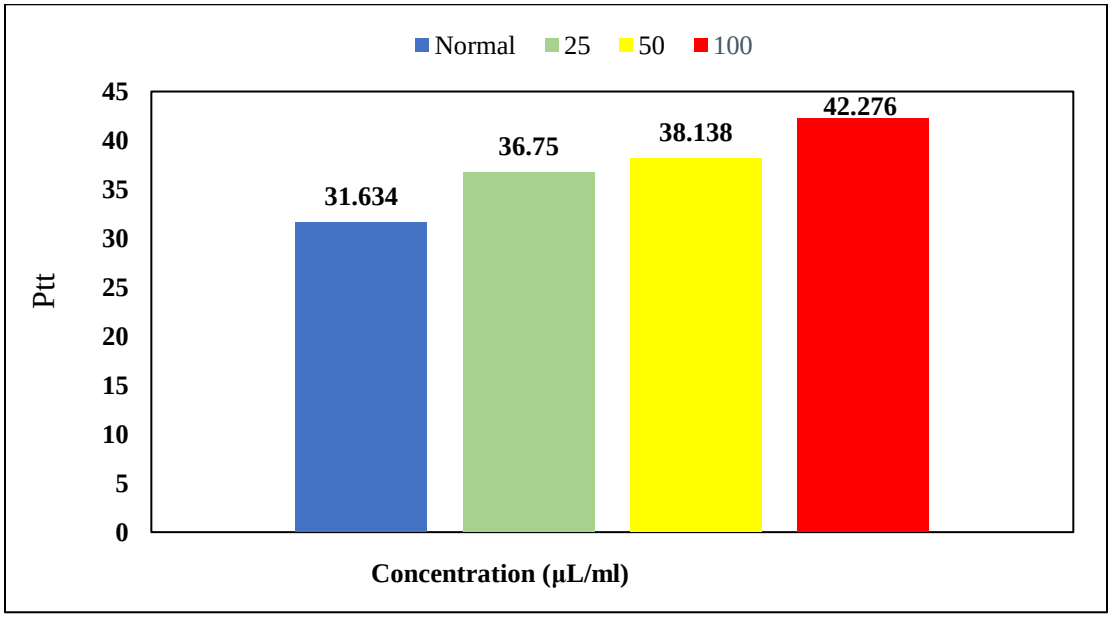

Figure 4.2: The effect of AgNPs concentration on the APTTs (n=90).

The values of mean and standard deviation of PT and APTT in the blood samples with and without AgNPs are determined by using paired t-test, and the results obtained are listed in Table 4.1. In general, significantly higher values of PT and APTT are found with AgNPs when compared with those without AgNPs, at the probability value of $P = 0.05$ [138].

Table 4.1: PT and PTT mean and standard deviation values in human blood for individuals with and without AgNPs from Karbala, Iraq.

	Mean (Sec)		(X – Y) Mean ± Sd (Unit)	Paired t-test			
	Without AgNPs (X) (n=90)	With AgNPs (Y) (n=90)		df	t_{calc}	t_{crit}	*Sig.(P)*
PT	12.902 ± 1.69	13.388 ± 1.74	10.641 ± 6.092	89	**16.571**	1.987	0.00
PTT	31.634 ± 6.68	42.276 ± 9.39	0.486 ± 0.791	89	**5.829**	1.987	0.00

Sd is the standard deviation, n_1, n_2 are the number of samples for individuals without and with AgNPs from Karbala, respectively, *df* = degree of freedom, $n_1 - 1$ for t-test, as described in Appendix C, t_{calc} are the calculated values for t-test, t_{crit} is a critical value at $P = 0.05$, the bold values indicate significant differences at the level of significance $P = 0.05$, Sig. = level of significance.

4.2.2 Effect of Health Status.

The influence of health status on the values of PT and APTT levels in blood samples are reported in Table 4.2 using a two-tailed t-test. No significant effects were found in the health status for both of PT and APTT at P = 0.05. The findings agree with those found in the literature [139]. On the other hand, one study in Najaf, Iraq has found significant differences in PT and APTT between hypertensive and normotensive patients [140].

Table 4.2: PT and PTT mean and standard deviation values in human blood for healthy individuals and patients from Karbala, Iraq.

	Mean ± SD (Sec)		Two-tailed t-test			
	Healthy ($n_1 = 30$)	Patients ($n_2 = 60$)	*df*	t_{calc}	t_{crit}	*Sig.(P)*
PT	12.640 ± 1.248	13.033 ± 1.870	88	1.039	2.021	0.301
PTT	30.020 ± 4.255	32.442 ± 7.512	88	1.636	2.021	0.105

Sd is the standard deviation, n_1, n_2 are the number of samples for health and patients, respectively, $df = (n_1+n_2-2)$, the degree of freedom for t-test determined as described in Appendix C, and t_{calc} are the calculated values for t-test, t_{crit} is a critical value at $P = 0.05$, the bold values indicate significant differences at the level of significance $P = 0.05$, Sig. = level of significance.

4.2.3 Influence of Gender

The purpose of this ersearch is to determine whether PT and APTT levels differ between males and females [141]. Therefore, the influence of gender on the values of Pt and APTT in the blood samples was determined. The samples (n = 90) are divided into two groups, namely females. The values of mean and standard deviation (±SD) for each group are presented in Table 4.3. The highest mean values in both groups are identified for APTT (males: 31.525 ± 7.505; and females: 31.842 ± 4.841). PT displayed the lowest values for both groups (males: 12.898 ± 1.906) and (females: 12.910 ± 1.207). The findings present that the PT and APTT levels of Females were slightly higher compared to males but there is no significant effect of gender on the values of PT and APTT.

Table 4.3: PT and PTT mean and standard deviation values in human blood for males and females from Karbala, Iraq.

	Mean ± SD (Sec)		Two-tailed t-test			
	Male ($n_1 = 59$)	Female ($n_2 = 31$)	*df*	t_{calc}	t_{crit}	*Sig.(P)*
PT	12.898 ± 1.906	12.910 ± 1.207	88	0.032	2.021	0.975
PTT	31.525 ± 7.505	31.842 ± 4.841	88	0.213	2.021	0.832

Sd is the standard deviation, n_1, n_2 are the number of samples for males anfemales, respectively, $df = (n_1+n_2-2)$, the degree of freedom for the t-test determined as described in Appendix C, and t_{calc} are the calculated values for t-test, t_{crit} is a critical value at $P = 0.05$, the bold values indicate significant differences at the level of significance $P = 0.05$, Sig. = level of significance.

4.2.4 Influence of Smoking Activity

The purpose of this study is to determine whether PT and APTT levels differ between smokers and non-smokers individuals [142]. Therefore, the effect of smoking activity on the levels of PT and APTT in has been studied and the results were reported in Table 4.4. It was found that there is no significant effect of smoking activity on PT and APTT in spite of the values of PT and APTT values are slightly higher in smokers compared to non-smokers.

Table 4.4: PT and PTT mean and standard deviation values in human blood for smokers and non-smokers from Karbala, Iraq.

	Mean ± SD (Sec)		Two-tailed t-test			
	Smokers ($n_1 = 45$)	Non-smoker ($n_2 = 45$)	*df*	t_{calc}	t_{crit}	*Sig.(P)*
PT	13.176 ± 2.098	12.629 ± 1.109	88	1.546	2.021	0.126
PTT	32.604 ± 8.021	30.664 ± 4.899	88	1.385	2.021	0.169

Sd is the standard deviation, n_1, n_2 are the number of samples for smokers and non-smokers, respectively, $df = (n_1+n_2-2)$, degree of freedom for t-test determined as described in Appendix C, and t_{calc} are the calculated values for the t-test, t_{crit} is a critical value at $P = 0.05$, the bold values indicate significant differences at the level of significance $P = 0.05$, Sig. = level of significance.

4.3 Conclusion

The use of Carbon dots (CDs) as bioimaging, biosensing, drug delivery, disease detection, materials science, and synthetic chemistry have recently been investigated by several studies. There are several methods were developed to prepare the CDs, for example, electrochemical oxidation, laser ablation, supported synthesis, and combustion/thermal MWA heating. Furthermore, solvothermal, hydrothermal, and microwave-assisted methods are useful because of their low-cost and simple operation [1]. The use of natural samples to produce CDs has several advantages such as being cost-effective, appropriate, and easily available in natural environments [2]. The main aim of this study was to develop and validate a new simple single-stage procedure to produce the CDs from Iraqi edible carrots by using refluxing Iraqi edible carrot with aqueous trisodium phosphate (TSP).

In consideration, different methods to prepare the CDs using the natural samples have been described in Chapter one. The chemical and physical properties, classification, and applications of CDs were also reported in this chapter.

The analytical methodological issues were described in Chapter 2, with appropriate green chemistry methods and optimised analysis conditions. Chapter 3 presented the results of synthesis of CDs, live cell imagining, and metal nanoparticles. The influence of AgNPs concentration, health status, gender, and smoking activity on the values of PT and APTT were reported in Chapter 4.

In the light of the results in this study, it can summaries the findings by the following points.

1- A convenient method to synthesis carbon dots from edible carrot was reported using commonly available chemical and labware.

2- Optimum synthetic parameters have been found, and the prepared CDs have been characterized by SEM, FTIR, 1H NMR, X-ray photoelectron spectroscopy (XPS), Energy Dispersive X-Ray Spectroscopy (EDX) and fluorescence spectroscopy.

3- It is found that 100 mM TSP is sufficient to produce CDs from 5 g of carrot. FTIR and 1H NMR analysis revealed that the carbonyl.

4- The application of CDs in optical imaging was demonstrated in Gram-negative and Gram-positive bacterial models.

5- FTIR and 1H NMR analysis revealed that the carbonyl containing phytonutrients undergone carbonization to yield blue luminescent CDs.

6- The prepared CDs have an ability to reduce metal ions like silver and gold to nanoparticles and stabilize them against aggregation.

7- As prepared AgNPs and AuNPs display excellent catalytic activity.

8- The simplicity of the CDs synthesis ensures their promising applications in the preparation of efficient nanocatalyst and in the development of cost-effective imaging agents.

4.4 Future Work

Further research could be developed from this study as there are no previously published studies about the synthesis carbon dots from edible carrot from Karbala (Iraq).

- As described in this study, CDs provide data about bioimaging, biosensing, drug delivery, disease detection. However, more research is needed to evaluate whether this CDs provides any advantages over these processes.

- The data from this study confirms that the CDs play a role in the direct reduction of silver ions to elemental silver (Ag_0) and gold ions to elemental gold (Au_0) without additional reducing and stabilizing agent. However, further studies are required using other elements.

- In general, significantly higher values of PT and APTT are found with AgNPs when compared with those without AgNPs, at the probability value of P = 0.05. However, further clinical studies are required using larger numbers of patients. In addition, other biological samples need to also be collected and analysed to enable a clearer picture of this study.

References

References

[1] C. Verma, A. Alfantazi, M. Quraishi, Quantum dots as ecofriendly and aqueous phase substitutes of carbon family for traditional corrosion inhibitors: a perspective, Journal of Molecular Liquids 343 (2021) 117648.

[2] M. Nasrollahzadeh, M.S. Sajadi, M. Atarod, M. Sajjadi, Z. Isaabadi, An introduction to green nanotechnology, Academic Press2019.

[3] K. Akbar, E. Moretti, A. Vomiero, Carbon dots for photocatalytic degradation of aqueous pollutants: recent advancements, Advanced Optical Materials 9(17) (2021) 2100532.

[4] N. Papaioannou, M.-M. Titirici, A. Sapelkin, Investigating the effect of reaction time on carbon dot formation, structure, and optical properties, ACS omega 4(26) (2019) 21658-21665.

[5] P. Velmurugan, R.V. Kumar, S. Sivakumar, A.V. Ravi, Fabrication of blue fluorescent carbon quantum dots using green carbon precursor Psidium guajava leaf extract and its application in water treatment, Carbon Letters 32(1) (2022) 119-129.

[6] M. Bottini, C. Balasubramanian, M.I. Dawson, A. Bergamaschi, S. Bellucci, T. Mustelin, Isolation and characterization of fluorescent nanoparticles from pristine and oxidized electric arc-produced single-walled carbon nanotubes, The Journal of Physical Chemistry B 110(2) (2006) 831-836.

[7] H.A. Nguyen, I. Srivastava, D. Pan, M. Gruebele, Unraveling the fluorescence mechanism of carbon dots with sub-single-particle resolution, Acs Nano 14(5) (2020) 6127-6137.

[8] P. Zhu, K. Tan, Q. Chen, J. Xiong, L. Gao, Origins of efficient multiemission luminescence in carbon dots, Chemistry of Materials 31(13) (2019) 4732-4742.

References

[9] L. Ai, Y. Yang, B. Wang, J. Chang, Z. Tang, B. Yang, S. Lu, Insights into photoluminescence mechanisms of carbon dots: advances and perspectives, Science Bulletin 66(8) (2021) 839-856.

[10] J. Liao, Y. Yao, C.H. Lee, Y. Wu, P. Li, In Vivo Biodistribution, Clearance, and Biocompatibility of Multiple Carbon Dots Containing Nanoparticles for Biomedical Application, Pharmaceutics 13(11) (2021).

[11] D. Zhao, Z. Zhang, C. Li, X. Xiao, J. Li, X. Liu, H. Cheng, Yellow-emitting hydrophobic carbon dots via solid-phase synthesis and their applications, ACS omega 5(35) (2020) 22587-22595.

[12] V. Rimal, P. Srivastava, Thermodynamic study of high thermal stability Carbon Dots, IOP Conference Series: Materials Science and Engineering, IOP Publishing, 2022, p. 012018.

[13] S. Agnello, F. Messina, Optical and electronic properties of carbon-based nanomaterials and composites, MDPI, 2020, p. 36.

[14] A. Döring, E. Ushakova, A.L. Rogach, Chiral carbon dots: synthesis, optical properties, and emerging applications, Light: Science & Applications 11(1) (2022) 75.

[15] P. Ranjan, R. Khan, S. Yadav, M.A. Sadique, S. Murali, M.K. Ban, Chapter 5 - Physical and chemical properties of carbon dots, in: R. Khan, S. Murali, S. Gogoi (Eds.), Carbon Dots in Agricultural Systems, Academic Press2022, pp. 117-133.

[16] B.D. Mansuriya, Z. Altintas, Carbon Dots: Classification, properties, synthesis, characterization, and applications in health care—An updated review (2018–2021), Nanomaterials 11(10) (2021) 2525.

[17] M. Liu, Optical properties of carbon dots: a review, Nanoarchitectonics (2020) 1-12.

References

[18] B.D. Mansuriya, Z. Altintas, Enzyme-free electrochemical nano-immunosensor based on graphene quantum dots and gold nanoparticles for cardiac biomarker determination, Nanomaterials 11(3) (2021) 578.

[19] I. Singh, R. Arora, H. Dhiman, R. Pahwa, Carbon quantum dots: Synthesis, characterization and biomedical applications, Turk. J. Pharm. Sci 15(2) (2018) 219-230.

[20] B.D. Mansuriya, Z. Altintas, Graphene quantum dot-based electrochemical immunosensors for biomedical applications, Materials 13(1) (2019) 96.

[21] Y. Wang, A. Hu, Carbon quantum dots: synthesis, properties and applications, Journal of Materials Chemistry C 2(34) (2014) 6921-6939.

[22] L. Tian, Z. Li, P. Wang, X. Zhai, X. Wang, T. Li, Carbon quantum dots for advanced electrocatalysis, Journal of Energy Chemistry 55 (2021) 279-294.

[23] S. Miao, K. Liang, J. Zhu, B. Yang, D. Zhao, B. Kong, Hetero-atom-doped carbon dots: Doping strategies, properties and applications, Nano Today 33 (2020) .

[24] Q. Xu, T. Kuang, Y. Liu, L. Cai, X. Peng, T.S. Sreeprasad, P. Zhao, Z. Yu, N. Li, Heteroatom-doped carbon dots: synthesis, characterization, properties, photoluminescence mechanism and biological applications, Journal of Materials Chemistry B 4(45) (2016) 7204-7219.

[25] J. Jana, Y.-L.T. Ngo, J.S. Chung, S.H. Hur, Contribution of carbon dot nanoparticles in electrocatalysis: Development in energy conversion process, Journal of Electrochemical Science and Technology 11(3) (2020) 220-237.

[26] B. Chen, S. Chai, J. Liu, C. Liu, Y. Li, J. He, Z. Yu, T. Yang, C. Feng, C. Huang, 2, 4, 6-Trinitrophenol detection by a new portable sensing gadget using carbon dots as a fluorescent probe, Analytical and bioanalytical chemistry 411(11) (2019) .

References

[27] F. Yuan, Y.-K. Wang, G. Sharma, Y. Dong, X. Zheng, P. Li, A. Johnston, G. Bappi, J.Z. Fan, H. Kung, Bright high-colour-purity deep-blue carbon dot light-emitting diodes via efficient edge amination, Nature Photonics 14(3) (2020) 171-176.

[28] W. Dong, R. Wang, X. Gong, C. Dong, An efficient turn-on fluorescence biosensor for the detection of glutathione based on FRET between N, S dual-doped carbon dots and gold nanoparticles, Analytical and bioanalytical chemistry 411(25) (2019)

[29] W. Dong, R. Wang, X. Gong, C. Dong, An efficient turn-on fluorescence biosensor for the detection of glutathione based on FRET between N, S dual-doped carbon dots and gold nanoparticles, Analytical and bioanalytical chemistry 411 (2019) 6687-6695.

[30] D. Li, C. Liang, E.V. Ushakova, M. Sun, X. Huang, X. Zhang, P. Jing, S.J. Yoo, J.G. Kim, E. Liu, Thermally activated upconversion near-infrared photoluminescence from carbon dots synthesized via microwave assisted exfoliation, Small 15(50) (2019) 1905050.

[31] P. Yang, Z. Zhu, T. Zhang, M. Chen, Y. Cao, W. Zhang, X. Wang, X. Zhou, W. Chen, Facile synthesis and photoluminescence mechanism of green emitting xylose-derived carbon dots for anti-counterfeit printing, Carbon 146 (2019) .

[32] F. Yan, Z. Bai, F. Zu, Y. Zhang, X. Sun, T. Ma, L. Chen, Yellow-emissive carbon dots with a large Stokes shift are viable fluorescent probes for detection and cellular imaging of silver ions and glutathione, Microchimica Acta 186 (2019) .

[33] K. Jiang, X. Feng, X. Gao, Y. Wang, C. Cai, Z. Li, H. Lin, Preparation of multicolor photoluminescent carbon dots by tuning surface states, Nanomaterials 9(4) (2019)

[34] S. Das, L. Ngashangva, P. Goswami, Carbon dots: an emerging smart material for analytical applications, Micromachines 12(1) (2021) 84.

References

[35] A. Emanuele, S. Cailotto, C. Campalani, L. Branzi, C. Raviola, D. Ravelli, E. Cattaruzza, E. Trave, A. Benedetti, M. Selva, Precursor-dependent photocatalytic activity of carbon dots, Molecules 25(1) (2019) 101.

[36] F. Wu, L. Yue, L. Yang, K. Wang, G. Liu, X. Luo, X. Zhu, Ln (III) chelates-functionalized carbon quantum dots: Synthesis, optical studies and multimodal bioimaging applications, Colloids and Surfaces B: Biointerfaces 175 (2019)

[37] L. Yue, H. Li, Q. Sun, J. Zhang, X. Luo, F. Wu, X. Zhu, Red-emissive ruthenium-containing carbon dots for bioimaging and photodynamic cancer therapy, ACS Applied Nano Materials 3(1) (2020) 869-876.

[38] Y. Ru, L. Ai, T. Jia, X. Liu, S. Lu, Z. Tang, B. Yang, Recent advances in chiral carbonized polymer dots: from synthesis and properties to applications, Nano Today 34 (2020) 100953.

[39] M. Chekini, E. Prince, L. Zhao, H. Mundoor, I.I. Smalyukh, E. Kumacheva, Chiral carbon dots synthesized on cellulose nanocrystals, Advanced Optical Materials 8(4) (2020) 1901911.

[40] B. Mansuriya, Z. Altintas, Carbon Dots: Classification, Properties, Synthesis, Characterization, and Applications in Health Care—An Updated Review (2018–2021). Nanomaterials 2021, 11, 2525, s Note: MDPI stays neutral with regard to jurisdictional claims in published , 2021.

[41] C. Rosso, G. Filippini, M. Prato, Carbon dots as nano-organocatalysts for synthetic applications, ACS Catalysis 10(15) (2020) 8090-8105.

[42] J. Zhang, Y.-q. Ma, N. Li, J.-l. Zhu, T. Zhang, W. Zhang, B. Liu, Preparation of Graphene Quantum Dots and Their Application in Cell Imaging, Journal of Nanomaterials 2016 (2016) 9245865.

[43] A. Ghaffarkhah, E. Hosseini, M. Kamkar, A.A. Sehat, S. Dordanihaghighi, A. Allahbakhsh, C. van der Kuur, M. Arjmand, Synthesis, applications, and

prospects of graphene quantum dots: a comprehensive review, Small 18(2) (2022) 2102683.

[44] B. Li, I. Eilks, A systematic review of the green and sustainable chemistry education research literature in mainland China, Sustainable Chemistry and Pharmacy 21 (2021) 100446.

[45] M.H. Facure, R. Schneider, L.A. Mercante, D.S. Correa, A review on graphene quantum dots and their nanocomposites: from laboratory synthesis towards agricultural and environmental applications, Environmental Science: Nano 7(12) (2020) 3710-3734.

[46] C. Ji, Y. Zhou, R.M. Leblanc, Z. Peng, Recent Developments of Carbon Dots in Biosensing: A Review, ACS Sensors 5(9) (2020) 2724-2741.

[47] R. Suresh, M. Pandiaraj, M. Sankaralingam, K. Giribabu, Graphene–metal chalcogenide modified electrochemical sensors, Graphene-based electrochemical sensors for biomolecules, Elsevier2019, pp. 139-153.

[48] R. Das, R. Bandyopadhyay, P. Pramanik, Carbon quantum dots from natural resource: A review, Materials today chemistry 8 (2018) 96-109.

[49] N. Dhenadhayalan, K.C. Lin, T.A. Saleh, Recent advances in functionalized carbon dots toward the design of efficient materials for sensing and catalysis applications, Small 16(1) (2020) 1905767.

[50] H. Li, X. He, Z. Kang, H. Huang, Y. Liu, J. Liu, S. Lian, C.H.A. Tsang, X. Yang, S.T. Lee, Water-soluble fluorescent carbon quantum dots and photocatalyst design, Angewandte Chemie International Edition 49(26) (2010) 4430-4434.

[51] S.Y. Lim, W. Shen, Z. Gao, Carbon quantum dots and their applications, Chemical Society Reviews 44(1) (2015) 362-381.

[52] P. Devi, S. Saini, K.-H. Kim, The advanced role of carbon quantum dots in nanomedical applications, Biosensors and Bioelectronics 141 (2019) 111158.

References

[53] R. Wang, K.-Q. Lu, Z.-R. Tang, Y.-J. Xu, Recent progress in carbon quantum dots: synthesis, properties and applications in photocatalysis, Journal of Materials Chemistry A 5(8) (2017) 3717-3734.

[54] Z. Zhang, T. Zheng, X. Li, J. Xu, H. Zeng, Progress of carbon quantum dots in photocatalysis applications, Particle & Particle Systems Characterization 33(8) (2016) 457-472.

[55] M.J. Molaei, Carbon quantum dots and their biomedical and therapeutic applications: a review, RSC Adv 9(12) (2019) 6460-6481.

[56] M. Farshbaf, S. Davaran, F. Rahimi, N. Annabi, R. Salehi, A. Akbarzadeh, Carbon quantum dots: recent progresses on synthesis, surface modification and applications, Artificial cells, nanomedicine, and biotechnology 46(7) (2018) 1331-1348.

[57] R.M. El-Shabasy, M. Farouk Elsadek, B. Mohamed Ahmed, M. Fawzy Farahat, K.N. Mosleh, M.M. Taher, Recent developments in carbon quantum dots: properties, fabrication techniques, and bio-applications, Processes 9(2) (2021) 388.

[58] S. Sun, W. Bao, F. Yang, X. Yan, Y. Sun, G. Zhang, W. Yang, Y. Li, Electrochemical synthesis of FeNx doped carbon quantum dots for sensitive detection of Cu2+ ion, Green Energy & Environment (2021).

[59] V. Magesh, A.K. Sundramoorthy, D. Ganapathy, Recent advances on synthesis and potential applications of carbon quantum dots, Frontiers in Materials (2022) 383.

[60] I. Singh, R. Arora, H. Dhiman, R. Pahwa, Carbon Quantum Dots: Synthesis, Characterization and Biomedical Applications, Turk J Pharm Sci 15(2) (2018) 219-230.

[61] V. Milosavljevic, A. Moulick, P. Kopel, V. Adam, R. Kizek, Microwave preparation of carbon quantum dots with different surface modification, Available from: web2. mendelu. cz/af_239_nanotech/J_Met_Nano/0314 (2014).

References

[62] R. Kumar, V.B. Kumar, A. Gedanken, Sonochemical synthesis of carbon dots, mechanism, effect of parameters, and catalytic, energy, biomedical and tissue engineering applications, Ultrason Sonochem 64 (2020) 105009.

[63] A. Sharma, J. Das, Small molecules derived carbon dots: synthesis and applications in sensing, catalysis, imaging, and biomedicine, Journal of nanobiotechnology 17(1) (2019) 1-24.

[64] V. Manikandan, N.Y. Lee, Green synthesis of carbon quantum dots and their environmental applications, Environmental Research 212 (2022) 113283.

[65] Y. Shi, X. Liu, M. Wang, J. Huang, X. Jiang, J. Pang, F. Xu, X. Zhang, Synthesis of N-doped carbon quantum dots from bio-waste lignin for selective irons detection and cellular imaging, International journal of biological macromolecules 128 (2019) 537-545.

[66] W. Zhang, Carbon Nanodots (CNDs): A Comprehensive Study of the Photoluminescence, Antioxidation and Cellular Uptake, The University of North Carolina at Greensboro, 2019.

[67] A. Vasin, D. Kysil, A. Rusavsky, O. Isaieva, A. Zaderko, A. Nazarov, V. Lysenko, Synthesis and Luminescent Properties of Carbon Nanodots Dispersed in Nanostructured Silicas, Nanomaterials 11(12) (2021) 3267.

[68] Y. Kwee, A.N. Kristanti, K. Siimon, N.S. Aminah, M. Zakki Fahmi, Carbon nanodots derived from natural products, South African Journal of Chemistry 75 (2021) 40-63.

[69] J. Liu, D. Li, K. Zhang, M. Yang, H. Sun, B. Yang, One-step hydrothermal synthesis of nitrogen-doped conjugated carbonized polymer dots with 31% efficient red emission for in vivo imaging, Small 14(15) (2018) 1703919.

[70] C. Xia, S. Zhu, S.-T. Zhang, Q. Zeng, S. Tao, X. Tian, Y. Li, B. Yang, Carbonized polymer dots with tunable room-temperature phosphorescence lifetime and wavelength, ACS applied materials & interfaces 12(34) (2020) 38593-38601.

References

[71] X. Huang, L. Yang, S. Hao, B. Zheng, L. Yan, F. Qu, A.M. Asiri, X. Sun, N-Doped carbon dots: a metal-free co-catalyst on hematite nanorod arrays toward efficient photoelectrochemical water oxidation, Inorganic Chemistry Frontiers 4(3) (2017) 537-540.

[72] S. Das, L. Ngashangva, P. Goswami, Carbon Dots: An Emerging Smart Material for Analytical Applications, Micromachines (Basel) 12(1) (2021).

[73] B. Wang, H. Cai, G.I. Waterhouse, X. Qu, B. Yang, S. Lu, Carbon Dots in Bioimaging, Biosensing and Therapeutics: A Comprehensive Review, Small Science (2022) 2200012.

[74] B. Wang, H. Cai, G.I. Waterhouse, X. Qu, B. Yang, S. Lu, Carbon dots in bioimaging, biosensing and therapeutics: a comprehensive review, Small Science 2(6) (2022) 2200012.

[75] X. Sun, Y. Lei, Fluorescent carbon dots and their sensing applications, TrAC Trends in Analytical Chemistry 89 (2017) 163-180.

[76] D. Yoo, Y. Park, B. Cheon, M.-H. Park, Carbon dots as an effective fluorescent sensing platform for metal ion detection, Nanoscale research letters 14(1) (2019) 1-13.

[77] G. Calabrese, G. De Luca, G. Nocito, M.G. Rizzo, S.P. Lombardo, G. Chisari, S. Forte, E.L. Sciuto, S. Conoci, Carbon Dots: An Innovative Tool for Drug Delivery in Brain Tumors, Int J Mol Sci 22(21) (2021).

[78] T. Kong, L. Hao, Y. Wei, X. Cai, B. Zhu, Doxorubicin conjugated carbon dots as a drug delivery system for human breast cancer therapy, Cell Prolif 51(5) (2018) e12488.

[79] Q. Zeng, D. Shao, X. He, Z. Ren, W. Ji, C. Shan, S. Qu, J. Li, L. Chen, Q. Li, Carbon dots as a trackable drug delivery carrier for localized cancer therapy in vivo, Journal of Materials Chemistry B 4(30) (2016) 5119-5126.

References

[80] J.R. Aguilar Cosme, H.E. Bryant, F. Claeyssens, Carbon dot-protoporphyrin IX conjugates for improved drug delivery and bioimaging, PLoS One 14(7) (2019) e0220210.

[81] A. Truskewycz, H. Yin, N. Halberg, D.T. Lai, A.S. Ball, V.K. Truong, A.M. Rybicka, I. Cole, Carbon dot therapeutic platforms: administration, distribution, metabolism, excretion, toxicity, and therapeutic potential, Small 18(16) (2022) 2106342.

[82] A. Khayal, V. Dawane, V.K. Yadav, K.K. Yadav, S.H. Khan, State of Art Technology: Synthesis of Carbon Dots and Their Potential Applications in Biomedical, Research and Environmental Remediation, (2021).

[83] K.K. Rana, S. Rana, Fundamentals, Representative Applications and Future Perspectives of Green Chemistry: A Short Review, Open Access Library Journal 1(5) (2014) 1-16.

[84] P.T. Anastas, J.C. Warner, Principles of green chemistry, Green chemistry: Theory and practice 29 (1998).

[85] A. DeVierno Kreuder, T. House-Knight, J. Whitford, E. Ponnusamy, P. Miller, N. Jesse, R. Rodenborn, S. Sayag, M. Gebel, I. Aped, A method for assessing greener alternatives between chemical products following the 12 principles of green chemistry, ACS Sustainable Chemistry & Engineering 5(4) (2017) 2927-2935.

[86] B.A. de Marco, B.S. Rechelo, E.G. Tótoli, A.C. Kogawa, H.R.N. Salgado, Evolution of green chemistry and its multidimensional impacts: A review, Saudi pharmaceutical journal 27(1) (2019) 1-8.

[87] S.L. Tang, R.L. Smith, M. Poliakoff, Principles of green chemistry: Productively, Green Chemistry 7(11) (2005) 761-762.

References

[88] S.Y. Tang, R.A. Bourne, R.L. Smith, M. Poliakoff, The 24 principles of green engineering and green chemistry:“Improvements Productively”, Green Chemistry 10(3) (2008) 268-269.

[89] B.T. Hoan, P.D. Tam, V.-H. Pham, Green synthesis of highly luminescent carbon quantum dots from lemon juice, Journal of Nanotechnology 2019 (2019).

[90] R. Atchudan, T.N. Jebakumar Immanuel Edison, M. Shanmugam, S. Perumal, T. Somanathan, Y.R. Lee, Sustainable synthesis of carbon quantum dots from banana peel waste using hydrothermal process for in vivo bioimaging, Physica E: Low-dimensional Systems and Nanostructures 126 (2021) 114417.

[91] A. Cayuela, M. Soriano, C. Carrillo-Carrión, M. Valcárcel, Semiconductor and carbon-based fluorescent nanodots: the need for consistency, Chemical Communications 52(7) (2016) 1311-1326.

[92] Q. Li, T.Y. Ohulchanskyy, R. Liu, K. Koynov, D. Wu, A. Best, R. Kumar, A. Bonoiu, P.N. Prasad, Photoluminescent carbon dots as biocompatible nanoprobes for targeting cancer cells in vitro, The Journal of Physical Chemistry C 114(28) (2010) 12062-12068.

[93] Z. Qian, X. Shan, L. Chai, J. Ma, J. Chen, H. Feng, Si-doped carbon quantum dots: a facile and general preparation strategy, bioimaging application, and multifunctional sensor, ACS applied materials & interfaces 6(9) (2014) .

[94] H. Ding, F. Du, P. Liu, Z. Chen, J. Shen, DNA–Carbon Dots Function as Fluorescent Vehicles for Drug Delivery, ACS Applied Materials & Interfaces 7(12) (2015) 6889-6897.

[95] K.B. Ayaz Ahmed, S.K. P, A. Veerappan, A facile method to prepare fluorescent carbon dots and their application in selective colorimetric sensing of silver ion through the formation of silver nanoparticles, Journal of Luminescence 177 (2016) 228-234.

References

[96] J. Zuo, T. Jiang, X. Zhao, X. Xiong, S. Xiao, Z. Zhu, Preparation and Application of Fluorescent Carbon Dots, Journal of Nanomaterials 2015 (2015) 787862.

[97] X. Guo, C.-F. Wang, Z.-Y. Yu, L. Chen, S. Chen, Facile access to versatile fluorescent carbon dots toward light-emitting diodes, Chemical communications 48(21) (2012) 2692-2694.

[98] W. Lu, X. Qin, S. Liu, G. Chang, Y. Zhang, Y. Luo, A.M. Asiri, A.O. Al-Youbi, X. Sun, Economical, green synthesis of fluorescent carbon nanoparticles and their use as probes for sensitive and selective detection of mercury (II) ions, Analytical chemistry 84(12) (2012) 5351-5357.

[99] B. Xu, C. Zhao, W. Wei, J. Ren, D. Miyoshi, N. Sugimoto, X. Qu, Aptamer carbon nanodot sandwich used for fluorescent detection of protein, Analyst 137(23) (2012) 5483-5486.

[100] P.-C. Hsu, H.-T. Chang, Synthesis of high-quality carbon nanodots from hydrophilic compounds: role of functional groups, Chemical communications 48(33) (2012) 3984-3986.

[101] C.-I. Wang, W.-C. Wu, A.P. Periasamy, H.-T. Chang, Electrochemical synthesis of photoluminescent carbon nanodots from glycine for highly sensitive detection of hemoglobin, Green Chemistry 16(5) (2014) 2509-2514.

[102] Z. Ma, H. Ming, H. Huang, Y. Liu, Z. Kang, One-step ultrasonic synthesis of fluorescent N-doped carbon dots from glucose and their visible-light sensitive photocatalytic ability, New Journal of Chemistry 36(4) (2012) 861-864.

[103] J. Liu, C. Li, F. Li, Fluorescence turn-on chemodosimeter-functionalized mesoporous silica nanoparticles and their application in cell imaging, Journal of Materials Chemistry 21(20) (2011) 7175-7181.

[104] Y.-Y. Zhang, M. Wu, Y.-Q. Wang, X.-W. He, W.-Y. Li, X.-Z. Feng, A new hydrothermal refluxing route to strong fluorescent carbon dots and its application as fluorescent imaging agent, Talanta 117 (2013) 196-202.

References

[105] B. De, N. Karak, A green and facile approach for the synthesis of water soluble fluorescent carbon dots from banana juice, Rsc Advances 3(22) (2013) 8286-

[106] C. Zhu, J. Zhai, S. Dong, Bifunctional fluorescent carbon nanodots: green synthesis via soy milk and application as metal-free electrocatalysts for oxygen reduction, Chemical communications 48(75) (2012) 9367-9369.

[107] S. Sahu, B. Behera, T.K. Maiti, S. Mohapatra, Simple one-step synthesis of highly luminescent carbon dots from orange juice: application as excellent bio-imaging agents, Chemical communications 48(70) (2012) 8835-8837.

[108] S. Han, H. Zhang, Y. Xie, L. Liu, C. Shan, X. Li, W. Liu, Y. Tang, Application of cow milk-derived carbon dots/Ag NPs composite as the antibacterial agent, Applied Surface Science 328 (2015) 368-373.

[109] V.N. Mehta, S. Jha, H. Basu, R.K. Singhal, S.K. Kailasa, One-step hydrothermal approach to fabricate carbon dots from apple juice for imaging of mycobacterium and fungal cells, Sensors and Actuators B: Chemical 213 (2015) 434-443.

[110] N. Wang, Y. Wang, T. Guo, T. Yang, M. Chen, J. Wang, Green preparation of carbon dots with papaya as carbon source for effective fluorescent sensing of Iron (III) and Escherichia coli, Biosensors and Bioelectronics 85 (2016) 68-75.

[111] X. Feng, Y. Jiang, J. Zhao, M. Miao, S. Cao, J. Fang, L. Shi, Easy synthesis of photoluminescent N-doped carbon dots from winter melon for bio-imaging, Rsc Advances 5(40) (2015) 31250-31254.

[112] M. Jayanthi, S. Megarajan, S.B. Subramaniyan, R.K. Kamlekar, A. Veerappan, A convenient green method to synthesize luminescent carbon dots from edible carrot and its application in bioimaging and preparation of nanocatalyst, Journal of Molecular Liquids 278 (2019) 175-182.

[113] S. Liu, T. Quan, L. Yang, L. Deng, X. Kang, M. Gao, Z. Xia, X. Li, D. Gao, N, Cl-codoped carbon dots from Impatiens balsamina L. stems and a deep eutectic

solvent and their applications for gram-positive bacteria identification, antibacterial activity, cell imaging, and ClO–sensing, ACS omega 6(43) (2021)

[114] R.C. Gosselin, K. Janatpour, E.C. Larkin, Y.P. Lee, J.T. Owings, Comparison of samples obtained from 3.2% sodium citrate glass and two 3.2% sodium citrate plastic blood collection tubes used in coagulation testing, American journal of clinical pathology 122(6) (2004) 843-848.

[115] M. Gunendren, S.S. Nordin, M.R. Ramachandran, N.A. Samad, Effect of Ocimum sanctum (Tulsi) aqueous leaf extract on prothrombin time (PT), activated partial thromboplastin time (APTT) and thrombin time (TT) of human plasma, Journal of Biomedical and Clinical Sciences (JBCS) 2(1) (2017) 62-68.

[116] D. Zamudio, A. Bartolomé, D. Cancho, N. Gijón, L. Gisbert, P. Redondo, S. García-del-Valle, Preoperative unexpected prolongation of the activated partial thromboplastin time and prothrombin time in adults. Do we need to pursue abnormal results? A retrospective analysis, Perioperative Care and Operating Room Management 24 (2021) 100204.

[117] C.P. Weiner, J. Brandt, A modified activated partial thromboplastin time with the use of amniotic fluid: Preliminary report of a new technique for detection of fetal lung maturity, American Journal of Obstetrics and Gynecology 144(2) (1982)

[118] Q. Wu, D. Kong, W. Peng, R. Zong, X. Yu, S. Feng, Deciphering the Biochemical Similarities and Differences Among Human Neuroglial Cells and Glioma Cells Using Fourier Transform Infrared Spectroscopy, World Neurosurgery 168 (2022)

[119] K.R. Ross, L.A. Todd, Field evaluation of a transportable open-path FTIR spectrometer for real-time air monitoring, Appl Occup Environ Hyg 17(2) (2002)

[120] D.L. Pavia, G.M. Lampman, G.S. Kriz, J.A. Vyvyan, Introduction to spectroscopy, Cengage learning2014.

References

[121] S. Oswald, X-Ray photoelectron spectroscopy in analysis of surfaces, Encyclopedia of Analytical Chemistry: Applications, Theory and Instrumentation (2006).

[122] D.N.G. Krishna, J. Philip, Review on surface-characterization applications of X-ray photoelectron spectroscopy (XPS): Recent developments and challenges, Applied Surface Science Advances 12 (2022) 100332.

[123] M. Balci, Basic 1H-and 13C-NMR spectroscopy, Elsevier2005.

[124] K.C. Wong, Review of NMR Spectroscopy: Basic Principles, Concepts and Applications in Chemistry, Journal of Chemical Education 91(8) (2014) .

[125] D. Shindo, T. Oikawa, Analytical electron microscopy for materials science, Springer Science & Business Media2013.

[126] M. Scimeca, S. Bischetti, H.K. Lamsira, R. Bonfiglio, E. Bonanno, Energy Dispersive X-ray (EDX) microanalysis: A powerful tool in biomedical research and diagnosis, Eur J Histochem 62(1) (2018) 2841.

[127] Q. Zhaosheng, S. Xiaoyue, C. Lujing, M. Juanjuan, C. Jianrong, F. Hui, Si-Doped Carbon Quantum Dots: A Facile and General Preparation Strategy, Bioimaging Application, and Multifunctional Sensor, (2014).

[128] K. Schröder, G. Bettermann, T. Staffel, T. Klein, T. Hofmann, Phosphoric Acid and Phosphates, Ullmann's Encyclopedia of Industrial Chemistry, Wiley-Vch, Weinheim, Germany, 1998.

[129] M.I. Alarcón-Flores, R. Romero-González, J.L.M. Vidal, F.J.E. González, A.G. Frenich, Monitoring of phytochemicals in fresh and fresh-cut vegetables: A comparison, Food Chemistry 142 (2014) 392-399.

[130] A.B. Siddique, A.K. Pramanick, S. Chatterjee, M. Ray, Amorphous carbon dots and their remarkable ability to detect 2, 4, 6-trinitrophenol, Scientific reports 8(1) (2018) 9770.

References

[131] B.A. Joda, Z.M. Abed Al-Kadhim, H.J. Ahmed, A.K. Al-Khalaf, A convenient green method to synthesize β-carotene from edible carrot and nanoparticle formation, Karbala International Journal of Modern Science 8(1) (2022) 20-27.

[132] F.A. Stevie, C.L. Donley, Introduction to x-ray photoelectron spectroscopy, Journal of Vacuum Science & Technology A: Vacuum, Surfaces, and Films 38(6) (2020) 063204.

[133] B. Shirley, E. Jarochowska, Chemical characterisation is rough: the impact of topography and measurement parameters on energy-dispersive X-ray spectroscopy in biominerals, Facies 68(2) (2022) 7.

[134] M.-M. Titirici, M. Antonietti, N. Baccile, Hydrothermal carbon from biomass: a comparison of the local structure from poly-to monosaccharides and pentoses/hexoses, Green Chemistry 10(11) (2008) 1204-1212.

[135] T.-Y. Wang, C.-Y. Chen, C.-M. Wang, Y.Z. Tan, W.-S. Liao, Multicolor functional carbon dots via one-step refluxing synthesis, ACS sensors 2(3) (2017)

[136] L. Tang, R. Ji, X. Cao, J. Lin, H. Jiang, X. Li, K.S. Teng, C.M. Luk, S. Zeng, J. Hao, Deep ultraviolet photoluminescence of water-soluble self-passivated graphene quantum dots, ACS nano 6(6) (2012) 5102-5110.

[137] X. Liu, J. Sun, Time-course effects of intravenously administrated silica nanoparticles on blood coagulation and endothelial function in rats, Journal of Nanoscience and Nanotechnology 13(1) (2013) 222-228.

[138] P. Peterson, E.L. Gottfried, The effects of inaccurate blood sample volume on prothrombin time (PT) and activated partial thromboplastin time (aPTT), Thrombosis and haemostasis 47(02) (1982) 101-103.

[139] N. Nnenna Adaeze, A. Uchenna Emeribe, I. Abdullahi Nasiru, A. Babayo, E.K. Uko, Evaluation of prothrombin time and activated partial thromboplastin time in hypertensive patients attending a tertiary hospital in calabar, Nigeria, Advances in Hematology 2014 (2014).

References

[140] G. Giacchetti, F. Turchi, M. Boscaro, V. Ronconi, Management of primary aldosteronism: its complications and their outcomes after treatment, Current Vascular Pharmacology 7(2) (2009) 244-249.

[141] A. Jiskani, S. Memon, L. Naseem, Prothrombin time (PT), activated partial thromboplastin time (APTT) and international normalized ratio (INR) as predictive factors of coagulopathy in newly diagnosed hypertensive patients, Hematol Transfus Int J 4(3) (2017) 84-88.

[142] O.O. Chizoba, E.H. Ebuka, Effects of cigarette smoking on some coagulation parameters of smokers in Nnewi metropolis, J Environ Occup Sci 6(1) (2017) 13.

Appendix A:
Documentation and Clinical Study

Study of Human Biological Samples (blood) in Karbala and London for Iraqi Individuals.

Code Number: ____ **Collection Date:** ____

Town/Province: _____

Type of sample:

Hair ____ Finger Nails ____ Toe Nails ____ Blood ____ Saliva ____

Residence: How long have you lived here? _____ years

Where did you live before? _____ town/city

Number of members of family _____ adults

_____ children

Personal Information: (For the sample code above)

Sex:		Male		Female
Age:		Years		Months
Height:		Metres		Centimetres
Weight:		Kilograms		

General Health: _____

_____

Do you have any permanent illness? ____ Yes ____ No

If yes: _____

_____

What temporary illness have you had in the last 12 months?

____ None Or _____

Smoking history:

Do you smoke? Yes No

If yes: How many cigarettes per day?

Number of smoking years: Years Months

Type of cigarette:

Diet : How many meals do you eat a day?

____ Number

What is your basic diet (sources and quantities)? List main foods for each meal*

Meal	Nutrition

*Note: Include all sources of protein, carbohydrate, fruits/vegetables and fats.

Drinking water: What sources of drinking water do you use? Used filter Yes No

____ Bottled ____ Tap ____ Other _____

Do you consume commercial beverages? If yes....

____ Name ____ Quantity per day/week

Do you apply any special treatments to your hair?

Special shampoos (dandruff, etc) ____ Dyes ____ Oxygenation ____

Spray ____ Hair gel ____ Others ____ _____

Do you apply any special treatments to you Nails? Yes or No:

Children only:

Does your child attend school? ____ Yes ____ No

If yes, School _____ Grade _____

How would you describe their academic achievement? _____

_____

Adults only:

Are you employed? ____ Yes ____ No

If yes: Where----------

Type of work----------

ALL INFORMATION WITHIN THIS QUESTIONAIRE IS CONFIDENTIAL TO THE PROJECT MANAGERS AND WILL NOT BE MADE AVAILABLE TO ANY OTHER INDIVIDUAL OR GROUP.

Appendix B: Publications

B1.1

A Green Method to Synthesis of Luminescent Carbon Dots from Iraqi Carrot Juice

Huda R. Mohaisen, Baker A. Joda, , Adnan Ibrahim Mohammed,
Department of Chemistry, Faculty of Science, University of Kerbala, Karbala, Iraq

Abstract In this research, an Iraqi edible carrot with aqueous trisodium phosphate (TSP) has been refluxed to produce blue-color luminescent carbon dots (CDs) using a simple single-stage method. Scanning Electron Microscopy (SEM) image confirmed that CDs are almost spherical in shape and the size is around 6.40 – 25.76 nm. The energy-dispersive X-ray (EDX) spectrum showed the existence of carbon in the samples. The Fourier-transform infrared (FTIR) spectrum of carrot extract (CE) and CDs is explained that the -C=O peak was found in 1740 and 1650 cm−1 in the CE but it is completely lost in CDs. This result indicates that the carbonyl group has undergone carbonization. 1H NMR spectra of CE and CDs confirmed that the signals found between 3 and 4 ppm in the CE were decreased considerably in CDs, confirming that the carbohydrates present in the carrot had undergone carbonization to produce luminescent CDs.

Keywords: Carbon dots, Carrot, Green Method, Karbala.

B1.2

Applications of Carbon Dots in Bioimaging and Preparation of Nanocatalyst

Huda R. Mohaisen, Baker A. Joda, Adnan Ibrahim Mohammed,
Department of Chemistry, Faculty of Science, University of Kerbala, Karbala, Iraq

Abstract In this research, the preparation of carbon dots (CDs) from edible carrots using a simple single-stage green method was used in bioimaging and the preparation of nanocatalyst. The produced CDs are used as luminophore to image bacteria through fluorescence microscopy. CDs have membrane good permeability and minimum toxicity against Gram-negative and Gram-positive bacteria. The CDs capability for direct reduction of silver ions to elemental silver (Ag0) and gold ions to elemental gold (Au0) without additional reducing and stabilizing agents was demonstrated. The resulting Ag and Au nanoparticles have a size of 8–22 nm and 5–15 nm, respectively. The catalytic activity of nanoparticles in the hydrogenation reaction was investigated. The results suggest that the nanoparticles had high catalytic activity in the sodium borohydride-mediated hydrogenation of nitroaromatic compounds.

Keywords: Carbon dots, Carrot, Bioimaging, Nanocatalyst, Karbala.

Appendix C: Statistics

C1. Statistical Equations Used in this Study (Miller & Miller, 2010; Farrant, 1997)

Arithmetic mean

The Arithmetic mean ($\bar{x}$) is the sum of measured value divided by the number of measurements (n):

$$x = \frac{\sum \bar{x_i}}{n}$$

Standard deviation (Sd)

The standard deviation (s) is a measure of the agreement between a set of n data points. It is also the measure of random error, the following equation used to calculate s:

$$s = \sqrt{\frac{\sum_i (x_i - \bar{x})^2}{n-1}}$$

where $x_i =$ x value and $\bar{x} =$ arithmetic mean of x values.

Variance (S^2)

Variance is the square of the standard deviation and is a measure of the extent to which results in a set of data differ from one another. The larger the variance, the greater the difference between the results.

Paired t-test

This test used to compare pairs of data, such as when a single sample has been measured by the two analytical techniques or prepared by the two digestion methods. The difference between the data values for the two different methods is used to calculate t-calculated (t_{calc}) value. This value

is compared with a t-critical (t_{crit}) value for n-1 degrees of freedom at the 95% confidence interval ($P < 0.05$), as shown:

$$t_{calc} = \frac{\bar{D}\sqrt{n}}{s_d}$$

$$s_d = \sqrt{\frac{\sum(D_i - \bar{D})^2}{N-1}}$$

where $\bar{D}_i$ is the individuals' difference between the two methods for each sample, with regard to sign; and D is the mean of all the individual differences.

Appendix D:

SEM Charts

D1: SEM for CDs

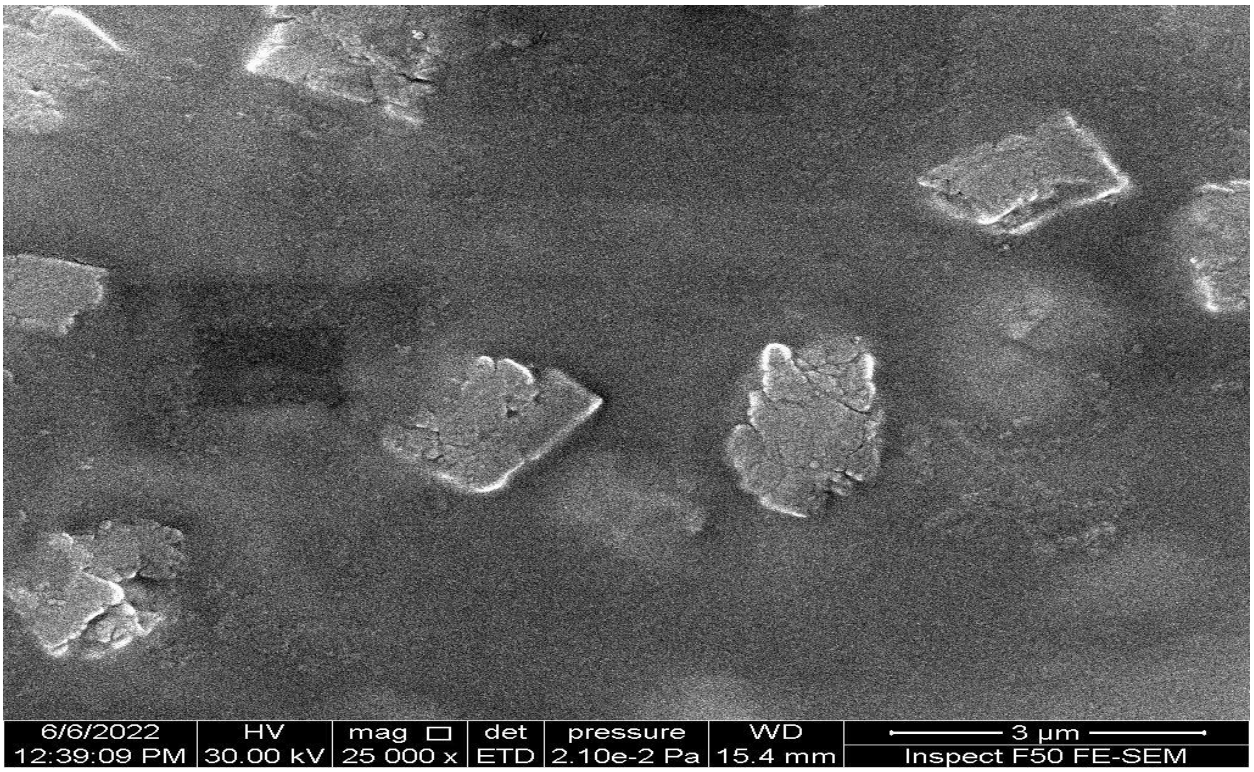

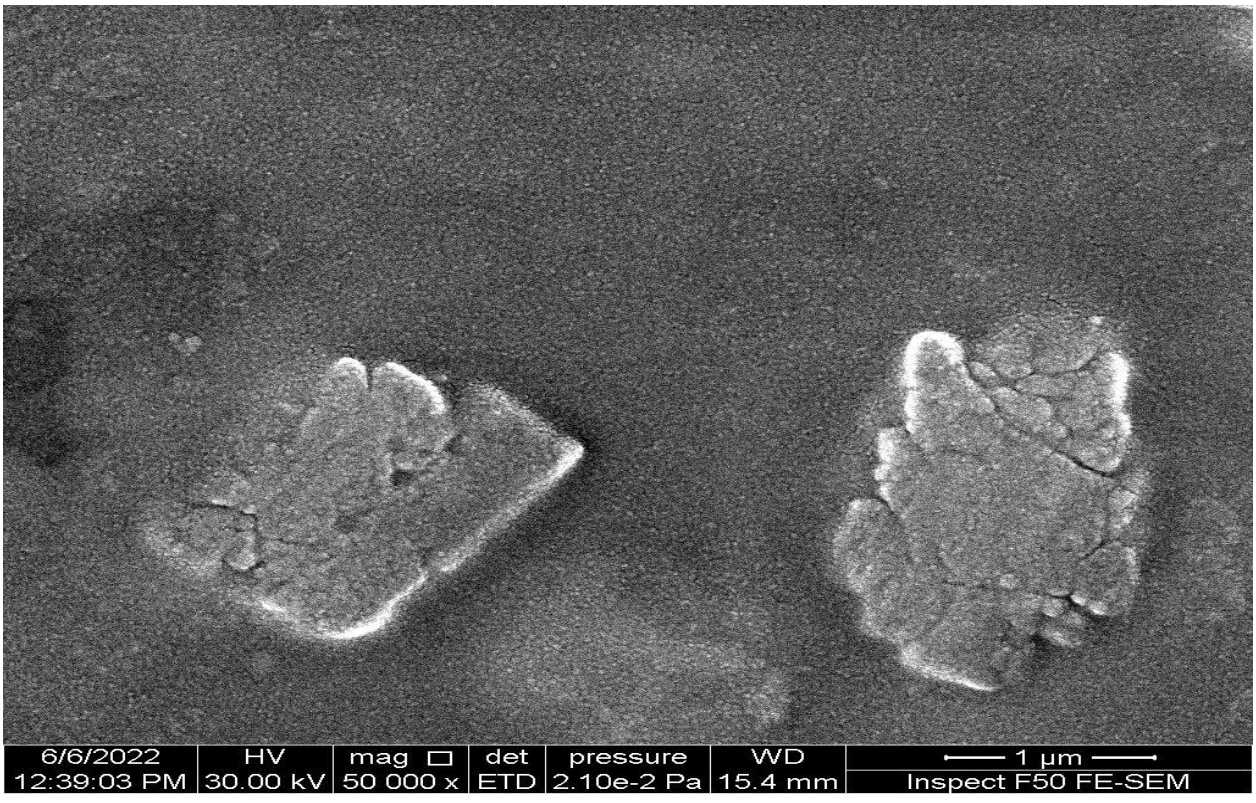

D2: SEM for NPs Ag

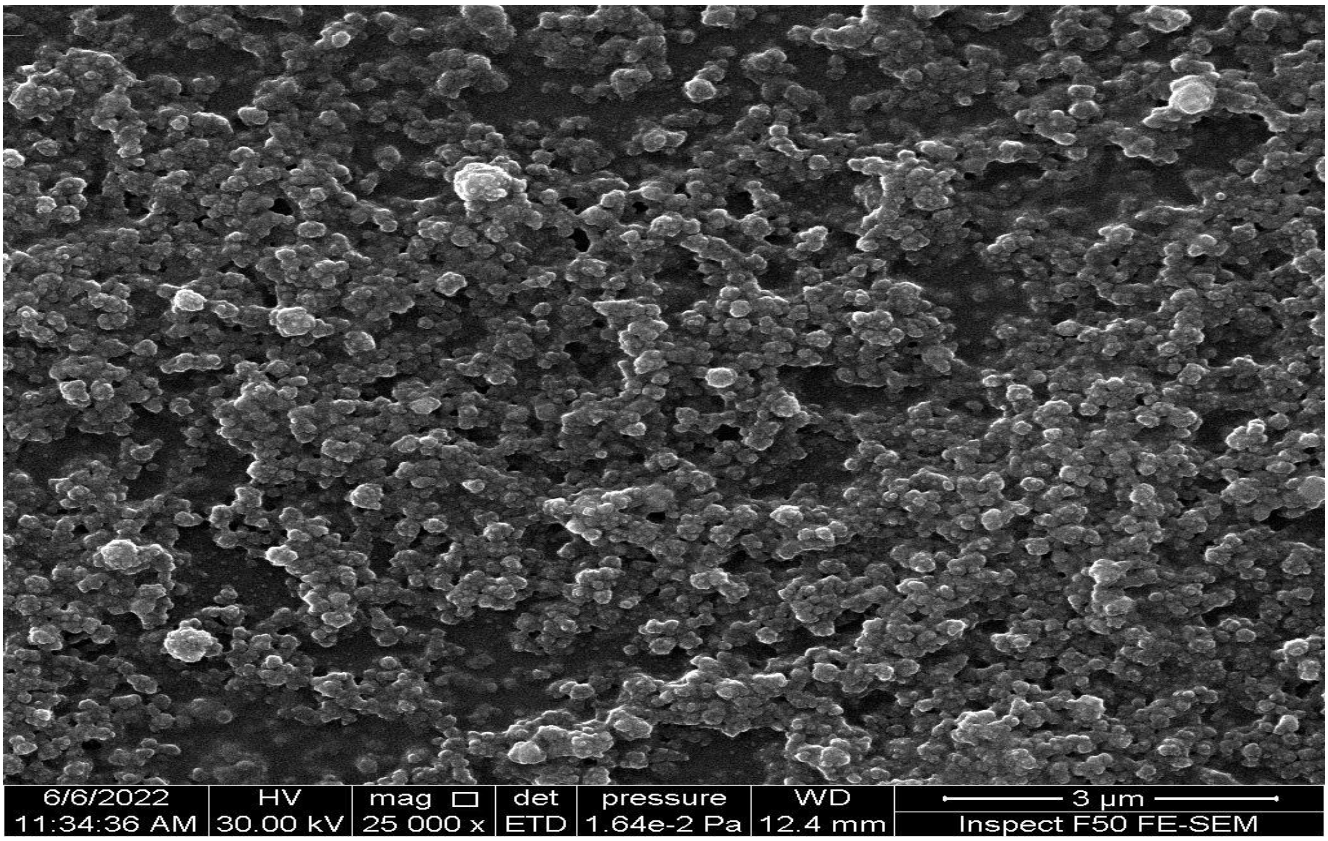

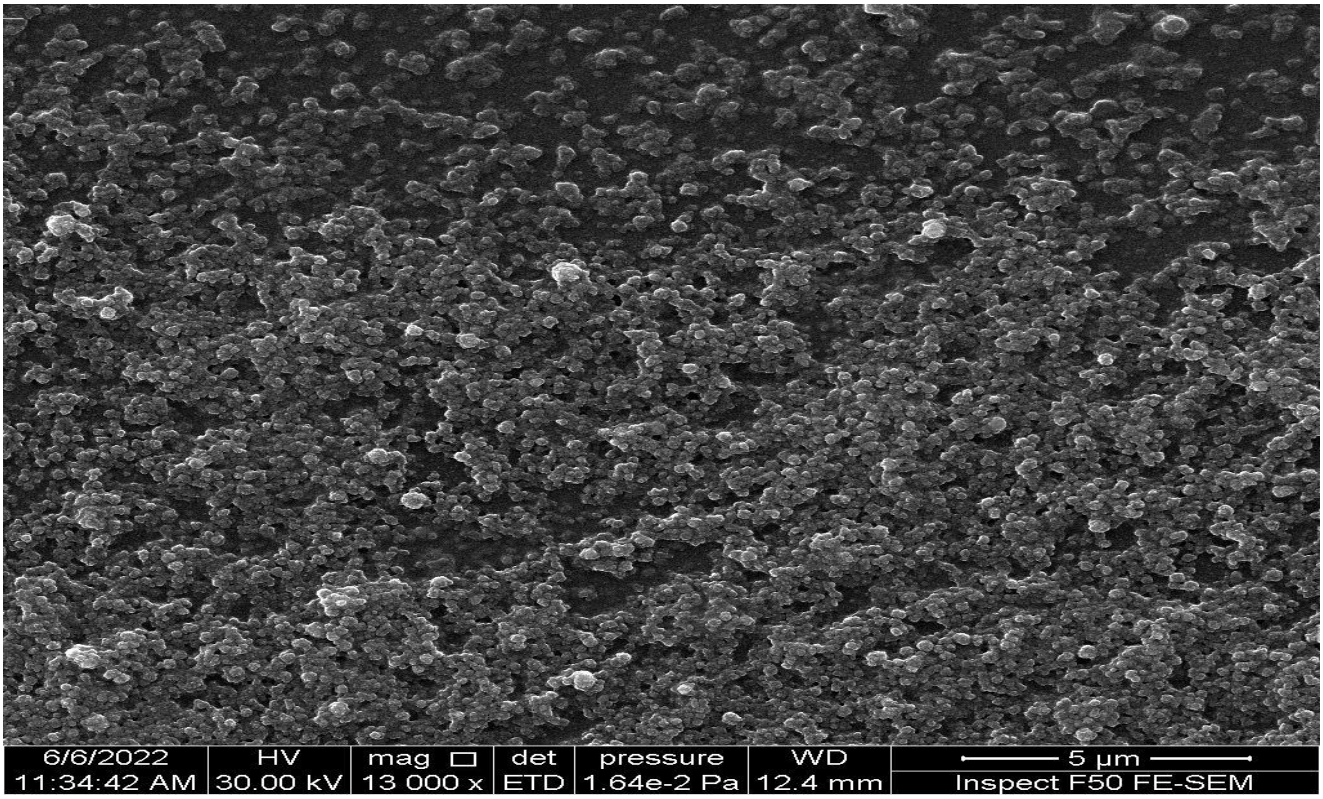

D3: SEM for NPS Au

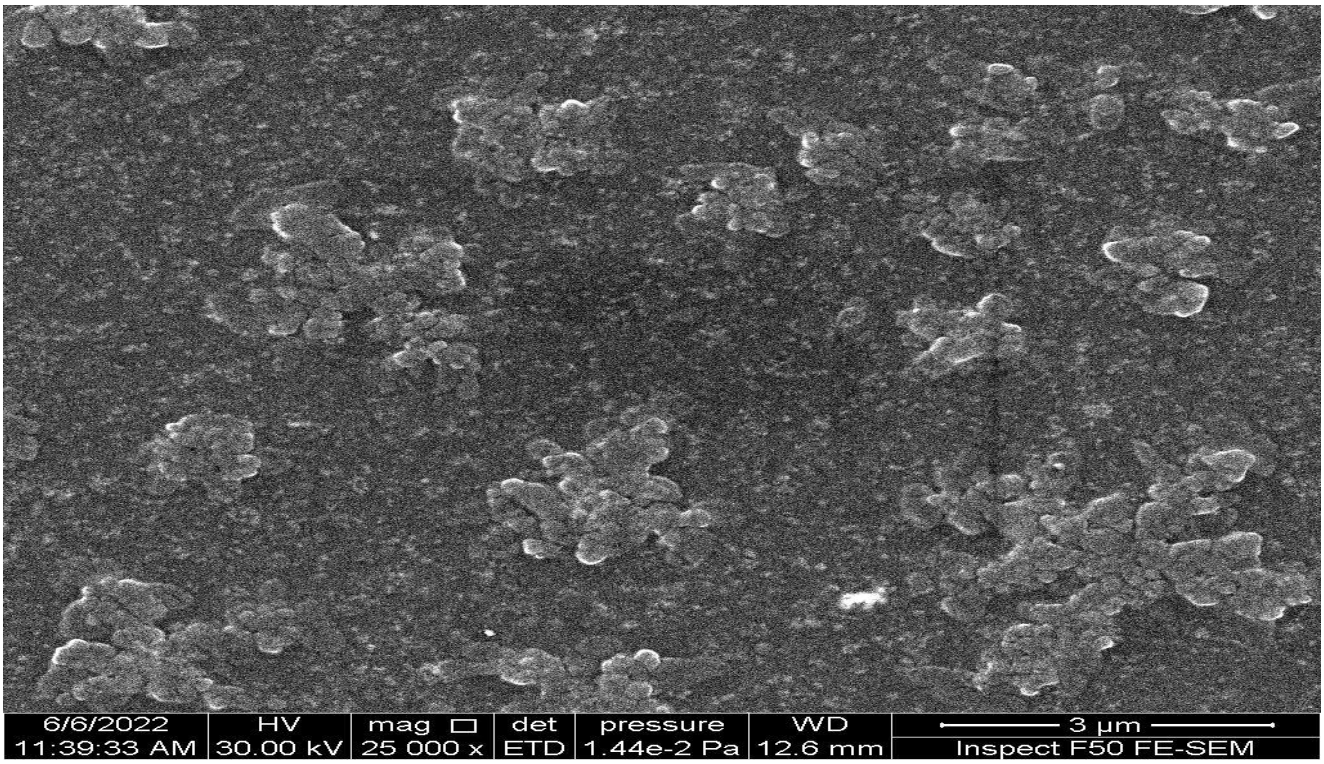

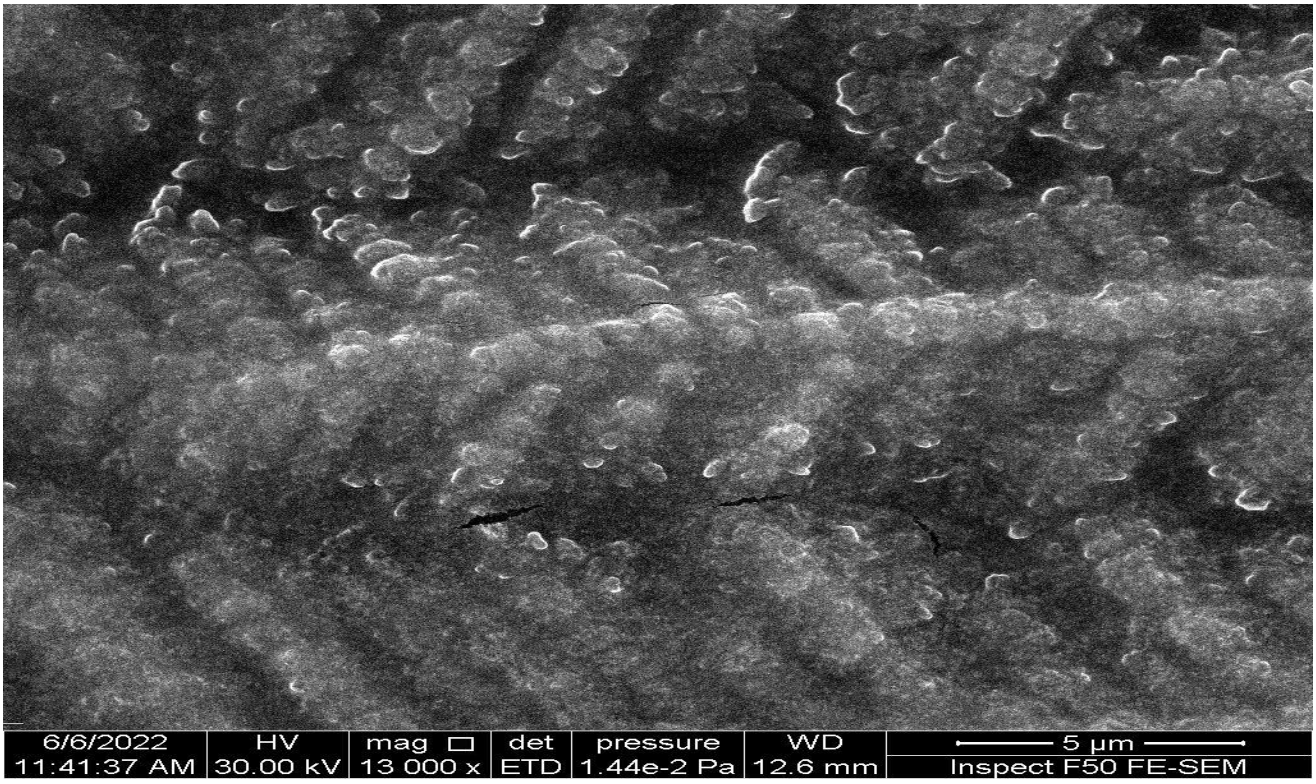

الخلاصة

في هذه الدراسة، تم استخدام طريقة بسيط بمرحلة واحدة تعتمد على التقطير العكسي (الأرتجاعي) للجزر العراقي الصالح للأكل مع فوسفات ثلاثي الصوديوم المائي (TSP) لتكوين نقاط الكربون المضيئة باللون الأزرق. تشير الدراسة إلى أن التقطير العكسي ل 5 جم من الجزر في 100 ملي مولاري من محلول مائي TSP ولمدة 120 دقيقة يكون كافٍ لإنتاج نقاط الكربون مضغوطة زرقاء عالية الإضاءة.

يوضح طيف الأشعة تحت الحمراء (FTIR) لمستخلص الجزر (CE) ونقاط الكربون (CDs) أن قمة C=O- التي تمت ملاحظتها عند $1740\ cm^{-1}$ و1650 في CE أختفت تمامًا في الأقراص المضغوطة، وهذا يشير إلى حدوث عملية الكربنة لمجموعة الكربونيل وتشكيل المزيد من الكربون المهجن sp^2.

علاوة على ذلك، أظهرت أطياف H NMR لـ CE وCDs أن عدد الإشارات التي لوحظت بين 3 و4 جزء في المليون في CE قد انخفضت بشكل كبير في CDs، مما يشير إلى أن بعض مخلفات السكر قد خضعت لعملية الكربنة. أكدت هذه النتائج أن الكربوهيدرات الموجودة في الجزر خضعت لعملية الكربنة لإنتاج نقاط الكربون المضيئة. أظهرت صورة فحص المجهري الإلكتروني (SEM) أن نقاط الكربون تكاد تكون كروية الشكل وحجمها يتراوح بين 6.40 - 25.76 نانومتر. أكدت نتائج طيف الأشعة السينية المشتت للطاقة (EDX) وجود نقاط الكربون في العينات المدروسة. تم استخدام نقاط الكربون التي تم إنتاجها كمصباح ضوئي لتصوير البكتيريا من خلال الفحص المجهري الفلوري لأن نقاط الكربون لها نفاذية جيدة للأغشية كما انها أقل سمية ضد البكتيريا سالبة الجرام وإيجابية الجرام.

تم إثبات قدرة نقاط الكربون على الاختزال المباشر لأيونات الفضة إلى عنصر الفضة (Ag^0) وأيونات الذهب إلى عنصر الذهب (Au^0) بدون عامل اختزال وتثبيت إضافي. يبلغ حجم الجسيمات النانوية الناتجة لكل من Ag وAu بمايساوي 20.40 - 59.44 و14.57 - 38.33 نانومتر، على التوالي.

تم تسجيل أعلى قيم لكل من PT وAPTT بوجود AgNPs أذا ما قورنت مع تلك التي لا تحتوي على AgNPs، عند $P = 0.05$.

جامعة كربلاء
كلية العلوم
قسم علوم الكيمياء

طريقة خضراء مناسبة لتخليق نقاط الكربون المضيئة من الجزر الصالح للأكل وتطبيقاته.

رسالة مقدمة الى

مجلس كلية العلوم- جامعة كربلاء

كجزء من متطلبات نيل شهادة الماجستير في الكيمياء

من قبل

هدى راضي محيسن الجليحاوي

بأشراف

أ.د. باقر عبد الزهرة جودة **أ.د. عدنان أبراهيم محمد**

١٤٤٤ هـ **٢٠٢٣ م**